

22719239

MICHIGAN STATE UNIVERSITY LIBRARIES



3 1293 00582 0323

LIBRARY
Michigan State
University

This is to certify that the

dissertation entitled

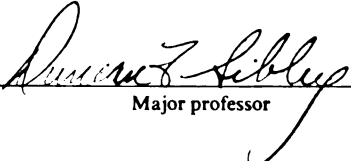
Dolomitization and Porosity evolution

presented by

Michael A. Miller

has been accepted towards fulfillment
of the requirements for

Doctoral degree in Geology


Major professor

Date 6/13/88

PLACE IN RETURN BOX to remove this checkout from your record.
TO AVOID FINES return on or before date due.

DATE DUE	DATE DUE	DATE DUE
_____	_____	_____
_____	_____	_____
_____	_____	_____
_____	_____	_____
_____	_____	_____
_____	_____	_____
_____	_____	_____

MSU is An Affirmative Action/Equal Opportunity Institution

**DOLOMITIZATION AND POROSITY
EVOLUTION**

By

Michael A. Miller

A DISSERTATION

**Submitted to
Michigan State University
in partial fulfillment of the requirements
for the degree of**

DOCTOR OF PHILOSOPHY

Department of Geology

1988

ABSTRACT
DOLOMITIZATION AND POROSITY EVOLUTION

By
Michael A. Miller

Dolomite rock texture, and therefore its porosity, is controlled by the interplay of factors that influence reaction kinetics. These factors include: 1) the surface area of the substrate, 2) the saturation state of the solution, 3) temperature, 4) substrate mineralogy, and 5) the role of inhibiting ions. Dolomite porosity is also affected by the flux of bicarbonate through the system in that this influences the amount of dolomite cement that can be precipitated.

In the Trenton dolomites (Michigan Basin) and the Sero Domi dolomites (Aruba, N.A.), the surface area of the substrate has a control on the resultant porosity of the dolomite. The dolomitization of a finely crystalline (high surface area) limestone, resulted in dense dolomite nucleation and a dolomite with porosities similar to, or lower than, the host. Dolomitization of a more coarsely crystalline (low surface area) limestone, resulted in less dense dolomite nucleation and a dolomite with porosities higher than the host.

In the Trenton Formation dolomites, the flow direction for the dolomitizing fluid can be inferred from the distribution of the dolomite and trace element gradients. The change in fluid chemistry of the dolomitizing solution across the study area had no significant influence on

the resultant porosity of the dolomites.

Limestones and dolomites with similar textures from the Sero Domi Formation and the Eniwetok Atoll were studied to assess the role of bicarbonate flux on the porosity evolution of the dolomites. It was determined that the flux of bicarbonate through the sediment was not a limiting factor in the porosity evolution of these dolomites.

ACKNOWLEDGEMENTS

This research was partially funded by both the National Science Foundation (EAR 82 14106) and the Department of Geological Sciences at Michigan State University. I wish to thank Eugene Shinn and the USGS at Fisher Island Station for the use of the drilling equipment on Aruba, NA. The government of Aruba and the Aruba Mining Company were also most helpful with equipment and support. A special thanks to Total Petroleum who granted the use of the Trenton cores and supplied the porosity and permeability data. Sampling of the Eniwetok core was granted by the Smithsonian Institution, with sampling directed by Warren Blow. Phil Koro of Schlumberer logging company was also helpful with the interpretation of the fracture identification log.

A special thanks to my thesis advisor Duncan Sibley for his support. I would also like to thank the other members of my committee Dave Long, Mike Velbel and Tom Vogel.

Thanks to all my fellow students who made my tenure at MSU a memorable experience. I would especially like to thank, Tim Flood PhD, Greg Giles, Nadine Romero, Jim Mills, Bill Sack, and Jerry Grantham for their support. Thanks to the various geochemistry types who helped so much with the collection of the trace element data and an occasional rod hockey game especially, Tim Wilson, Dale Rezabeck and Nancy Fegan.

I would also like to gratefully acknowledge the help and support of Robert Hayes of the MDNR.

As always, I would like to thank my parents Robert and Dorothy Miller for their unmitigated moral and financial support.

Finally, I would like to thank my wife and best friend Beth for her unerring support through the past five years.

TABLE OF CONTENTS

ACKNOWLEDGEMENTS	ii
LIST OF TABLES	vii
LIST OF FIGURES	x
INTRODUCTION	1
PREVIOUS WORK	3
MODEL RELATING SUBSTRATE SURFACE AREA AND SATURATION STATE OF THE SOLUTION TO DOLOMITE POROSITY	5
Model For Dolomite Porosity	9
Reactant Surface Area in Nature	16
Substrate Surface Area Affects (Examples)	19
Ranges of Solution Chemistry in Nature	21
Solution Chemistry Affects (Examples)	23
METHODS	25
OBSERVED AFFECTS OF SUBSTRATE SURFACE AREA AND SATURATION STATE OF THE SOLUTION TO DOLOMITE POROSITY	27
The Ordovician Trenton Formation Jackson County, Michigan	27

TABLE OF CONTENTS (cont'd.)

Relationship of the Trenton Dolomites to Fractures	63
Discussion of Substrate Surface Area Affects	71
Discussion of Solution Chemistry Affects	78
Pliocene Sero Domi Formation Aruba, Netherlands Antilles	84
Discussion of Substrate Surface Area Affects	92
BICARBONATE FLUX	94
Pliocene Sero Domi Formation Aruba, Netherlands Antilles	98
Origin of the Sero Domi Dolomites	110
Discussion of the Bicarbonate Flux Model	115
Eocene Carbonates From the Eniwetok Atoll	116
Discussion of the Bicarbonate Flux Model	123
DISCUSSION OF DOLOMITE POROSITY	124
SUMMARY	126
CONCLUSIONS	128
APPENDIX I	130
APPENDIX II	136
APPENDIX III	148

TABLE OF CONTENTS (cont'd.)

APPENDIX IV	153
REFERENCES	158

LIST OF TABLES

Table	1.	BET specific surface area as a function of grain size.	18
Table	2.	The saturation indexes of the solutions with respect to dolomite	22
Table	3.	Variation of crystal sizes in Trenton limestone clasts	38
Table	4.	Oxygen and carbon isotope analyses of the Trenton limestones	43
Table	5.	Minor and trace element compositions (ppm) of the Trenton limestones.	44
Table	6.	Dolomite crystal size distribution in the clasts and the matrix between the clasts from the Trenton.	50
Table	7.	Oxygen and carbon isotope analyses of the Trenton dolomites.	54
Table	8.	Oxygen and carbon isotope analyses of dolomites from the partially dolomitized cores, Trenton Formation.	55
Table	9.	Strontium concentration (ppm) of the Trenton Formation dolomites.	56
Table	10.	Manganese, iron and zinc concentrations (ppm) of the Trenton Formation dolomites..	58
Table	11.	Stable isotopic and trace element compositions of some ancient dolomites.	61

LIST OF TABLES (cont'd.)

Table 12.	Comparison of oxygen isotopic signatures between Trenton dolomite types.	69
Table 13.	Comparison of manganese concentrations (ppm) between Trenton dolomite types.	70
Table 14.	Comparison of iron concentrations (ppm) between Trenton dolomite types.	72
Table 15.	Point counting results for the Trenton dolomite textural comparison.. . . .	73
Table 16.	Porosity and permeability of the Boe Doei carbonates (Aruba, N.A.).	87
Table 17.	Oxygen and carbon isotope analyses of the Sero Domi limestones, (Boe Doei).	89
Table 18.	Stable isotope and trace element analyses of the Sero Domi dolomites (Boe Doei).	91
Table 19.	Darcy velocities and mass fluxes.	97
Table 20.	Oxygen and carbon isotope analyses of the Sero Domi limestones (Rooi Hundu).	100
Table 21.	Stable isotope and trace element analyses of the Sero Domi dolomites (Rooi Hundu).	105
Table 22.	Porosity and permeability of the Rooi Hundu carbonates (Aruba, N.A.).	108
Table 23.	Stable isotopic and trace element compositions of selected Cenozoic dolomites.	114
Table 24.	Porosities and permeabilities of the Eniwetok carbonates.	121

LIST OF TABLES (cont'd.)

Table AI-1.	Comparison of Compensated Neutron and Whole Core Porosity of the Trenton Dolomites .	131
Table AII-1.	Whole Core Porosity Analyses of the Trenton Formation Carbonates	136
Table AIV-1.	Compensated Neutron Log Porosity Comparison of the Nonconglomeritic Zones in the Trenton Formation Dolomites	153
Table AIV-2.	Whole Core Porosity Comparison of the Conglomeritic Horizon in the Trenton Formation Dolomites	155

LIST OF FIGURES

Figure 1.	Model of dolomite porosity evolution in a generic substrate	10
Figure 2.	Model of dolomite porosity evolution in a generic wackestone	14
Figure 3.	Schematic cross-section of the Red River Dolomites, Montana	24
Figure 4.	Location Map for the Trenton Formation Study Area in Jackson County, Michigan	28
Figure 5.	Map of wells that were used in the study.	29
Figure 6.	Study area map with well lease names listed. Cores used in this study are circled	30
Figure 7.	Generalized isopach map of the Trenton Formation in the study area.	31
Figure 8.	Top of the Trenton Formation contour map	33
Figure 9.	West to east cross-section A-A' through the Trenton Formation in the study area.	34
Figure 10.	North to south cross-section B-B' through the Trenton Formation in the study area.	36
Figure 11.	Rounded quartz grains in the matrix between dolomitized clasts in the Trenton.	39
Figure 12.	Blocky low magnesium calcite cement filling molds in the Trenton limestone	40

LIST OF FIGURES (cont'd.)

Figure 13.	Cemented fracture in a limestone clast that is broken off at the edge of the clast.	41
Figure 14.	Composition of the Trenton Formation limestone clasts.	45
Figure 15a.	Trenton dolomite observed in plane light.	47
15b.	Trenton dolomite as viewed in blue-violet light.	47
Figure 16.	Comparison of the crystal sizes between the dolomitized clasts and the dolomitized matrix between the clasts in the Trenton Formation.	49
Figure 17.	Large dolomite crystals replacing allochems and smaller dolomite crystals replacing mud in the Trenton Formation.	52
Figure 18.	Late iron-rich dolomite cement in the Trenton Formation dolomites.	53
Figure 19.	Comparison of porosity between limestone and dolomite clasts in the Trenton.	62
Figure 20.	Fossil moldic porosity in the Trenton dolomites.	64
Figure 21.	Dolomite clasts with varying porosity in close proximity.	65
Figure 22.	Rose diagram of the fracture trend in the Trenton in the study area.	66
Figure 23.	Nonplanar dolomite crystal replacing calcite cement in the Trenton	75

LIST OF FIGURES (cont'd.)

Figure 24.	Oxygen isotopic signature of the dolomites versus distance from west to east for the Trenton dolomites	82
Figure 25.	Location map for the Sero Dumi Formation outcrops on Aruba, N.A.	85
Figure 26.	Percent porosity versus depth for the carbonates from Boe Doei	86
Figure 27.	Blade shaped cement crystal included in a dolomite crystal from Boe Doei	90
Figure 28.	Dolomite crystals from the partial and complete dolomites from Boe Doei.	93
Figure 29a.	Typical limestone from Rooi Hundu.	101
29b.	Dolomite from Rooi Hundu showing mimic replacement of the coralline algae	102
29c.	Foram mold in the dolomites from Rooi Hundu.	103
Figure 30.	Coralline algae fractured around what is currently a foram mold from Rooi Hundu.	104
Figure 31.	Percent porosity versus depth for the carbonates from Rooi Hundu.	107
Figure 32.	Location map for the core used from the Eniwetok Atoll.	117
Figure 33.	Selective replacement of the muds by dolomite and the resistance of coarsely crystalline fossil fragments	118
Figure 34.	Dolomite cementation after calcite cementation on Eniwetok.	119

LIST OF FIGURES (cont'd.)

Figure 35.	Percent porosity versus depth for the carbonates from Eniwetok.	120
-------------------	--	------------

INTRODUCTION

Dolomitization is a process that is governed by factors that influence reaction kinetics (Machel and Mountjoy, 1986). Nucleation and growth rates of the dolomite crystals influence the texture and therefore the porosity of the resultant dolomite. Recent laboratory experiments have delineated several key parameters affecting reaction kinetics: a) Mg/Ca ratio in the solution and substrate mineralogy (Gaines, 1980); b) crystal size of the reactant (Sibley et al, 1987); c) temperature (Katz and Matthews, 1977); and d) the effects of inhibiting ions, such as SO_4^{2-} (Baker and Kastner, 1981).

In addition to reaction kinetics, the flux of bicarbonate through the system is an important consideration in the evolution of dolomite porosity. Bicarbonate flux is important in that it influences the amount of dolomite cement that can be precipitated.

Most dolomites have very complicated diagenetic histories. Consequently, in most studies examining dolomite porosity, the factors affecting porosity are difficult to constrain. This study is significant in that constraints can be imposed to evaluate the effects of; 1) substrate surface area, 2) saturation state of the solution, and 3) the flux of bicarbonate on the resultant dolomite porosity. Several hypotheses are tested in this study; 1) that crystal size of the reactant creates variations in resultant dolomite porosity, 2) that changes in the fluid chemistry of the dolomitizing solution create variations in the porosity of the resultant dolomite and 3) that the mere flux of bicarbonate through the carbonate system is not the limiting factor in dolomite porosity development.

Samples from the Ordovician Trenton Formation (Michigan Basin), the

Pliocene Sero Domi Formation on Aruba (Netherlands Antilles), and the Miocene carbonates on the Eniwetok Atoll (South Pacific) were used in this study. Samples from the Trenton Formation were studied because they contain carbonate conglomerates. The individual clasts in the conglomerate have a wide range in composition. This provides an opportunity to examine what influence the variation in substrate texture has on dolomite porosity within a close proximity. It is highly improbable that clasts of strikingly different textures immediately adjacent to one another experienced differences in solution chemistry and temperature. The Trenton dolomites also provided an opportunity to look at how changes in solution chemistry might affect dolomite porosity. These changes in solution chemistry were inferred from the spatial distribution of the dolomites and trace element gradients.

Samples from the Sero Domi Formation on Aruba, were studied because they contain dolomites and limestones with similar original depositional textures. This allows one to determine whether or not dolomitization creates or destroys porosity. The amount of bicarbonate transported into or out of the system can then be determined for mass flux modelling.

The dolomites from the Eniwetok Atoll were studied to see how fabric-selective dolomitization would affect dolomite porosity. Previous work on these dolomites also provides constraints on the timing of dolomitization and the type of dolomitizing solution for mass flux modelling. Saller (1984a) presents a reasonable case for dolomitization by deep seawater. Through the use of strontium isotopes in the dolomites he was able to constrain the timing for the dolomitization process. Using petrographic data obtained in this study and the data provided by Saller

(1984a), one can model the flux of bicarbonate through the original carbonate substrate.

In the Trenton and Sero Domi dolomites, it will be shown how the crystal size of the reactant (limestone) produces the textural/porosity variations observed. Additionally, in the Trenton dolomites, it will be shown that changes in dolomitizing fluid chemistry did not affect the porosity of the resultant dolomite. In the Eniwetok and Sero Domi dolomites, it will also be shown that the bicarbonate flux was adequate to produce the observed porosities.

PREVIOUS WORK

Porosity evolution of dolomites is most commonly explained by "volume shrinkage", a model attributed to deBeaumont in 1836 (Van Tuyl, 1914). The model was discussed in greater detail by Murray (1960) and Weyl (1960). They called it the "local source theory", because the source of CO_3^{2-} was assumed to be derived from the CaCO_3 being replaced. The model is based on the dolomitization of a limestone via the following equation:



The resultant dolomite will occupy 13 percent less volume than the original volume of the calcite. This occurs due to the molar volume difference between two moles of calcite and one mole of dolomite. Since

dolomitization via this reaction should result in a porous dolomite, a strict application of this model universally does not seem warranted due to the existence of many low porosity dolomites.

Other models attribute the porosity of dolomites to the dissolution rate of calcite being greater than the precipitation rate of dolomite during the replacement process (Murray, 1930 and Landes, 1946). However, studies of partial and complete dolomitization by Lucia (1962), Jodry (1969) and Choquette and Steinen (1985), infer that dolomitization initially decreased porosity and then increased porosity. These studies are not consistent with the dissolution rate of calcite being more rapid than the precipitation rate of dolomite.

Wardlaw (1979) suggested that porosity in dolomite can be attributed to contact inhibition. Contact inhibition is the tendency for crystals to stop growing when they come into contact. He suggested that contact inhibition between dolomite crystals is greater than the inhibition between calcite crystals, which tend to form compromise boundaries and destroy porosity. This suggestion however, is in direct conflict with the fact that compromise boundaries and intergrown dolomite crystals are observed through standard petrographic and SEM examination. Schmoker and Halley (1982) suggest that dolomites are more resistant to the "porosity reducing effects of burial" than limestones.

Limestone and dolomite porosities have been compared in many studies (Lucia, 1962; Jodry, 1969; Schmoker and Halley, 1982; Halley and Schmoker, 1983; Longman, Fertal and Glennie, 1983; Baum, Harris and Drez, 1985; Schmoker, Krystinik and Halley, 1985; and Choquette and Steinen, 1985). These studies however, produce no consistent trends in dolomite porosity data. For example, Longman et al (1983), Baum et al

(1985) and Choquette and Steinen (1985) showed that dolomites were more porous than their associated limestones. Lucio (1962), Jodry (1969) and Choquette and Steinen (1985), inferred that dolomitization initially decreased porosity and then increased porosity. Halley and Schmoker (1983) showed that no difference in porosity exists between limestones and dolomites of the Cenozoic of Southern Florida. Schmoker and Halley (1982) also show that shallowly buried dolomites from south Florida are less porous than their associated limestones. Finally, Schmoker et al (1985) found that limestone reservoirs in the United States are actually more porous and permeable than dolomite reservoirs.

None of the models presented can account for the wide range of dolomite porosities observed in nature.

The texture, i.e. porosity, of non-detrital rocks is the result of several factors influencing crystal nucleation and crystal growth. Two of these factors are; 1) the surface area of the substrate, and 2) the saturation state of the solution. The effects of these two parameters on dolomite porosity will be addressed in the following section. The influence of bicarbonate flux on dolomite porosity will be addressed in a later section.

MODEL RELATING SUBSTRATE SURFACE AREA AND SATURATION STATE OF THE SOLUTION TO DOLOMITE POROSITY

If the flux of bicarbonate through the system is not a limiting factor, the nucleation rate of the dolomite can determine the texture of the

dolomite and consequently its porosity. Two factors which can affect nucleation rate are; 1) the surface area of the reactant particles, and 2) the supersaturation of the solution with respect to the products. How these two parameters can influence nucleation rate is addressed below.

The heterogeneous nucleation rate of a phase can be related to the number of active sites (potential nucleation sites) by the following equation from Christian (1975, eq. 52.34):

$$I \approx (N)^{1/3} L (kT/h) \exp \{-(\Delta G_c + \Delta g^*)/kT\} \quad (2)$$

where N = Number of atoms per unit volume which are on dislocation lines

L = Dislocation density

ΔG = Critical free energy for homogeneous nucleation

Δg^* = Free energy of activation per atom

k = Boltzmann's constant

h = Planck's constant

T = Temperature

It is assumed that the number of active sites (dislocations) is directly proportional to the surface area of the reactant, and therefore, the nucleation rate is directly proportional to the surface area of the reactant. An increase in the surface area of the reactant will cause a corresponding increase in the nucleation rate.

The influence of the saturation state of the solution on the heterogeneous nucleation rate is observed by substituting the free energy term for homogeneous nucleation into the preceding equation. The free

energy term for homogeneous nucleation is given by the following equation from Christian (1975, eq. 46.20):

$$\Delta G_e = 4\delta^3 n^3 / 27(g^v - g^l)^2 \quad (3)$$

where

δ = Surface free energy

n = Shape factor

g = Gibb's function per atom (l - liquid, v - vapor)

Substituting this equation into equation (2) above one can see that the nucleation rate is an exponential function of the saturation state.

This relationship can also be seen in the following equation from Boistelle (1982):

$$I = N_0 v \exp [-16 B^2 s^3 / 3(kt)^3 (\ln S)^2 \exp (-G_{vdiff}/kt)] \quad (4)$$

where

N_0 = no. of solute molesules/ volume of solution

v = frequency with which a critical nucleus becomes supercritical

B = volume of a molecule inside the nucleus

s = interfacial surface free energy between the nucleus and the solution,

S = degree of supersaturation,

G_{vdiff} = energy barrier encountered by the bulk solution for volume diffusion from the bulk solution to the nucleus.

We lack the necessary data on the surface free energy of the dolomite nucleus, the shape factor of the dolomite nucleus, and the dislocation density of the substrate, to apply these equations quantitatively to dolomitization. Qualitatively however, from equation (2) it can be seen that a direct relationship exists between the dislocation density and the nucleation rate. From equations (3) and (4) it can be seen that a linear relationship also exists between $\log I$ and the degree of supersaturation. The slope of the curve will be determined by factors in the numerator of the exponent.

In summary, the rate of nucleation is directly proportional to the number of active sites on the substrate, which in turn is directly proportional to the surface area of the reactant. An increase in the surface area of the reactant will therefore, cause a corresponding increase in the nucleation rate. The rate of nucleation is also an exponential function of the degree of supersaturation with respect to the product phase. An increase in the saturation state of the solution will therefore, cause a corresponding increase in the nucleation rate.

The porosity evolution of a dolomite is also influenced by the dissolution rate of the parent limestone. From observations in the partially dolomitized rocks from the Trenton Formation in this study, it appears that dissolution of the limestone host occurs at the limestone-dolomite interface and not whole-sale throughout the sediment. This is evidenced in the partial dolomites in that no partially dissolved parent mud or allochems are observed. If whole-sale calcite dissolution was occurring in the host, there should be evidence of dissolution in both the mud, and the allochems, in the partial dolomites. If dissolution of the parent limestone occurs at the limestone-dolomite interface and no

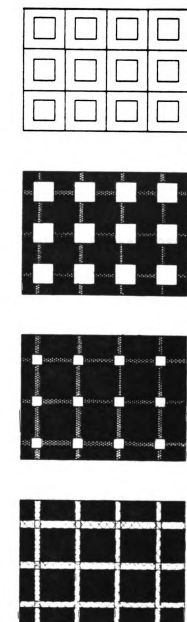
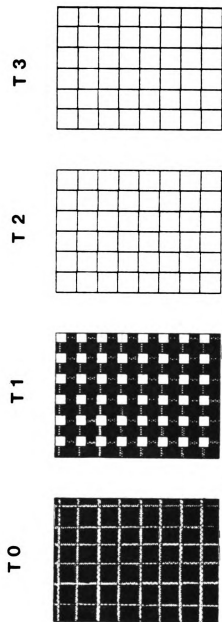
dolomite nucleates on the substrate, then dissolution will not occur. This unreplaced host can then be dissolved out at some later time creating porosity.

Model for Dolomite Porosity

The model of dolomite porosity proposed has two parts, 1) the influence of the substrate surface area, and 2) the influence of the saturation state of the solution. These two situations will be examined in relation to varying amounts of bicarbonate.

First, if the growth of the nuclei is not limited by other kinetic factors, then the porosity of the product will be directly related to the surface area of the reactant. The affect of substrate surface area and solute flux will first be examined using a generic substrate, and then using a generic wackestone. In figure 1, substrate (a) has a high density of dolomite nuclei, and substrate (b) has a low density of dolomite nuclei. The evolution of the porosity to total exclusion of porosity in both substrates is depicted. Both substrates begin the process with the same porosity. In an open system with a solution of constant composition and temperature, and with excess bicarbonate moving through the substrate, the crystals in both substrates will grow at the same rate. After a short period of growth (T1), substrate (a) with the high nucleation density has a lower porosity than substrate (b) with the low nucleation density. This is due to the tighter initial packing of the nuclei. After a longer period of growth (T2), the porosity of the substrate (a) with the high nucleation density has been totally occluded, but substrate (b) with the lower nucleation density still

Figure 1. Model of dolomite porosity evolution in a generic substrate. Substrate (a) has a high density of dolomite nuclei and substrate (b) has a low density of dolomite nuclei. The substrate in both cases has the same original porosity. As dolomitization ensues, substrate (a) will lose its porosity more rapidly than substrate (b) due to the greater number of dolomite crystals growing. At time T2 substrate (a) has lost its porosity, whereas substrate (b) still retains porosity. With continued dolomitization, substrate (b) will lose its porosity as well at a later time (T3).



- LIMESTONE
- DOLOMITE
- POROSITY

Figure 1

has porosity. If substrate (b) remains in the dolomitizing solution, it will eventually lose its porosity and become occluded as well (T3). The product in this sample will have a larger crystal size than the product formed from the nuclei that were more densely packed initially. The density of the nuclei will then, determine which portions of the substrate will lose their porosity first, and which portions of the substrate will retain their porosity the longest. Substrates with a higher number of nuclei per unit mass of reactant would have more closely packed products and therefore a lower porosity than the corresponding substrate with less dense nucleation at any time (T) as the sediment approaches zero porosity.

The dolomitization of finely crystalline reactants (i.e. mud or cryptocrystalline allochems) will result in dense dolomite nucleation. This dense nucleation will result in a finely crystalline dolomite with a relatively low porosity. The dolomitization of a coarsely crystalline substrate (e.g. microcrystalline allochems) will result in a lower density of dolomite nuclei. This lower nucleation density is manifested in the formation of a coarsely crystalline dolomite with a relatively high porosity.

Considering the same situation with a limited amount of bicarbonate, initially the substrate with the higher nucleation density will become more porous due to the more rapid dissolution of the local carbonate to produce the dolomite. As dolomitization continues however, and dolomite cement is added, the substrate with the more densely packed dolomite crystals will result in the lower porosity dolomite.

Second, the porosity of the dolomite is a function of the saturation state of the solution. The nucleation rate of dolomite is an exponential function of the degree of supersaturation with respect to the product

phase. An increase in the degree of supersaturation will therefore behave in a similar fashion as an increase in the surface area of the substrate. A high saturation state will result in a high nucleation rate and therefore a high density of dolomite nuclei. A solution with a high saturation state should therefore result in dense nucleation and tightly packed products. This is similar to the effect produced by a finely crystalline substrate. Solutions with a high saturation state will cause dense nucleation and will result in a low porosity product. Conversely, a solution with a low saturation state will result in a low density of nuclei and a high porosity product. Therefore at time T (any time before the total occlusion of porosity) the substrate subjected to the solution with a higher saturation state will result in a dolomite with a lower porosity than the same substrate subjected to a solution with a lower saturation state.

The effects of substrate surface area, saturation state of the solution and time are demonstrated on a generic wackestone in figure 2. In this wackestone, the carbonate mud portion will have a high density of dolomite nuclei due to its high surface area. There are also some coarsely crystalline fossil fragments in this wackestone that will have a lower density of nucleation sites due to the lower surface area of these grains. If this wackestone is subjected to a solution that is highly supersaturated with respect to dolomite, very dense nucleation will occur in the mud portion of the wackestone due to both the high surface area of the substrate and the high saturation state. The more coarsely crystalline portions of the sample will have fewer dolomite nuclei (IIA). Given an adequate flux of HCO_3^- , the dolomite nuclei will grow rapidly and impinge on one another. The product will be a dolomite with a porosity similar to or lower than the limestone that it replaced. The dolomite will retain the

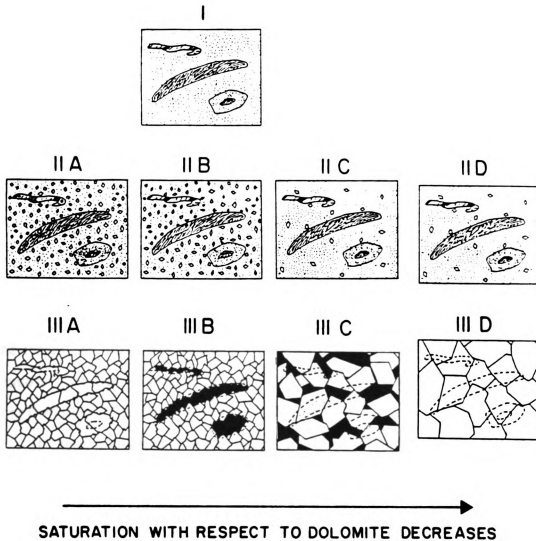


Figure 2. Model of dolomite porosity evolution in a generic wackestone. Where (I) represents the generic wackestone, (II) is the onset of dolomitization showing the distribution of the nuclei, and (III) is the completely dolomitized result (diagram from Sibley and Gregg, 1987).

original limestone texture (IIIA) due to the dense initial nucleation. Due to the externally derived HCO_3^- , dolomite cementation may occur and produce a dolomite with a lower porosity than the original limestone.

If the same wackestone is subjected to a solution with a slightly lower saturation state (IIB) and little externally derived HCO_3^- , there is still relatively high nucleation density in the mud portions of the sample, due to its high surface area, but little or no nucleation in the more coarsely crystalline portions of the rock. The more coarsely crystalline portions of the substrate will therefore be much slower to dissolve and remain unreplaced. The coarsely crystalline substrate will be slower to dissolve because the dolomite does not nucleate on it. Since dissolution occurs at the limestone-dolomite contact, if there is no nucleation there will be no dissolution. These unreplaced fragments can later dissolve, in which case fossil moldic porosity will result (IIIB).

If the same wackestone is subjected to a solution with an even lower saturation state (IIC) and very little externally derived bicarbonate, there is a lower density of dolomite nuclei. This results in large dolomite rhombs that are not packed as closely as the rhombs in case A (IIIC), and no dolomite cementation. A dolomite which has a porosity that is increased over the precursor limestone is produced. With the low nuclei density in the host, the fine textural detail of the host is obliterated.

In the first three cases presented, the amount of time was a fixed quantity. In example D, the effect of a prolonged time in a dolomitizing solution with a low saturation state is presented. In case D, there are few nuclei in the substrate due to the low saturation state. This low saturation state also results in a slow growth rate. If however, this solution is

fluxed through the sediment over a sufficient period of time, then the dolomite rhombs would eventually impinge on one another and result in a low porosity dolomite (IID), that shows textural obliteration.

The previous examples were sediments that experienced one dolomitization event. For each succeeding event of dolomitization a new set of factors needs to be analyzed.

Reactant Surface Area in Nature

A mudstone will have a higher number of possible nucleation sites per unit volume than a coarse crystalline grainstone due to the higher surface area of the micrite per unit volume. Therefore, dolomite should nucleate more rapidly and more densely in mudstones as compared to grainstones. This assumes that the number of active sites on a crystal surface is directly proportional to its surface area. There are no data available on the surface area of natural reactants in situ. This appears to be a good working hypothesis however since Bartlett (1964) conducted dolomitization experiments with substrates of different surface area, and found that dolomitization did indeed occur more rapidly in substrates with a higher surface area to volume ratio. This is also consistent with the common observation that mudstones and the mud in packstones are often preferentially dolomitized (Chilingar, 1956; Powers, 1962; Murray and Lucia, 1967; Armstrong, 1970; Wardlaw, 1979; Ruzyla and Friedman, 1985; Gawthorpe, 1987).

The magnitude of the surface area effect of nonallochems on nucleation rate can be estimated by comparing crystal size differences of

micrite and microspar. The size range of micrite is 1-4 microns and the size range of microspar is 4-50 microns (Bathurst, 1975). If one assumes that the crystals are cubes, the difference in surface area between micrite and microspar is approximately four orders of magnitude from 6 microns to 15,000 microns. The magnitude of the surface area effect of allochems on nucleation rate is difficult to estimate. The sizes of allochems and cement however can vary by much more than size differences observed between micrite and microspar. The crystal sizes of allochems and cement can range from microns to millimeters.

Crystal size differences occur not only between mudstones and grainstones, but also between different fossil types. Walter and Morse (1984) have shown that fossil types have a wide variety of BET surface areas, and that these surface area measurements can vary by at least an order of magnitude (Table 1). Differences in the reactivity of these fossils to dolomitization are contingent upon not only differences in crystal size, but also to differences in mineralogical composition, chemical composition and microstructure (Sibley, 1982; Bullen and Sibley, 1984). From petrographic observation and experimental studies one can see the differences in behavior of different fossils to dolomitization. For example, certain fossils are replaced mimetically, nonmimetically, not replaced at all, or entirely dissolved out (Murray, 1960; Sibley, 1982; Bullen and Sibley, 1984). If these effects were due entirely to differences in crystal size, the following would occur. Red algae which have cryptocrystalline calcite skeletons (i.e. high surface area) are more likely to be replaced mimetically, whereas some molluscs which have microcrystalline calcite skeletons (i.e. low surface area) are more likely to be nonmimetically replaced or remain unreplaced. This difference in

TABLE 1. BET SPECIFIC SURFACE AREA AS A FUNCTION OF GRAIN SIZE

Grain Type	Median Grain Diameter (Microns)	Observed Specific Surface Area (m^2g^{-1})	Observed/Geometrically Predicted Surface Area
Echinoid	81	0.14	5.7
	275	0.09	12.4
	513	0.08	20.5
Coral	51	0.23	5.9
	81	0.22	8.9
	275	0.17	23.4
	513	0.12	30.8
<i>Halimeda</i>	81	2.04	82.6
	215	2.10	225.8
	513	2.11	541.2

(Walter and Morse, 1984)

textural response is best explained by the different number of potential nucleation sites and therefore a different rate of nucleation.

Diagenesis can cause an increase in the crystal size of the CaCO_3 , therefore decreasing the density of potential dolomite nucleation sites. Samples having undergone aggrading neomorphism and/or coarsely crystalline cementation should therefore result in a substrate with a lower density of dolomite nuclei per unit volume.

Substrate Surface Area Affects (Examples)

There are few published analyses where the distribution of dolomite, dolomite paragenesis, original lithologies, solution chemistry and porosity are adequately described. The following examples of dolomite porosity evolution are consistent with our ideas concerning the influence of substrate surface area on dolomite porosity. In these studies, however, it is not possible to assess what affects differences in original mineralogy and/or changes in fluid chemistry had on the dolomite porosity development.

Jodry (1969) examined dolomites from a reef and associated carbonates (Silurian, Michigan Basin). He chronicled the evolution of the porosity for a variety of original rock textures from 100 percent limestone to 100 percent dolomite. He concluded that the "rocks with the least porosity development were micrite", with the resultant dolomites exhibiting an average porosity of 1.8 percent. Dolomitized micrites also had a small dolomite crystal size in comparison to the dolomitized

reef-framework. He observed that very large crystals of dolomite and higher porosity (12.5 percent) were apparent in dolomites that had replaced reef-framework material. This porosity development is consistent with a substrate surface area control on porosity.

Barrett (1986) suggested that the replacement dolomite of the Smackover Formation (southern Alabama) and its porosity distribution, were a function of changes in the magnesium flux and anisotropies in the carbonate fabric. The effect of the carbonate fabric on porosity is observed in the completely dolomitized areas. In these areas, the low porosity dolomites were correlated with changes to finer-grained carbonate substrates.

Armstrong (1970) examined dolomites from the Lisburne Group (Alaska). In these dolomites, finer crystalline dolomite replaced the carbonate mudstones and more coarsely crystalline dolomites replaced packstones and grainstones. Abundant visible porosity was noted in the dolomitized packstones and grainstones.

Fisher and Rodda (1969) examined dolomites from the Edwards Formation (Texas). They suggest that there are two types of dolomite present, 1) a stratal dolomite - which is fine grained, has a uniform grain size, a tightly knit fabric, is very slightly porous and permeable, and is associated with carbonate mudstones, and 2) massive dolomite - fine to coarse grained, has a variable rhomb size, a loosely knit fabric, is moderately porous and permeable, and is associated with fossiliferous carbonate grainstones. The stratal dolomite is inferred to have formed prior to lithification and the massive dolomite formed after lithification. The differences in porosity between the two dolomite types may be due to the initial differences in substrate surface area, and to the lithification

process which would increase the crystal size of the substrate. The variable rhomb sizes in the massive dolomite may have resulted from; 1) coarsely crystalline dolomite replacing the coarsely crystalline fossils that had been lithified and 2) the finely crystalline rhombs (similar in size to the stratal dolomites) replacing the mud matrix.

Ranges of Solution Chemistry in Nature

Dolomitizing solutions consisting of a wide range of fluid compositions have been inferred by many researchers. The differences in the saturation indexes (IAP/Ksp) of these solutions with respect to dolomite is examined below.

Dolomitizing solutions produced by various mixing proportions of fresh water and seawater have been invoked by Badiozamani (1973); Hanshaw, Beck and Dieke (1971); Choquette and Steinen (1980); Sears and Lucia (1980); Ward and Halley (1985) and many others. The saturation index of this mixture using Badiozamani's (1973) data is approximately 14 (Table 2). Seawater has been suggested as a dolomitizing solution by Saller (1984a); Mullins et al (1985); Corbello and Land (1987), Aharon et al (1987) and others. Seawater, with a saturation index of approximately 2990 (Table 2) with respect to dolomite is more highly supersaturated with respect to dolomite than mixed waters.

Refluxing brines (which can have a wide range of compositions) have also been suggested as a possible dolomitizing solution (Adams and Rhodes, 1960; Deffeyes et al, 1965; Sears and Lucia, 1980; Clement, 1985; Rosen et al, 1988). The saturation index of the Dead Sea brine (Krumgalz et al,

TABLE 2. THE SATURATION INDEXES OF THE SOLUTIONS WITH RESPECT TO STOICHOOMETRIC DOLOMITE

Solution Type	Saturation Index
<u>Mixed Water</u> ⁺	1.38×10^1
<u>Sea Water</u> ⁺⁺	2.99×10^3
<u>Brine</u> ⁺⁺⁺	4.85×10^5

⁺ Badiozamani (1973) Mix consists of 95% freshwater and 5% sea water.

⁺⁺ Activity coefficients from Millero and Schreiber (1982) with absolute concentrations from Drever (1982).

⁺⁺⁺ Dead sea brines approximately 10X the concentration of sea water (Krumgalz and Millero, 1982).

1982) which has been used for flux modelling is approximately 4.9×10^5 (Table 2). Although this particular brine has a higher saturation index than sea water, not all evaporatively concentrated waters are even supersaturated with respect to dolomite (Gueddari, 1983).

The evaporatively concentrated brine has the highest saturation index of the waters examined and the mixed water solution has the lowest. The higher saturation index in the brine would lead to a greater nucleation rate for the brine dolomites. The lower saturation index in the mixed water would lead to a lower nucleation rate for the mixed water dolomites.

Solution Chemistry Affects (Examples)

There are two examples where the porosity of the dolomites appears to be directly related to the saturation state of the dolomitizing solution (Longman et al, 1983 and Barrett, 1986). These studies however, do not attempt to correlate the stratigraphic distribution of the dolomite with changes in dolomite crystal chemistry, nor do they provide enough detailed information to assess the role that changes in substrate surface area may have in the porosity evolution of the dolomite.

Longman et al (1983) examined dolomites from the Red River Formation (Ordovician, Williston Basin) detailing the dolomite distribution and porosity trends (Figure 3). They showed dolomite pods under the C anhydrite which crosscut bedding planes. The abundance of dolomite decreased around the periphery of the pods, suggesting a decrease in the Mg/Ca ratio of the dolomitizing solution. Near the source of the

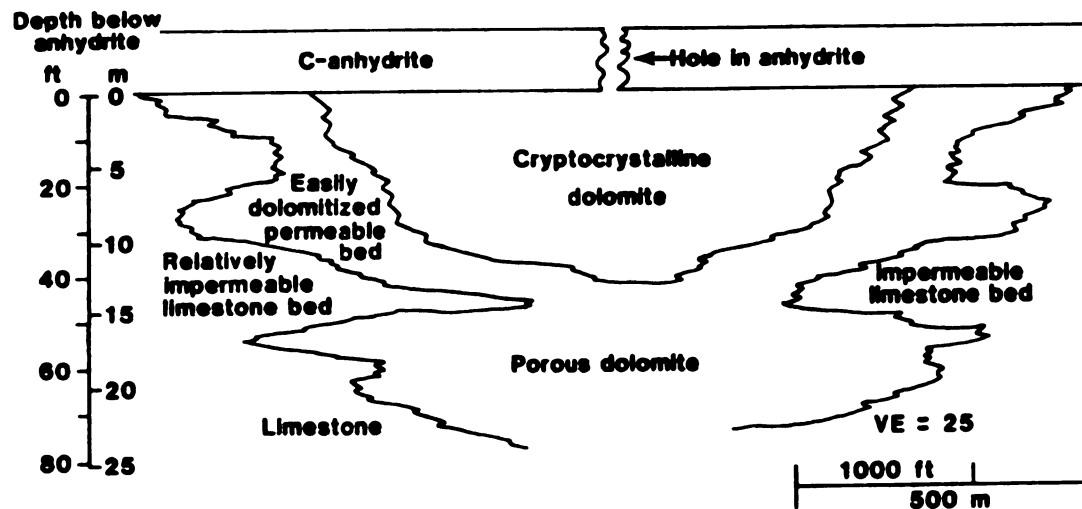


Figure 3. Schematic cross-section of the Red River Dolomites, Montana (Longman et al, 1983). Note the dolomite near the inferred source of the dolomitizing solution (break in the C anhydrite) is cryptocrystalline and has a low porosity. Dolomites farther away from the source of the solution are more coarsely crystalline and have a higher porosity.

dolomitizing solution (an inferred break in the C anhydrite), the dolomite is finely crystalline with low porosity. Near the limestone-dolomite contact, the dolomite is more coarsely crystalline and porous. These dolomite and porosity trends are interpreted to be related to decreases in the saturation state of the solution with respect to dolomite.

Barret (1986) examined dolomites from the Smackover Formation (Jurassic, Alabama) detailing the dolomite distribution and porosity trends. It was suggested that areas of high magnesium flux determined the amount and distribution of replacement dolomite and therefore its porosity. Areas of high magnesium flux resulted in greater dolomite replacement, the formation of sucrosic dolomite and consequently greater porosity.

In this study constraints will be placed on the sediments to determine what effects substrate surface area, solution chemistry or bicarbonate flux would have on the evolution of dolomite porosity.

METHODS

Porosity analyses reported in this study come from three sources. Core Labs (Mt Pleasant, MI) performed whole core and plug porosity analyses on selected samples from all sample locations. After these values were obtained, thin section point count (500pts/slide) porosities were determined on samples impregnated with blue epoxy or epoxy spiked with a fluorescent dye. Fluorescent dyes were used to help determine microporosity in the dolomites (Yanguas and Dravis, 1985). Regional trends in the Trenton porosity were also determined from compensated neutron porosity logs. A comparison of the dolomite whole-core porosity and the

compensated neutron log porosity was conducted in order to determine regional trends in dolomite porosity (APPENDIX I). Through the use of a T-test, it was found that there was no significant difference in porosity between the two methods.

Fossil percentages in the dolomites were obtained through point counts of thin sections under fluorescent light (Dravis and Yurewicz, 1985), diffused plane light, and plane light. Thin sections of the Trenton Formation impregnated with fluorescent epoxy and viewed with a fluorescence microscope reveal little or no microporosity. This indicates that the thin section point counts are not biased by visible porosity.

Stoichiometry of the dolomites was determined by X-ray diffraction analyses (Graf and Goldsmith, 1956). Major and trace element analyses of the limestones and dolomites were performed on a Perkin-Elmer #560 AAS. The analytical and machine precision for strontium and manganese was less than $\pm 1\%$, for zinc $\pm 4\%$, and for iron $\pm 20\%$. All samples were powdered to pass a 60 micron sieve and dissolved in glacial acetic acid following the method outlined by Barber (1974).

Carbon and oxygen isotopic analyses were performed at the University of Michigan Stable Isotope Laboratory. All samples were roasted under vacuum at 380°C for one hour to remove volatile contaminants. Calcite and dolomite samples were reacted in anhydrous phosphoric acid at 50°C , and CO_2 was prepared in an extraction line coupled directly to the inlet of a VG 602E ratio mass spectrometer. Isotopic compositions were then converted to PDB and corrected for ^{17}O according to Craig's (1957) procedure. No fractionation correction was applied for the dolomite-phosphoric acid reaction. Precision of the isotopic data is better than 0.10 per mil (‰)

for both oxygen and carbon determinations. The precision of data is based on a daily analysis of NBS 20.

**OBSERVED AFFECTS OF SUBSTRATE
SURFACE AREA AND SATURATION STATE
OF THE SOLUTION ON DOLOMITE POROSITY**

**The Ordovician Trenton Formation
Jackson County, Michigan**

The Trenton Formation (Ordovician, Michigan Basin) was studied because it contains carbonate conglomerates and consequently provides substrate textural variations within close proximity. In studying clasts of strikingly different textures immediately adjacent to one another, differences in solution chemistry and/or temperature can be dismissed. The Trenton dolomites also provided an opportunity to look at how changes in solution chemistry might affect dolomite porosity. These changes in solution chemistry were inferred from the spatial distribution of the dolomites and trace element gradients.

The Trenton Formation is composed of mudstones and wackestones that were deposited in a deep subtidal environment (Wilson and Sungepta, 1985). In this study five cores from north central Jackson County were examined (Figures 4 and 5). An isopach map of the Trenton Formation in the Michigan Basin (Figure 6), indicates that the study area lies between what are interpreted to have been two Trenton platforms. An isopach map of the study area (Figure 7) reveals an anomalous local thickening of the Trenton,

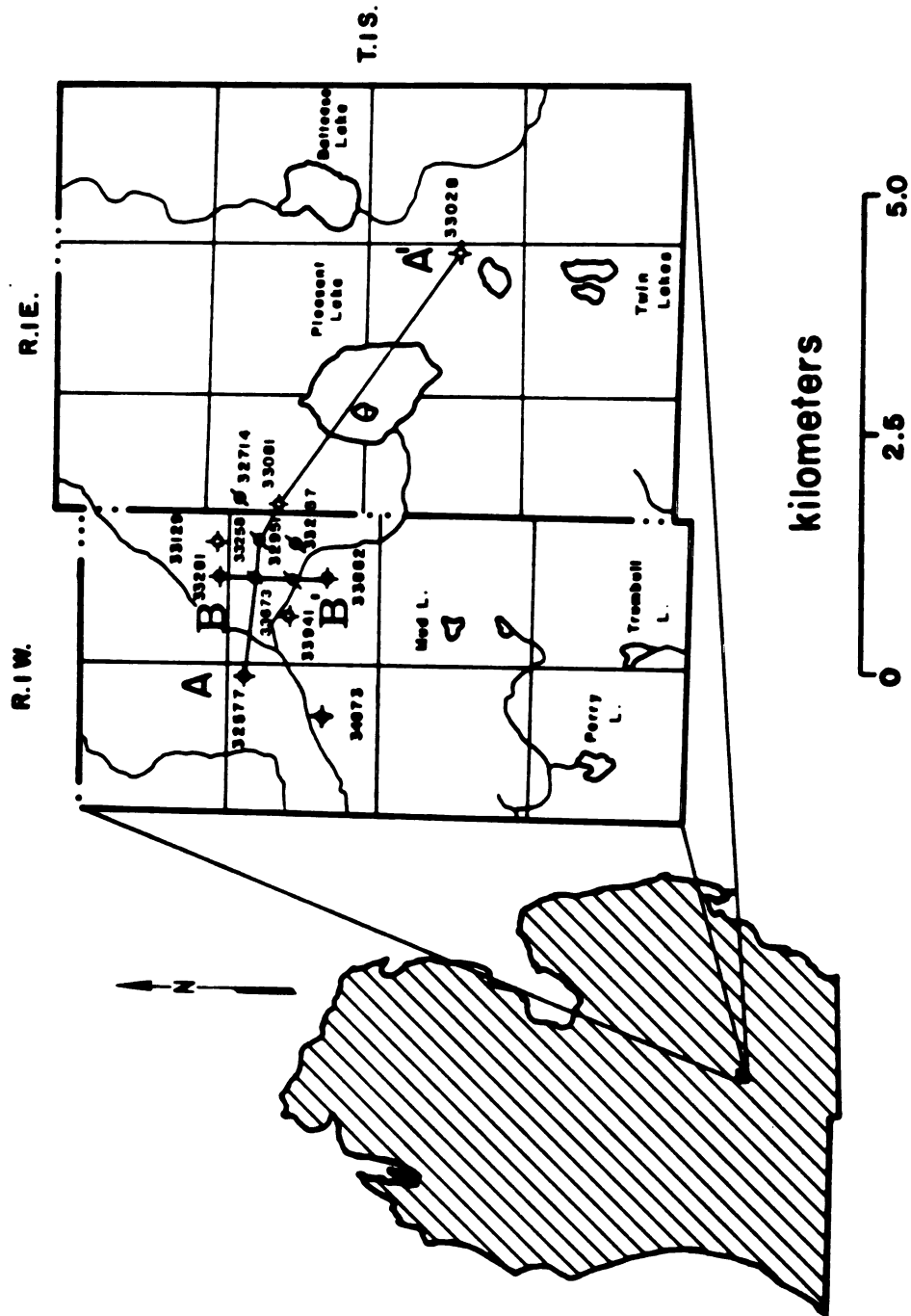


Figure 4. Location Map for the Trenton Formation Study Area in Jackson County, Michigan. The lines of section A-A' and B-B' are also shown.

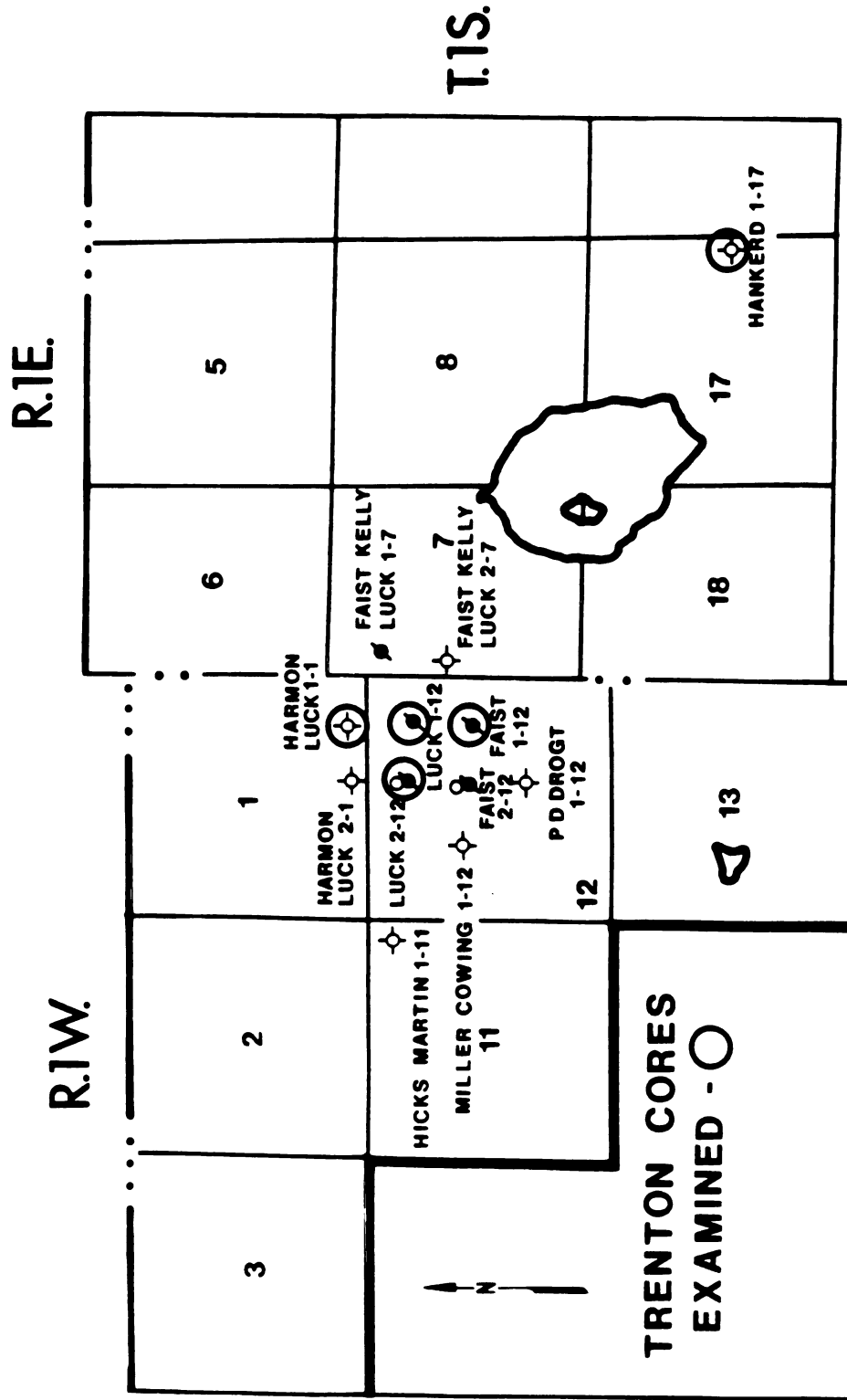


Figure 5. Study area map with the well lease names listed. Cores used in this study are circled.

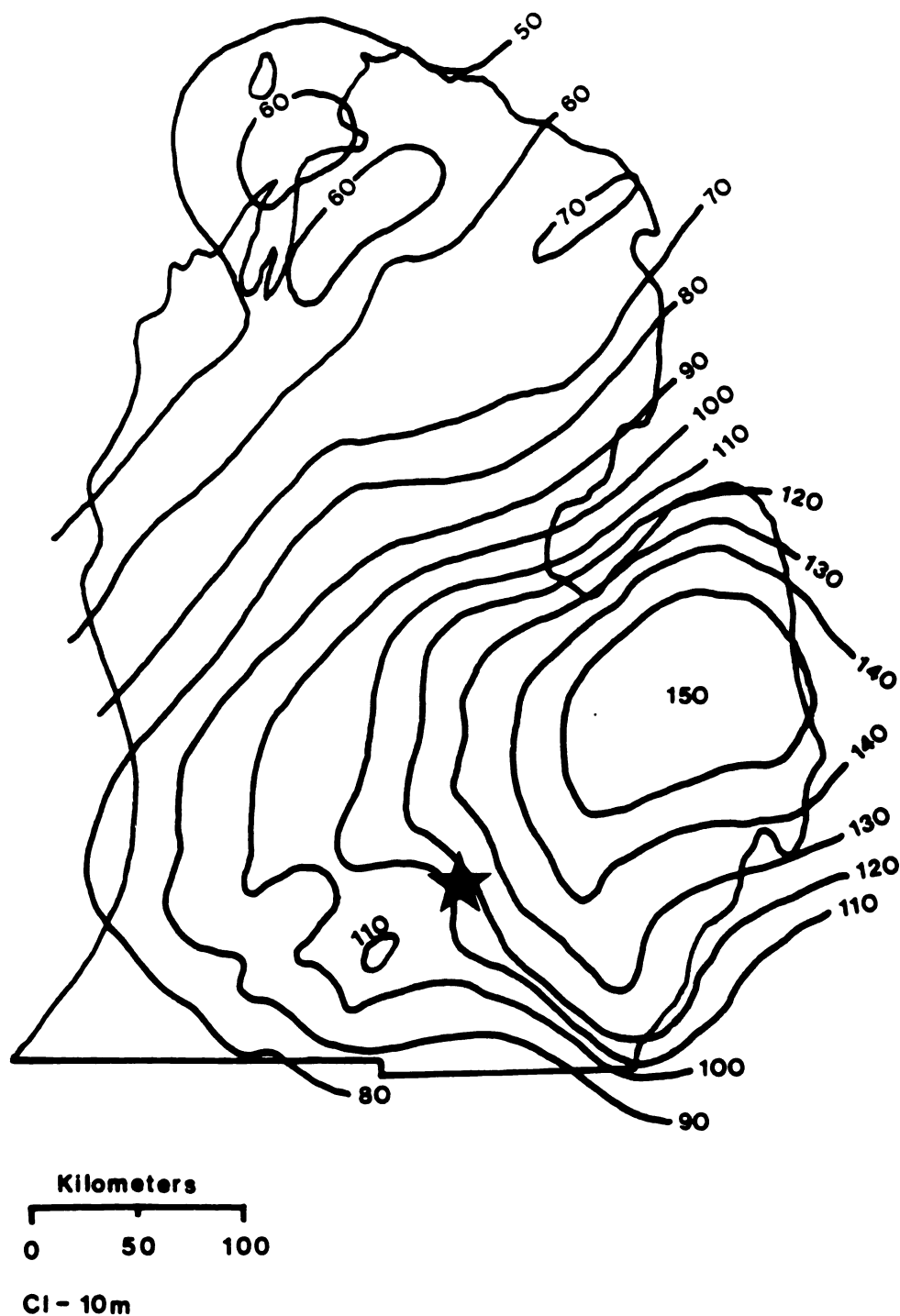


Figure 6. Generalized isopach map (contours in meters) of the Trenton Formation in Michigan (from Wilson and Sengupta, 1985). Note the position of the study area (star) between what are thought to have been two Trenton platforms.

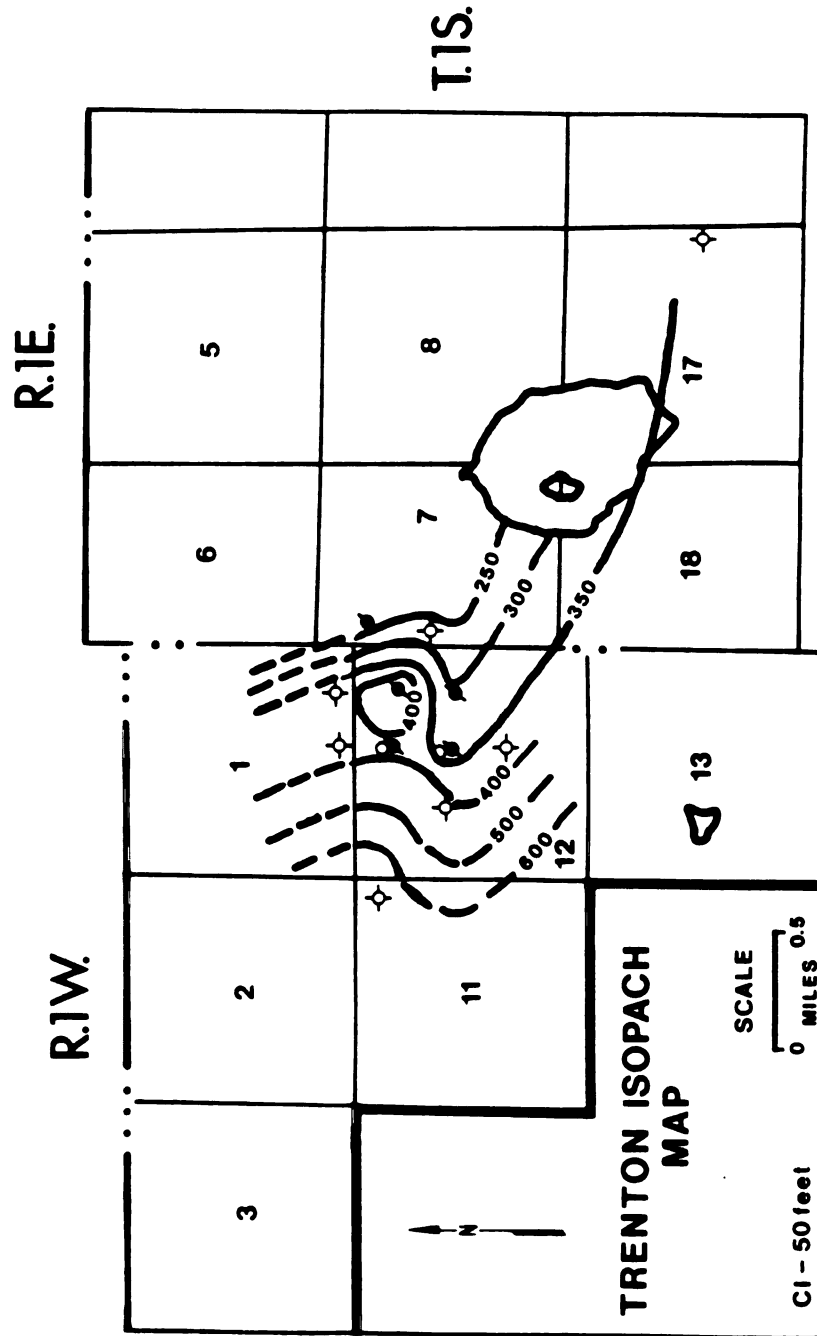


Figure 7. Isopach map of the Trenton Formation in the study area. Note the anomalous thickening in the Trenton.

a feature that has also been seen in the Trenton from the nearby Northville Trend (Mesher, 1980). A contour map of the top of the Trenton in the study area (Figure 8), shows that there is no discernable local dip direction. The regional dip in this area of the basin is to the north. Most of the Trenton Formation in the study area is limestone, however, the cored intervals contain partially and completely dolomitized strata.

The limestones are dominantly dark grey nodular mudstones and wackestones. The allochems in the limestones are chiefly echinoid and brachiopod fragments, with minor amounts of lithoclasts, trilobites, molluscs and pellets. Clasts are common in the upper part of the cores (Figures 9 and 10). The clasts in this zone range in size from a few millimeters to five centimeters. The clasts range in composition from mudstones to crinoid-brachiopod-mollusc packstones, and generally comprise about 65 percent of the rock volume where present. The crystal sizes of the constituents in the limestone clasts vary widely (Table 3). The fact that the clasts are rounded suggests that these clasts are detrital and not collapse breccias. This is also supported by the presence of rounded detrital quartz grains in the matrix between the clasts but not within the clasts themselves (Figure 11). Molluscs in the limestones and in the lithoclasts are often dissolved away with the molds being filled by an equant blocky spar cement (Figure 12). Cementation occurred prior to the deposition of the clasts. This is evidenced by cemented fractures in the clasts which end abruptly at clast edges (Figure 13). These fractures do not extend into the matrix and would not have survived transport if they had not been previously cemented.

Oxygen isotopic compositions of whole-rock limestone analyses range from -7.66 to -5.06 ‰ and average -6.39 ‰ PDB. Carbon isotopic

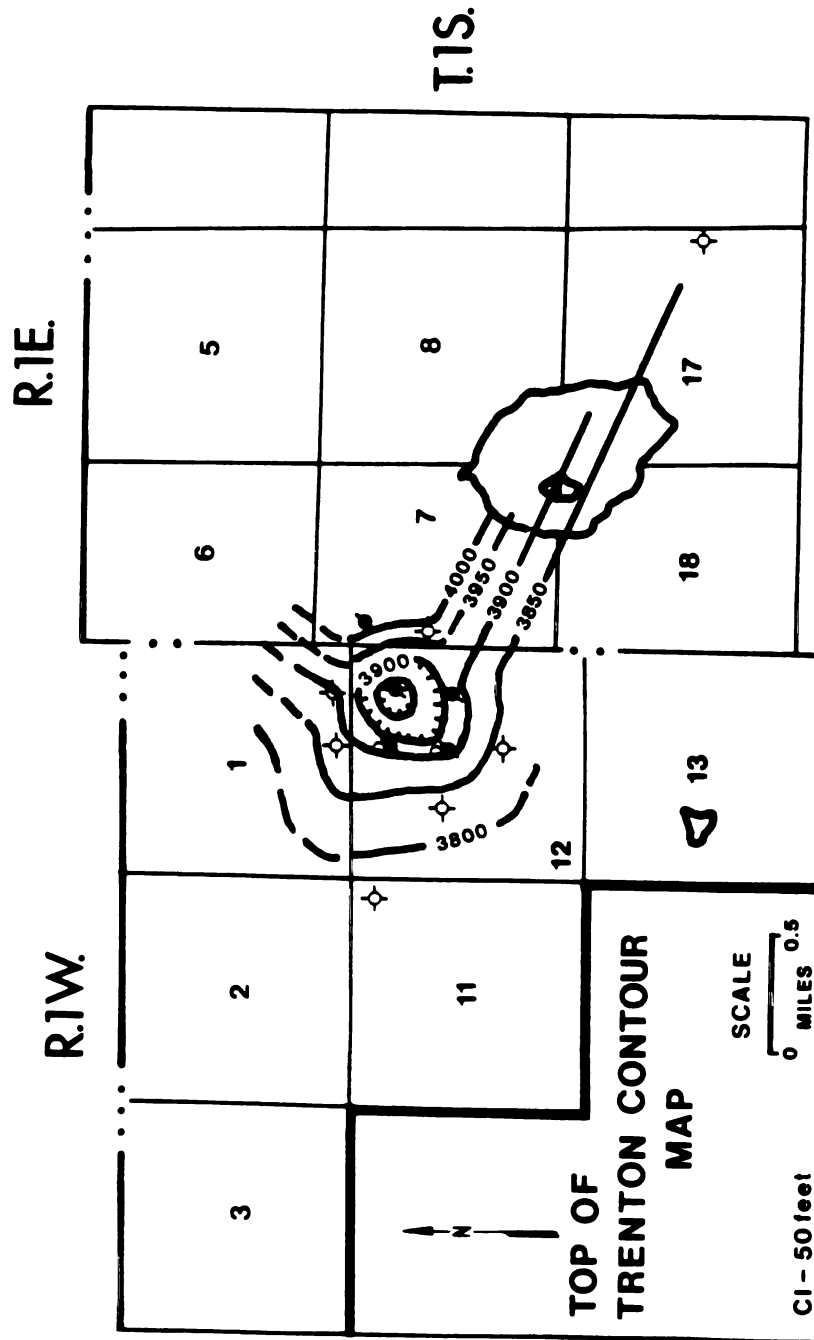


Figure 8. Top of the Trenton Formation contour map.

Figure 9. Cross-section A-A' showing the distribution of dolomite and lithoclasts. Gamma logs and neutron porosity logs for the wells are also shown. Note the increase in neutron porosity in the horizons containing dolomitized lithoclasts. Also shown are the cored intervals of the wells.

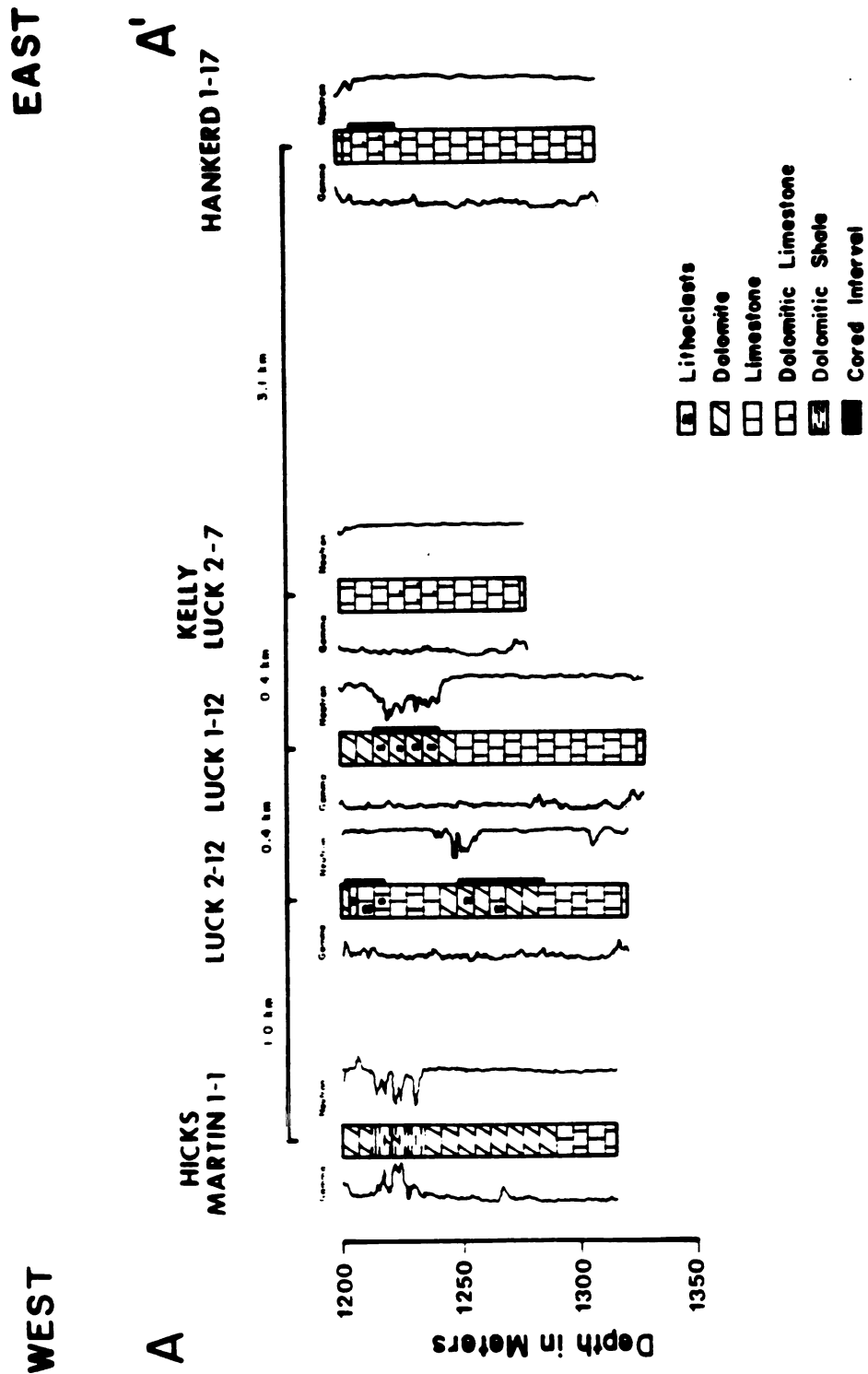


Figure 9

Figure 10. Cross-section B-B' showing the distribution of dolomite and lithoclasts. Gamma logs and neutron porosity logs for the wells are also shown. Note the increase in neutron porosity in the horizons containing dolomitized lithoclasts. Also shown are the cored intervals of the wells.

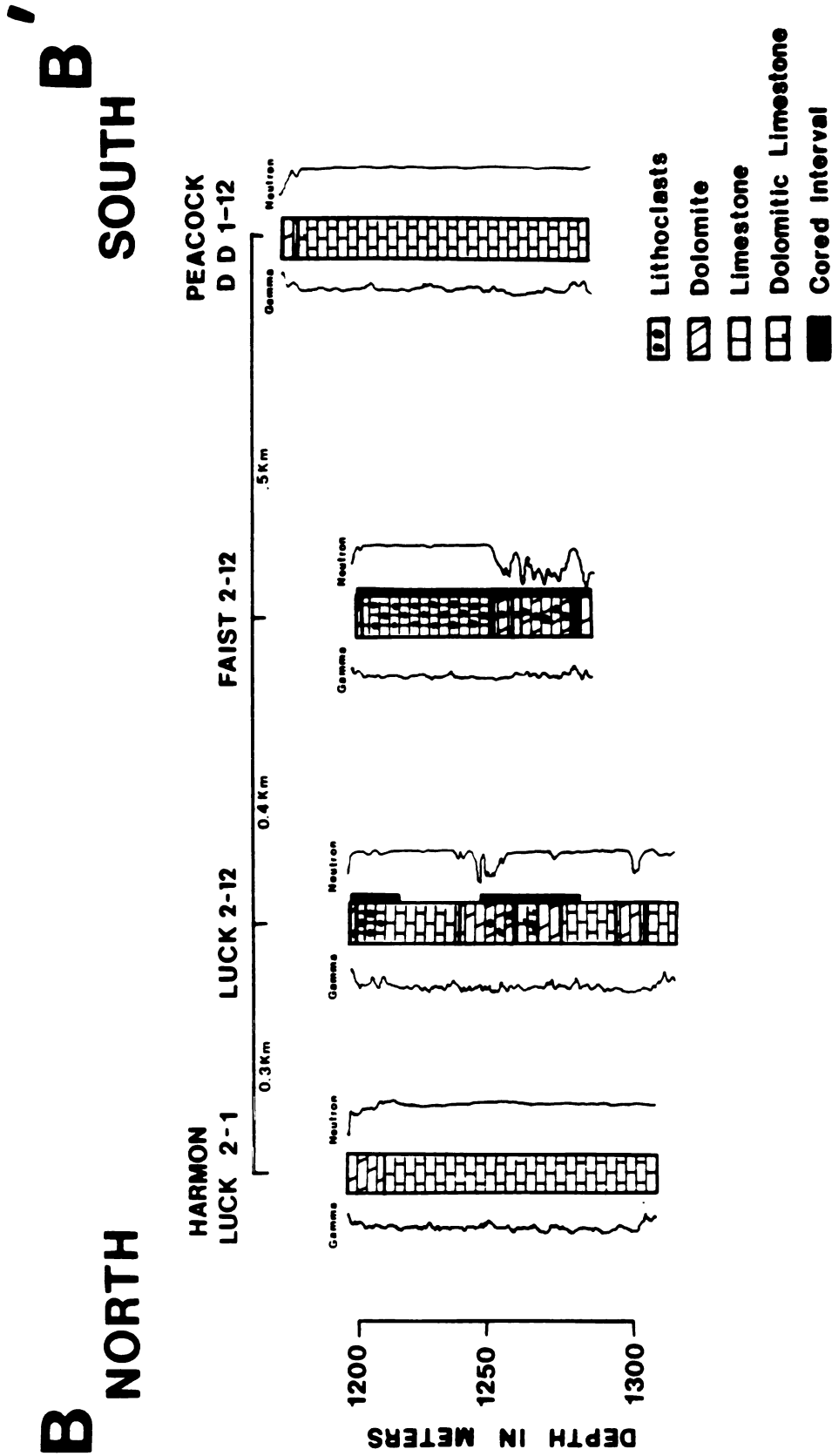


Figure 10

TABLE 3. VARIATION OF CRYSTAL SIZES (MICRONS) IN TRENTON LIMESTONE CLASTS

	MUD (1-4 μ M)	MICROSPAR (4-50 μ M)	SPAR		ALLOCHEMS	
			Short	Long*	Short	Long
RANGE IN SIZE	1 - 4	4 - 17	1 - 40	6 - 50	6 - 810	12 - 2010
MEAN SIZE	2	7	13	30	145	537
STANDARD DEVIATION	1	3	22	32	160	554
NUMBER OF SAMPLES	122	150	30	30	98	98

*Micrite and Microspar are considered to be spherical in shape. Spar and Allochems are not and therefore they will have a maximum and minimum for both their short and long dimension.

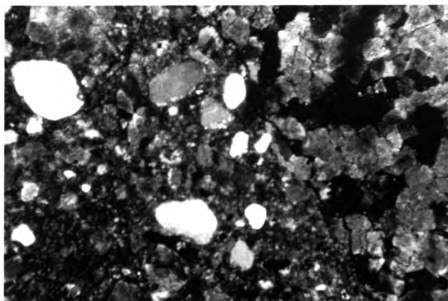


Figure 11. Rounded quartz grains in the matrix between dolomitized clasts in the Trenton. Width of field = 3.8 mm



Figure 12. Blocky low magnesium calcite cement filling fossil molds in the Trenton limestone. Width of field = 0.6mm.

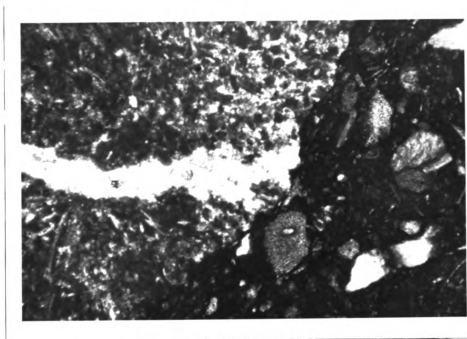


Figure 13. Cemented fracture in a limestone clast that is broken off at the edge of the clast. Width of field = 3.8mm.

compositions of the whole rock limestone range from 1.01 to - 0.03 ‰ and average 0.15 ‰ PDB (Table 4). The oxygen isotopic signature of these limestones is approximately one per mil lighter than the isotopic composition of Ordovician sea water as estimated by Taylor and Sibley (1986).

The minor and trace element compositions of the limestones are presented in table 5. The strontium concentrations of the limestones range from 562 to 235 ppm and average 405 ppm. The manganese concentrations of the limestones range from 772 to 189 ppm and average 404 ppm. The iron concentrations of the limestones range from 3606 to 1219 ppm and average 2146 ppm. And finally, the zinc concentrations of the limestones range from 10 to 3 ppm and average 6 ppm.

The amount of dolomite in the cores decreases gradually from west to east and abruptly to the north and south (Figures 9 and 10). The dolomite is planar to nonplanar, uniform to nonuniform (Sibley and Gregg, 1987) with rhombs ranging from 25 to 1050 micrometers. The dolomite crystals exhibit both undulose and nonundulose extinction. Inclusions in the dolomites are so abundant that the dolomites appear light brown in plane light. The original composition of the dolomitized limestones is difficult to determine because most of the fossils in the dolomites are either ghosts (particularly crinoids) or molds. However, the dolomitization crosscuts lithologies, and therefore sections with undolomitized limestone clasts probably represent the precursors to the dolomitized clasts. In the horizons that have not been dolomitized, clasts range in composition from mudstones to packstones (Figure 14). In order to decipher the original texture of the dolomites, diffuse plane light and fluorescence microscopy

TABLE 4. OXYGEN AND CARBON ISOTOPE ANALYSES OF THE TRENTON LIMESTONES

Sample	Lithology	$\delta^{18}\text{O}_{\text{PDB}}$ (‰)	$\delta^{13}\text{C}_{\text{PDB}}$ (‰)
T Luck 2-12			
C1B2	Limestone	-5.17	-0.43
C2B2	-	-6.47	-0.31
C2B11	-	-6.60	-0.09
C3B9	-	-6.42	0.41
	-	-6.75	0.32
T Honkerd			
C1B15	-	-7.43	0.84
T Faist			
4939	-	-7.66	1.01
142-14	-	-5.06	-0.03
4945	-	-5.99	-0.33
		Mean = -6.39	0.15
		S.D. = 0.89	0.52

TABLE 5. MINOR AND TRACE ELEMENT CONCENTRATIONS (PPM) OF THE TRENTON FORMATION LIMESTONES.

Sample		Strontium	Manganese	Iron	Zinc
T Luck 2-12					
C1B2		255	772	2831	3
C1B9	a	326	379	1219	9
	b	559	386	1440	4
C2B9	a	552	470	1767	12
	b	302	456	2006	3
C2B11		408	356	1950	10
C3B2		418	238	1312	9
C3B13		485	406	2439	4
T Foist 1-12					
C1B2		489	658	3606	7
C1B3		525	489	2304	4
C1B7		375	380	2363	4
C1B12		235	282	2381	7
C1B15		312	263	1456	5
C1B16		377	387	2771	3
C1B18		300	189	2387	4
<u>C1B20</u>		<u>562</u>	<u>358</u>	<u>2111</u>	<u>10</u>
Mean =		405	404	2146	6
S.D. =		111	148	632	3

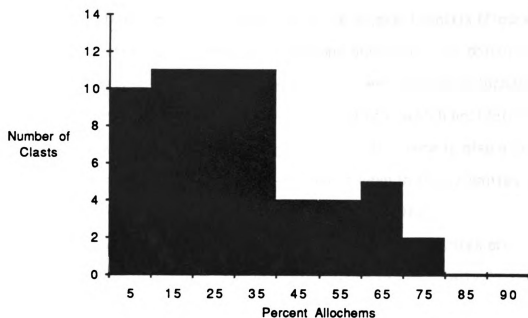
Trenton Limestone

Figure 14. Composition of the Trenton Formation limestone clasts. The percent of allochems in the limestone versus the number of clasts counted with this percentage of allochems. The limestones range in composition from mudstones to packstones.

were used to enhance fossil fragments (Figure 15 a and b). Areas that were originally allochems often appear as grey inclusions in diffuse plane light. In the dolomitized conglomerates, the dolomite which replaced the matrix between clasts is finer than the dolomite which replaced the clasts (Figure 16 and table 6). Within the dolomitized clasts, the fossils are replaced by rhombohedra that are larger than those in the adjacent matrix (Figure 17). In areas of partial dolomitization in the conglomeratic zone, dolomite preferentially replaced the matrix within the clasts and not allochems. There is a small amount of ferroan dolomite cement which postdates the initial and major dolomitization event (Figure 18). There is also a minor amount of late sulphide mineralization that is seen in the dolomites. Minor stylolitization is observed between some dolomite clasts.

The stable isotopic compositions of the Trenton dolomites are presented in tables 7 and 8. The oxygen isotopes of the totally dolomitized cores range from -6.49 to -10.42 ‰ and average -7.84 ‰ PDB (Table 7). The oxygen isotopes of the dolomites in the partially dolomitized cores range from -6.07 to -7.63 ‰ and average -6.57 ‰ PDB (Table 8).

The carbon isotopes of the totally dolomitized cores ranges from 0.58 to -0.67 ‰ and average -0.02 ‰ PDB. The carbon isotopes of the dolomites in the partially dolomitized cores range from 1.01 to -0.43 ‰ and average 0.15 ‰ PDB. These values are similar to limestone values for the Ordovician (Veizer and Hoefs, 1976).

The dolomites are only slightly calcium rich with a mean value of 51 mole percent calcium (XRD). The trace element concentrations of the dolomites are presented in tables 9 and 10. The strontium concentration of the dolomites ranges from 319 ppm to 96 ppm and averages 182 ppm.

Figure 15a. Trenton dolomite observed in plane light. Replaced allochems appear as faint ghosts.

Figure 15b. Trenton dolomite as viewed in blue-violet light. Note the ease with which allochems are observed.

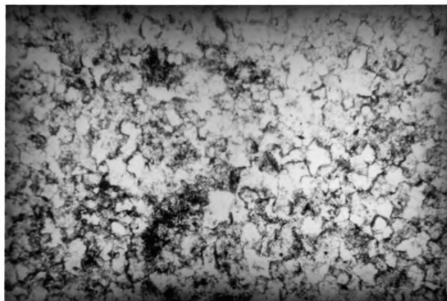


Figure 15a

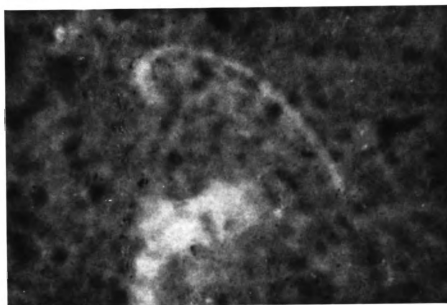


Figure 15b

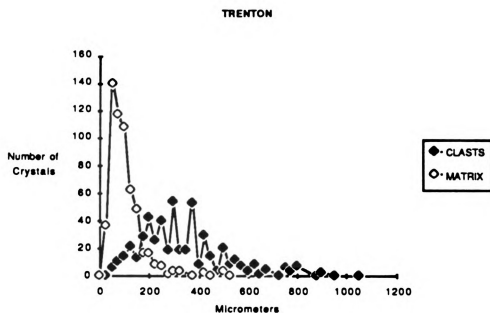


Figure 16. Comparison of the crystal sizes between the dolomitized clasts and the dolomitized matrix between the clasts in the Trenton Formation.

TABLE 6. DOLOMITE CRYSTAL SIZE DISTRIBUTION IN CLASTS FROM THE TRENTON FORMATION.

SIZE (MICRONS)	LUCK 1-12 C1 B1	LUCK 1-12 C1 B8	LUCK 1-12 C3 B2	LUCK 1-12 C3 B5	LUCK 1-12 C3 B12	TOTAL
1-25	1	0	0	0	0	1
26-50	1	1	2	0	2	6
51-75	1	2	3	1	4	11
76-100	2	4	4	2	3	15
101-125	6	3	5	2	6	22
126-150	3	2	3	2	3	13
151-175	4	8	6	6	5	29
176-200	20	4	7	7	4	42
201-225	9	5	4	2	6	26
226-250	7	3	9	9	12	40
251-275	7	2	3	5	2	19
276-300	20	7	5	8	14	54
301-325	3	8	0	4	4	19
326-350	3	11	0	4	1	19
351-375	14	13	7	10	9	53
376-400	3	0	1	3	2	9
401-425	8	3	3	9	7	30
426-450	7	0	2	5	0	14
451-475	1	2	0	0	1	4
476-500	10	1	1	3	5	20
501-525	3	0	0	3	3	9
526-550	4	1	1	4	2	12
551-575	3	2	0	2	0	7
576-600	2	0	0	2	0	4
601-625	2	3	1	1	2	9
626-650	1	0	0	1	0	2
651-675	2	1	1	1	0	5
676-700	0	0	0	0	0	0
701-725	1	0	0	0	0	1
726-750	2	1	0	1	2	6
751-775	0	1	1	1	1	4
776-800	4	2	1	1		8
801-825	0	0	0	0		0
826-850	0	0	0	0		0
851-875	0	1	0	0		1
876-900	2		0	1		3
901-925	0		0			0
926-950	1		0			1
951-975			0			0
976-1000			0			0
1001-1025			0			0
1026-1050			1			1
Total						519

TABLE 6 cont'd. DOLOMITE CRYSTAL SIZE DISTRIBUTION IN THE MATRIX FROM THE TRENTON FORMATION.

SIZE (MICRONS)	LUCK 1-12 C1 B1	LUCK 1-12 C1 B8	LUCK 1-12 C3 B2	LUCK 1-12 C3 B5	LUCK 1-12 C3B12	TOTAL
1-25	12	3	7	11	4	37
26-50	34	20	36	28	22	140
51-75	36	25	19	14	24	118
76-100	33	23	18	11	23	108
101-125	23	16	5	9	10	63
126-150	25	3	2	7	12	49
151-175	3	0	4	5	5	17
176-200	10	0	1	2	4	17
201-225	7	1	0	0	1	9
226-250	3	0	3	0	1	7
251-275	2	0	0	0	0	2
276-300	0	1	2	1	0	4
301-325	1	1	1	1	1	4
326-350	0		0	0	0	0
351-375	1		0	0	0	1
376-400	0		0	0	0	0
401-425	2		1	0	0	3
426-450	0			0	1	1
451-475	0			0	0	0
476-500	2			1	1	4
501-525	1					1
Total						585

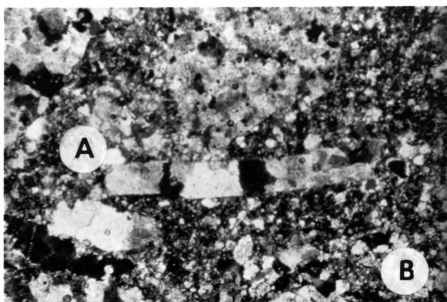


Figure 17. Large dolomite crystals replacing the allochems (A) and smaller dolomite crystals replacing the adjacent matrix (B). Width of field = 3.8mm.

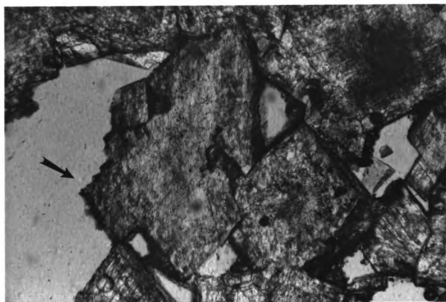


Figure 18. Late iron-rich dolomite cement in the Trenton Formation dolomites. Width of field = 3.8mm.

TABLE 7. OXYGEN AND CARBON ISOTOPE ANALYSES OF THE TRENTON DOLOMITES.

Sample	Lithology	$\delta^{18}\text{O}_{\text{PDB}}$ (‰)	$\delta^{13}\text{C}_{\text{PDB}}$ (‰)
T Luck 1-12			
C1B1	100 % Dolomite	-7.71	-0.08
C1B5	"	-8.11	0.28
C1B8	"	-7.21	-0.67
	"	-6.49	0.50
	"	-7.30	-0.09
C2B1	"	-7.68	-0.27
	"	-7.22	-0.09
C3B2	"	-7.50	0.24
	"	-7.71	0.05
C3B12	"	-8.35	0.14
T Luck 2-12			
C2B3	"	-6.88	0.25
C2B6	"	-8.11	-0.26
	"	-8.57	-0.53
C2B6	"	-7.63	0.04
C2B7	"	-7.29	0.03
C2B7	"	-7.32	0.12
T Faist			
4896	"	-8.05	-0.28
4898	"	-8.35	-0.23
4899	"	-8.91	-0.08
<u>4900</u>	"	<u>-10.42</u>	<u>0.58</u>
Mean =		-7.84	-0.02
S.D. =		0.85	0.31

TABLE 8. OXYGEN AND CARBON ISOTOPE ANALYSES OF DOLOMITES FROM THE PARTIALLY DOLOMITIZED CORES, TRENTON FORMATION.

Sample	Lithology	$\delta^{18}\text{O}_{\text{PDB}}$ (‰)	$\delta^{13}\text{C}_{\text{PDB}}$ (‰)
T Harkerd 1-17			
C1B2	Partial Dolomite	-6.95	-0.01
C1B3	"	-7.63	-0.12
C1B6	"	-6.20	-0.14
T Harmon Luck 1-1			
4930	"	-6.07	0.09
4941	"	-6.21	0.51
4950	"	-6.36	0.37
		Mean = -6.57	0.12
		S.D. = 0.60	0.26

TABLE 9. STRONTIUM CONCENTRATION (PPM) OF THE TRENTON FORMATION DOLOMITES.

Sample			Lithology	Nonporous Clasts	Nonporous Portions of Porous Clasts
T Luck 1-12					
C1B1	a		Dolomite	130	
	b		"	134	129
	c		"	155	
C1B5	a		"	157	
	b		"	127	122
C2B1			"		159
C3B5	a		"	155	
	b		"	140	139
	c		"	150	123
C3B12			"	162	188
C3B16	a		"		181
	b		"		141
C3B17	a		"	202	139
	b		"	161	
C3B21			"	129	
C5B2			"	144	
T Luck 2-12					
C2B3	a		"	203	
	b		"	102	
C2B6	a		"	135	125
	a		"	96	
C2B7	a		"	<u>149</u>	<u>125</u>
Mean =				146	143
S.D. =				27	23

Table 9 (cont'd.)

Sample	Lithology	Strontium
T Harkerd 1-17		
4829	Dolomite	174
4832	-	235
4833	-	251
4834	-	203
4837	-	277
4839	-	319
4841	-	275
4845	-	311
4849	-	196
4854	-	232
4855	-	205
4857	-	263
4863	-	202
4865	-	273
4867	-	303
<u>4871</u>	-	<u>256</u>
Mean =		248
S.D. =		44

TABLE 10. MANGANESE, IRON AND ZINC CONCENTRATIONS (PPM) OF THE TRENTON FORMATION DOLOMITES.

Sample			Lithology	Manganese	Iron	Zinc
T Luck 1-12						
C1B1	a		Dolomite	2079	28200	3
	b		"	2001	25057	2
	c		"	1622	29329	5
C1B5	a		"	1777	21015	5
	b		"	1791	21733	2
C3B5	a		"	1714	17778	2
	b		"	1708	18913	1
	c		"	1685	19090	2
C3B12			"	1819	18188	3
C3B17	a		"	1518	19262	3
	b		"	1589	18329	4
C3B21			"	1557	27143	2
C5B2			"	1768	36486	9
T Luck 2-12						
C2B3	a		"	1736	19634	4
	b		"	1850	18329	5
	c		"	1385	15676	6
	d		"	1489	16221	5
C2B6	a		"	1298	25891	2
	b		"	1425	23056	2
	c		"	2078	34918	10
	d		"	1636	18879	5
C2B7	a		"	1268	22112	2
	b		"	1213	24563	2
	c		"	1626	22677	5
	d		"	<u>1287</u>	<u>27236</u>	<u>6</u>
Mean =				1637	22789	4
S.D. =				241	5456	3

Table 10 (Cont'd)

T Harkerd 1-17

4829	-	1386	14460	4
4832	-	1456	14779	1
4833	-	952	8789	3
4834	-	1710	17297	3
4837	-	1012	9903	5
4839	-	1144	10750	2
4841	-	1019	8938	7
4845	-	961	9551	4
4849	-	986	9230	5
4854	-	683	5733	5
4855	-	1114	11515	3
4857	-	1980	18450	1
4863	-	664	6000	1
4865	-	1691	15445	3
4867	-	997	8273	5
<u>4871</u>	-	<u>572</u>	<u>4978</u>	<u>3</u>
Mean =		1145	10543	3
S.D. =		399	4714	2

Strontium concentrations in these dolomites are similar to the concentrations in other Ordovician dolomites (Weber, 1964) but higher than many other ancient dolomites (Table 11). The strontium concentration in the dolomites is roughly half of the strontium concentration in the limestones (Table 5). The manganese concentration of these dolomites ranges from 2079 ppm to 572 ppm and averages 1445 ppm. These concentrations are higher than other Ordovician dolomites (Weber, 1964) and other ancient dolomites (Table 11) but are similar to the concentrations of other Trenton dolomites (Taylor and Sibley, 1986). The iron concentration of these dolomites ranges from 36,486 ppm to 4978 ppm and averages 18,140 ppm. These concentrations are higher than the iron concentrations of other Ordovician dolomites (Weber, 1964) but is similar to other Trenton dolomites (Taylor and Sibley, 1986). The zinc concentrations of these dolomites ranges from 10 ppm to 1 ppm and averages 4 ppm. These concentrations are lower than other Ordovician dolomites (Weber, 1964).

The whole core porosity of the Trenton Formation carbonates is presented in Appendix II. The average porosity of the limestones is 1.3 percent, the average porosity of the partial dolomites is 1.9 percent, and the average porosity of the dolomites is 3.1 percent. Whole core porosities of the clast rich horizons are 0.8 percent ($n = 32$) for the limestones and 3.5 percent ($n = 92$) for the dolomites. The porosity difference between individual limestones clasts is low compared to the porosity difference between individual dolomite clasts (Figure 19). The porosity in the limestones occurs generally as fossil moldic (50 percent of the total porosity). The dolomite porosity values determined by point counting were found by subtracting the late ferroan dolomite and anhydrite cements, both

TABLE 11. STABLE ISOTOPIC (PDB) AND TRACE ELEMENT COMPOSITIONS (PPM) OF SOME ANCIENT DOLOMITES

Location	Sr	Mn	Fe	$\delta^{13}\text{C} \text{ ‰}$	$\delta^{18}\text{O} \text{ ‰}$	Proposed Origin
Ordovician, Tennessee (Churnet and Miers, 1981)	24	247				Fresh & Mixed
Ordovician-Silurian, Nevada (Dunham & Olsen, 1980)	49		476	+2.4	+2.0	Mixed
Mississippian, Illinois (Choquette & Steinen, 1980)	166			+2.4	+2.0	Mixed
Ordovician, Wisconsin (Beddozement, 1973)	37			-1.0	-4.5	Mixed
Ordovician, N.W.T., Canada (Lend et al, 1975)	81	46		+0.4	-3.3	Mixed
Silurian, Michigan (Sears & Lucia, 1980)	114			+3.6	-7.4	Refluxing Brines
Devonian, Alberta, Canada (Mattes & Mountjoy, 1980)	57	59	343	+3.0	-5.0	Burial
Bowlend Basin, England (Gawthorpe, 1987)	60			+0.5	-6.3	Burial

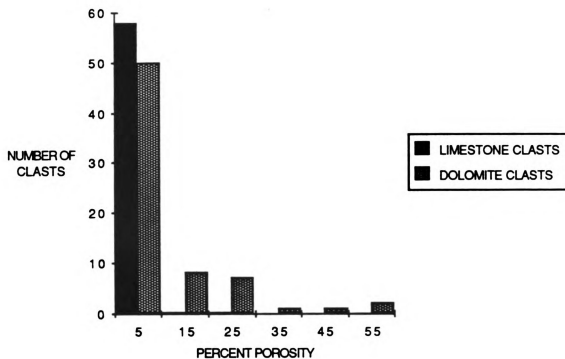


**Figure 19. Comparison of porosity between limestone and dolomite clasts..
Note the large range in porosity between the individual dolomite clasts.**

of which are very rare volumetrically comprising less than one percent of the total volume. The porosity in the dolomites generally occurs as intercrystalline (89 percent), but can locally be attributed directly to fossil molds (11 percent) (Figure 20). Dolomite clasts of differing porosity are in close proximity and are often in contact with each other (Figure 21). Horizons with dolomitized clasts generally have higher porosities (based on compensated neutron logs, Figures 9 and 10) than dolomitized horizons without dolomitized clasts, and higher than the limestone sections.

Relationship of the Trenton Dolomites to Fractures

Taylor and Sibley (1986) characterized the Trenton Formation dolomites of the Michigan Basin into three distinct types based on major and minor element chemistry, oxygen isotope ratios, and rock texture. These dolomite types are; 1) cap dolomite, 2) regional dolomite, and 3) fracture related dolomite.

The dolomites in this study are the fracture related type. Looking at the areal distribution of the dolomite, the dolomite abundance in the area decreases from west to east and from north and south. Two fracture identification logs were run in the study area and indicate that the Trenton Formation is locally highly fractured. The trends of the fractures are N 27° W and N 21° E (Figure 22). The northwest-southeast fracture trend is similar to the regional fracture trends of the Albion-Scipio and the Northville oil fields (Ells, 1962; Shaw, 1975 and Mesher, 1980).

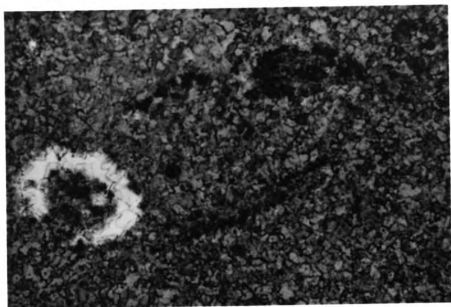


Figure 20. Fossil moldic porosity in the Trenton dolomites. Width of field 3.8mm.

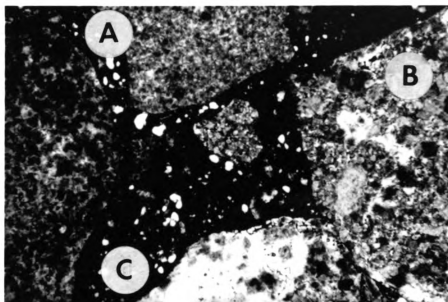


Figure 21. Dolomite clasts with varying porosity in close proximity. The view presented is in plane light so the porosity appears white. A low porosity clast (A), a moderate porosity clast (B) and a high porosity clast (C) are in close proximity.

Figure 22. Rose diagram depicting the fracture pattern in the Trenton as derived from two fracture identification logs run in the study area. The trends of the fracture set are N 27° W and N 21° E.

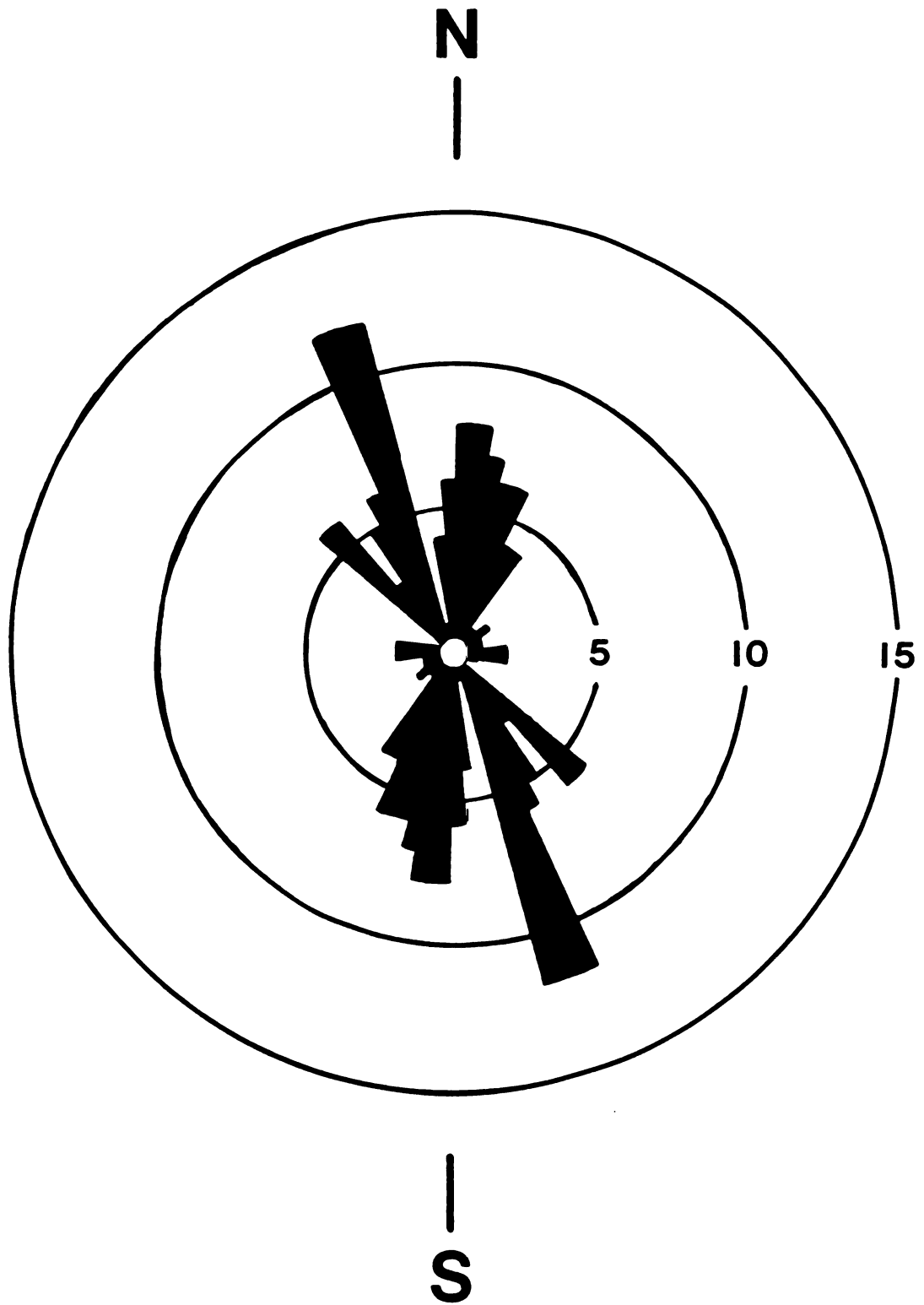


Figure 22

The anomalous thickening in the Trenton as seen from the isopach map is similar to the pattern in the Northville Trend. This thickening is suggested to be due to fault related differential subsidence in the area (Mesher, 1980). Donald Ferguson (personal communication; Total Petroleum Company) indicated that the Trenton was highly fractured locally, and that there was probably some type of horst and graben structure in the area. These assessments were based on proprietary geophysical information.

The oxygen isotopes of these dolomites average -7.64‰ PDB. The oxygen isotopes of these dolomites were compared to dolomites in the area that were studied by Taylor (Table 12). The isotopic ratios in this study are not significantly different from the Albion-Scipio or the Northville fracture related dolomites. Both of these areas are considered to be high temperature, fracture-related dolomites (Taylor and Sibley, 1986). The oxygen isotopic values in this study are also, however, not significantly different from the cap dolomites studied by Taylor (1982), which are considered to be lower temperature dolomites. This may be explained by either of the following; 1) that the dolomites in this study formed from a solution that had a relatively low temperature, 2) or that there was a lower water/rock ratio in these dolomites which affected the $^{18}\text{O}/^{16}\text{O}$ equilibrium ratios of these dolomites. With a lower water/rock ratio, a greater percentage of the dolomites' isotopic signature would be inherited from the precursor limestone, which is heavier than the associated dolomites (Table 4).

Manganese concentrations in these dolomites are consistent with the values of the Trenton fracture related dolomites, and are significantly lower than the cap dolomites (Table 13).

Iron concentrations in these dolomites are significantly higher than

TABLE 12. COMPARISON OF OXYGEN ISOTOPIC SIGNATURES BETWEEN DOLOMITE TYPES

	This Study	Fracture Related		Cap
		(Albion-Scipio)	(Northville)	
1	-7.7	-8.6	-7.9	-6.7
2	-8.1	-7.4	-7.3	-7.7
3	-7.2	-8.4	-8.1	-7.6
4	-6.5	-7.8	-8.5	-8.4
5	-7.3	-9.4	-8.0	-8.0
6	-7.7	-8.2	-7.4	-7.2
7	-7.2	-6.5	-8.6	-7.6
8	-7.5	-9.1	-9.0	-7.6
9	-7.7	-9.1	-9.0	-7.8
10	-8.4	-6.9	-9.0	-7.8
11	-6.9	-9.1	-9.2	-7.0
12	-8.1	-9.7		
13	-8.6	-8.2		
14	-7.6	-8.8		
15	-7.3	-9.1		
16	-7.3	-8.2		
17	-8.1	-8.1		
18	-8.4			
19	-8.9			
20	-10.4			
<hr/>				
Mean =	-7.8	-8.4	-8.4	-7.6
S.D. =	0.8	0.9	0.7	0.5

TABLE 13. COMPARISON OF MANGANESE CONCENTRATIONS (PPM) BETWEEN TRENTON DOLOMITE TYPES.

	Average	Standard Deviation	Number of Samples
This Study	1384	414	44
Fracture Dolomites [†]	1477	520	33
Cap Dolomites [†]	3786	1323	40

[†]Taylor and Sibley, 1986

the values of the Trenton fracture related dolomites (although the ranges in values overlap), and are significantly lower than the cap dolomites (Table 14).

Textural characteristics of these dolomites are similar to those described by Taylor (1982) for the fracture related dolomites, and to those described by Mattes and Mountjoy (1980) for epigenetic dolomites. These dolomites are generally coarse grained and nonplanar. Fossils are generally not well preserved, and minor saddle dolomite is present. The dolomites in the western portion of the study area have a higher percentage of dolomite crystals with nonplanar boundaries (Table 15). The higher percentage of nonplanar boundaries may indicate precipitation at an elevated temperature (Gregg and Sibley, 1984).

Discussion of Substrate Surface Area Affects

In the Trenton Formation, one can constrain a number of factors influencing the porosity of the dolomites, and subsequently show the effect that the substrate surface area had on the resultant porosities. The following parameters are constrained: 1) the porosity variation observed is not an inherited property of the parent limestone, 2) the porosity variation is not a function of variance in solution chemistry or temperature, and 3) that parent mineralogy has no verifiable control on the resultant dolomite porosities.

First, the porosity difference observed between clasts in the dolomites of the Trenton Formation was not inherited from the parent limestone. High and low porosity clasts in the dolomite are often in direct

TABLE 14. COMPARISON OF IRON CONCENTRATIONS (PPM) BETWEEN TRENTON DOLOMITE TYPES.

	Average	Standard Deviation	Number of Samples
This Study	18,142	7,666	41
Fracture Dolomites ⁺	6,976	6,634	28
Cap Dolomites ⁺	109,500	44,436	96

⁺Taylor and Sibley, 1986

TABLE 15. POINT COUNTING RESULTS FOR DOLOMITE TEXTURAL COMPARISON

SAMPLE	PLANAR		NONPLANAR		TOTAL
	UN	NON	UN	NON	
(WEST)					
T LUCK 1-12 C3 B21	(2)	13 (11)	(30)	87 (57)	200
T LUCK 1-12 C1 B8	(0)	17 (17)	(5)	83 (78)	201
T LUCK 1-12 C3 B2	(0)	14 (14)	(0)	86 (86)	180
	Mean =	15	Mean =	85	TOTAL 581
(EAST)					
T HANKERD 1-17 C1 B8	(0)	35 (35)	(4)	65 (61)	187
T HANKERD 1-17 C1 B2	(0)	27 (27)	(11)	73 (62)	96
T HANKERD 1-17 C1 B7	(0)	31 (31)	(0)	69 (69)	201
T HANKERD 1-17 C1 B15	(0)	31 (31)	(1)	69 (68)	209
T HANKERD 1-17 C1 B3	(0)	28 (28)	(1)	72 (71)	206
T HANKERD 1-17 C1 B14	(0)	26 (26)	(1)	74 (73)	215
T HANKERD 1-17 C1 B12	(0)	25 (25)	(4)	75 (71)	71
T HANKERD 1-17 C1 B3	(0)	29 (29)	(2)	71 (69)	231
	Mean =	29	Mean =	71	TOTAL 1416

UN = Percent of crystals with an undulose extinction

NON = Percent of crystals with a nonundulose extinction

contact with each other. Due to the immediate proximity of the clasts it is therefore reasonable to assume that the clasts were subjected to the same amount of bicarbonate flux. The existence of dolomite clasts with approximately 60% porosity precludes the possibility that the observed porosity in the dolomites was due to porosity in the original limestones. The low average porosity of the dolomite (3 % - APPENDIX II) indicates that there has been at least 10% dolomite cement precipitated, according to the volume shrinkage theory. If one assumes an average porosity of 10% for the parent limestone, approximately 20% dolomite cement must have been precipitated in order to produce the current average dolomite porosity of 3%. Due to the large amount of dolomite cement in these clasts, the porosity of the precursor limestone clasts would have to have been unrealistically high. It is not likely that a clast of 80% porosity for example, could have been transported and redeposited intact.

It is not likely that the limestone clasts had a wide difference in porosity prior to dolomitization. The limestone clasts experienced a porosity loss due to calcite cementation prior to dolomitization. In the partial dolomites, dolomite crystals are observed replacing calcite cement (Figure 23). This episode of cementation is also evidenced by the cemented fractures in the limestone clasts. The fractures in the clasts end abruptly at the clasts' edge and do not extend into the matrix (Figure 13). It is not likely that these fractures would have survived transport if they had not been previously cemented. If the limestones had an initially high porosity, one would expect that in the partial dolomites there should be some dolomite cement precipitated in the voids. This is not observed in the partial dolomites. Also there is a minor amount of late evaporite cement in the dolomites. If there was abundant porosity in the limestones, one would

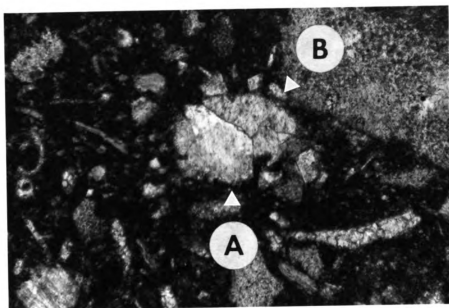


Figure 23. Nonplanar dolomite crystal (A) replacing calcite cement (B) in the Trenton. Width of Field = 1.5mm.

also expect to see evaporite cement in these voids. No evaporite cement is observed in the limestones. The differences in porosity between individual dolomite clasts was therefore not inherited from the limestone clasts, and must then be the result of the dolomitization process.

Second, the close proximity of porous and nonporous dolomite clasts (often in direct contact with each other) indicates that differences in temperature and/or solution chemistry are not responsible for the observed porosity differences. The porosity differences between clasts then, could be the result of differences in substrate texture and/or mineralogy.

It is unlikely that the substrate had a significantly different mineralogy. Rao et al (1987) have shown that dolomite replacing low magnesium calcite and aragonite result in dolomites with significantly different strontium contents. The dolomite that replaced low magnesium calcite averages 210 ppm strontium and the dolomite that replaced aragonite averages 660 ppm strontium. The similarity in the strontium concentration observed between nonporous clasts and the nonporous portions of porous clasts in these dolomites (Table 9) suggests that the parent mineralogy of the clasts was similar. A difference in substrate mineralogy is also not likely with the evidence of calcite cementation prior to dolomitization. The metastable phases of aragonite and high magnesium calcite are generally the first phases affected by diagenesis. It is likely that if these metastable phases were in the sediment prior to the calcite cementation, they would have been converted to more stable low magnesium calcite.

There are several observations that are consistent with the hypothesis that an original difference in substrate texture caused the differences in porosity observed. Differences in the substrate texture between clasts

(Figure 14), and crystal sizes between constituents (Table 3), have been demonstrated. Rhombohedra size variation within and between the dolomite clasts suggests that the texture of the substrate did have an effect on dolomite nucleation density and therefore its resultant texture. For example, where discernable, the dolomite rhombohedra that replaced fossils are larger (due to low nucleation density) than the rhombs that replaced the adjacent matrix (due to high nucleation density) (Figure 17). Also, the highly porous clasts in the dolomite have large dolomite crystal sizes and the low porosity clasts have relatively smaller dolomite crystals. This demonstrates the direct relationship that substrate texture had on the resultant dolomite texture/porosity. Dolomitized clasts also directly show some fossil moldic porosity. This also demonstrates the direct relationship that differences in substrate texture had on the resultant dolomite porosity.

These observations are consistent with the hypothesis of substrate influence on texture and therefore porosity. According to this hypothesis, the variability of the constituents in the clasts resulted in the porosity differences observed between dolomite clasts. Specifically, the porosities in the dolomites are directly related to the amount of coarsely crystalline allochems, cement and/or neospar in the original limestone. This is based on the assumption that the coarsely crystalline portions of the substrate would resist dolomitization. This is evidenced in the partial dolomites where finely crystalline mud is replaced by dolomite and the coarsely crystalline allochems are not. The coarsely crystalline portions of the substrate were therefore unreactive to the onset of dolomitization. The resistance to dolomitization by coarsely crystalline portions of the substrate is also evidenced in the totally dolomitized rocks by the

existence of fossil moldic porosity. These coarsely crystalline portions of the substrate resisted dolomitization and occupied space during much of the dolomite replacement and cementation. These coarsely crystalline portions of the substrate were then later dissolved out, leaving a high-porosity clast. The coarsely crystalline fossil and/or spar-rich limestone clasts (low surface area) provided fewer nucleation sites than the finely crystalline mud rich clasts (high surface area) for the dolomitization episode. This resulted in the clasts with the higher concentration of coarsely crystalline fragments becoming the dolomite clasts with the higher porosity. Dense nucleation and interference of dolomite rhombs occurred in substrates that had a high surface area (mudstones) resulting in the lower porosity clasts.

Discussion of Solution Chemistry Affects

The distribution of the dolomite in this section of the Trenton suggests that the solution flowed in a general easterly direction, because the dolomite decreases in abundance to the east (Figure 9). Trace elements and oxygen isotopes of the Trenton dolomites were examined in order to confirm the flow direction of the dolomitizing fluid.

Veizer (1983) and Parker et al (1985) suggested that changes in the gradients of trace elements may indicate the direction of fluid flow during diagenesis. Land, Salem and Morrow (1975), Land, (1980), Gregg (1988) and Machel (1988) suggest that trends in trace elements can be used to determine the fluid flow direction of dolomitizing solutions, if the system is not completely open. Trace elements can be used because during

dolomitization elements will fractionate between the dolomite and the aqueous phase. Elements with a distribution coefficient of less than one will fractionate to the aqueous phase. The actual amount of a phase that is incorporated into a crystal is a function of the distribution coefficient, and the total concentration of the species in solution (Veizer, 1983). In the case of a distribution coefficient less than one, as the solution evolves, the concentration of the species in solution will increase. The crystals forming in the downflow direction should therefore have a higher concentration of this species in the crystal lattice. This scheme assumes a constant distribution coefficient. Although changes in temperature, solution chemistry and many other factors may affect distribution coefficients, the magnitude of these effects on the distribution coefficients for dolomites are not known. In this study the distribution coefficients are assumed to be constant. Elements with a distribution coefficient greater than one will tend to be incorporated into growing crystals. The concentration of this species in solution will therefore decrease in the downflow direction. The dolomite crystals in the downflow direction will therefore have a lower concentration of this species.

The actual distribution coefficient of Sr^{2+} is still under debate (Land, 1980). It is agreed however, that it is less than one (Land, 1980, Veizer, 1983, Burns and Baker, 1987). The dolomite crystals in the downflow direction should therefore become enriched in Sr^{2+} . The Sr^{2+} concentrations of the dolomites in the Trenton Formation average 143 ppm (sd = 26, n = 29) for the Total Luck wells (west) and 245 ppm (sd = 43, n = 20) for the Total Hankerd well (east). A W-test was conducted on the Sr^{2+} concentrations from the Total Luck wells, and it was determined that these values were from a normally distributed population (Appendix III). A

standard T-test was then conducted on the two populations. The Sr^{2+} concentrations from the Total Luck wells and the Total Hanked wells are significantly different at the 98% confidence interval (Appendix III). This type of trend in the Sr^{2+} concentration is consistent with the stratigraphic distribution suggesting an easterly fluid flow.

Much less is known about the distribution coefficients of manganese, iron and zinc in dolomites. However, the distribution coefficients of all of these elements are considered to be greater than one (Land, 1980, Veizer, 1983). The Mn^{2+} concentrations in the dolomites of the Trenton Formation average 1637 ppm (sd = 241, n = 24) for the Total Luck wells (west) and 1145 ppm (sd = 399, n = 16) for the Total Hanked well (east). A W-test was conducted on the Mn^{2+} concentrations from the Total Luck wells, and it was determined that these values were from a normally distributed population (Appendix III). A standard T-test was then conducted on the two populations. The Mn^{2+} concentrations from the Total Luck wells and the Total Hanked wells are significantly different at the 95% confidence interval (Appendix III). This trend in Mn^{2+} concentration is also consistent with an easterly fluid flow.

The Fe^{2+} concentrations in the dolomites of the Trenton Formation average 22,789 ppm (sd = 5456, n = 25) for the Total Luck wells (west) and 10,543 ppm (sd = 4714, n = 16) for the Total Hanked well (east). A W-test was conducted on the Fe^{2+} concentrations from the Total Luck wells, and it was determined that these values were from a normally distributed population (Appendix III). A standard T-test was then conducted on the two populations. The Fe^{2+} concentrations from the Total Luck wells and the Total Hanked wells are significantly different at the 98% confidence interval (Appendix III). This trend in Fe^{2+} concentration is

also consistent with an easterly fluid flow.

The Zn^{2+} concentrations in the dolomites of the Trenton Formation average 4 ppm. The lack of any trend in Zn^{2+} concentration may be due to the low absolute concentration of zinc in the solution.

Oxygen isotopic composition of the dolomites could also be an indicator of fluid flow in these dolomites. If these dolomites were precipitated from a dolomitizing solution with an elevated temperature, then as the solution moved away from its source it should cool and produce a dolomite with a less depleted isotopic signature. Consequently, the trend that should be observed in the Trenton dolomites is an enrichment in the oxygen isotopic signature of the dolomites in an easterly direction. The oxygen isotopic composition of the Trenton dolomites from the Total Luck 2-12 well (west) to the Total Hankerd well (east) are presented in figure 24. There is a general increase in the oxygen isotopic signature from west to east. This data also supports an easterly direction for fluid flow. It is possible however, that this trend simply reflects the effects of a lower water/rock ratio. In this case, the oxygen isotopic composition of the substrate would have an increased role in determining the final isotopic composition of the dolomite.

There is also a change in dolomite texture which is consistent with fluid flow in an easterly direction. Gregg and Sibley (1984) determined that the temperature of the dolomitizing fluid had an effect on the texture of the dolomite. Specifically, a solution with a high temperature will result in a higher proportion of nonplanar dolomite. The change in texture observed is a statistically higher proportion of planar dolomite (CI 95%) in the eastern portion of the study area. This change in texture is consistent with fluid flow in an easterly direction, with the temperature of the

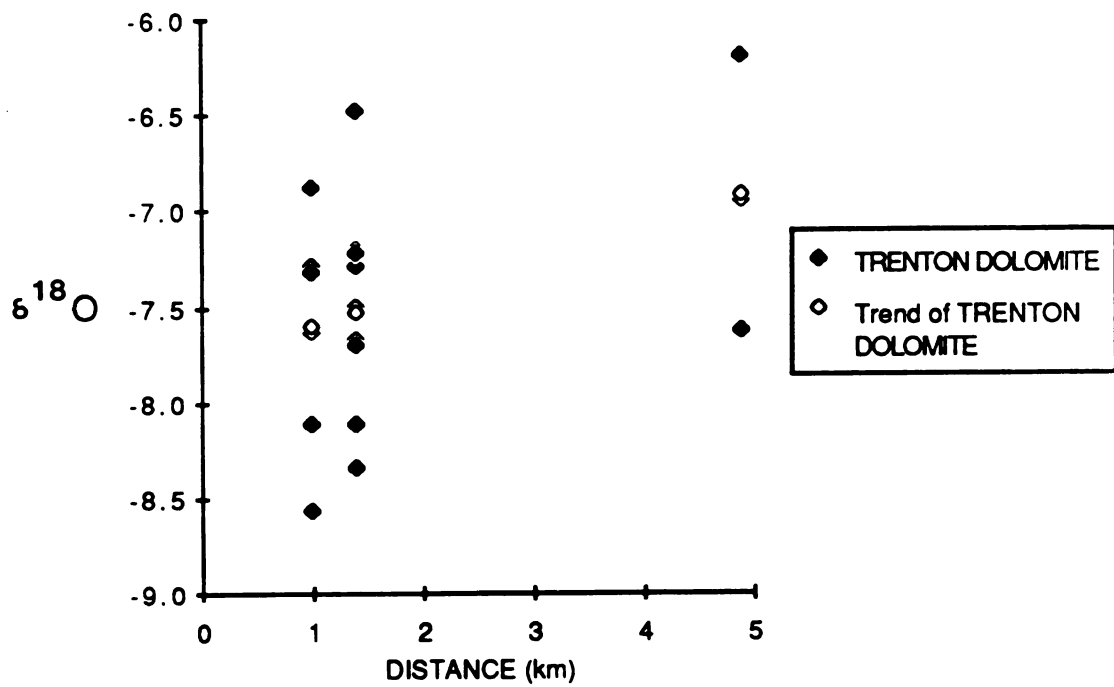


Figure 24. Oxygen isotopic signature of the dolomites versus distance from west to east for the Trenton dolomites. The trend is towards a heavier oxygen isotopic signature of the dolomites towards the east.

solution decreasing away from the source.

Evidence that the dolomitizing solution flowed in an easterly direction is: 1) the stratigraphic distribution of the dolomites, 2) the changes in the trace element compositions of the dolomites, 3) the trend in the oxygen isotopic composition and 4) the difference in the texture of the dolomites. Therefore the saturation state of the solution with respect to dolomite should decrease in this direction. Recall from above that solutions with a higher saturation state should result in a higher density of dolomite nuclei, resulting in a lower dolomite porosity.

One can look at the porosity of the dolomites across the field to determine if the change in saturation state that dolomitized these rocks caused a difference in porosity. Compensated neutron log porosities of the Total Hicks-Martin 1-11 well in the west and the Total Luck 2-12 well in the east were compared (APPENDIX IV). There is no statistical difference in the porosities between the two wells. A comparison of the whole core porosities between the conglomeritic portions of the Emil Faist 2-12 (west) and the Total Luck 1-12 (east) wells was also made (APPENDIX IV). There was also no significant difference in the porosities between these wells. This indicates that the change in fluid chemistry that these limestones experienced did not significantly influence the porosity of the resultant dolomite. This is not to say however, that greater changes in fluid chemistry could not have an influence on porosity.

**Pliocene Sero Domi Formation
Aruba, Netherlands Antilles**

Two outcrop locations of the Sero Domi Formation on the island of Aruba were examined. The two outcrops investigated in this study (Figure 25) are steeply dipping forereef deposits. The outcrop at Boe Doei will be examined first with regard to the effects of substrate surface area on dolomite porosity. The outcrop at Rooi Hundu will be examined later with regard to the bicarbonate flux model. The island of Aruba, Netherlands Antilles is located approximately 30 kilometers north of the peninsula of Paraguaná, Venezuela. The upper Sero Domi Formation exposed on the island of Aruba is composed of a series of forereef limestones and dolomites (DeBuissonje, 1974). The rocks are predominantly coralline algal grainstones and packstones (Sibley, 1980; 1982). The dolomites at both locations are conformably overlain by limestones.

The rocks at Boe Doei dip approximately 11° to the north. The limestones exposed are mainly wackestones. The major allochem in these samples is pelagic foraminifera (*Globogerina* sp.) which can comprise up to 44 percent of the rock volume. Minor amounts of coralline algae and echinoderms are also present. There is little or no evidence of compaction in these rocks. X-ray diffraction analysis indicates that the rock is low magnesium calcite. There is a euhedral blade-shaped calcite cement in the limestones which comprises up to 25 percent of the rock volume. The porosity of these rocks averages 17.1 percent (Figure 26 and Table 16). The permeabilities of these rocks vary widely from 1.5 to 9530 md (Table 16). Whole rock oxygen isotopic composition of the limestones ranges from -3.76 to -2.20 ‰ and averages -3.15 ‰ PDB. Whole rock carbon isotopic

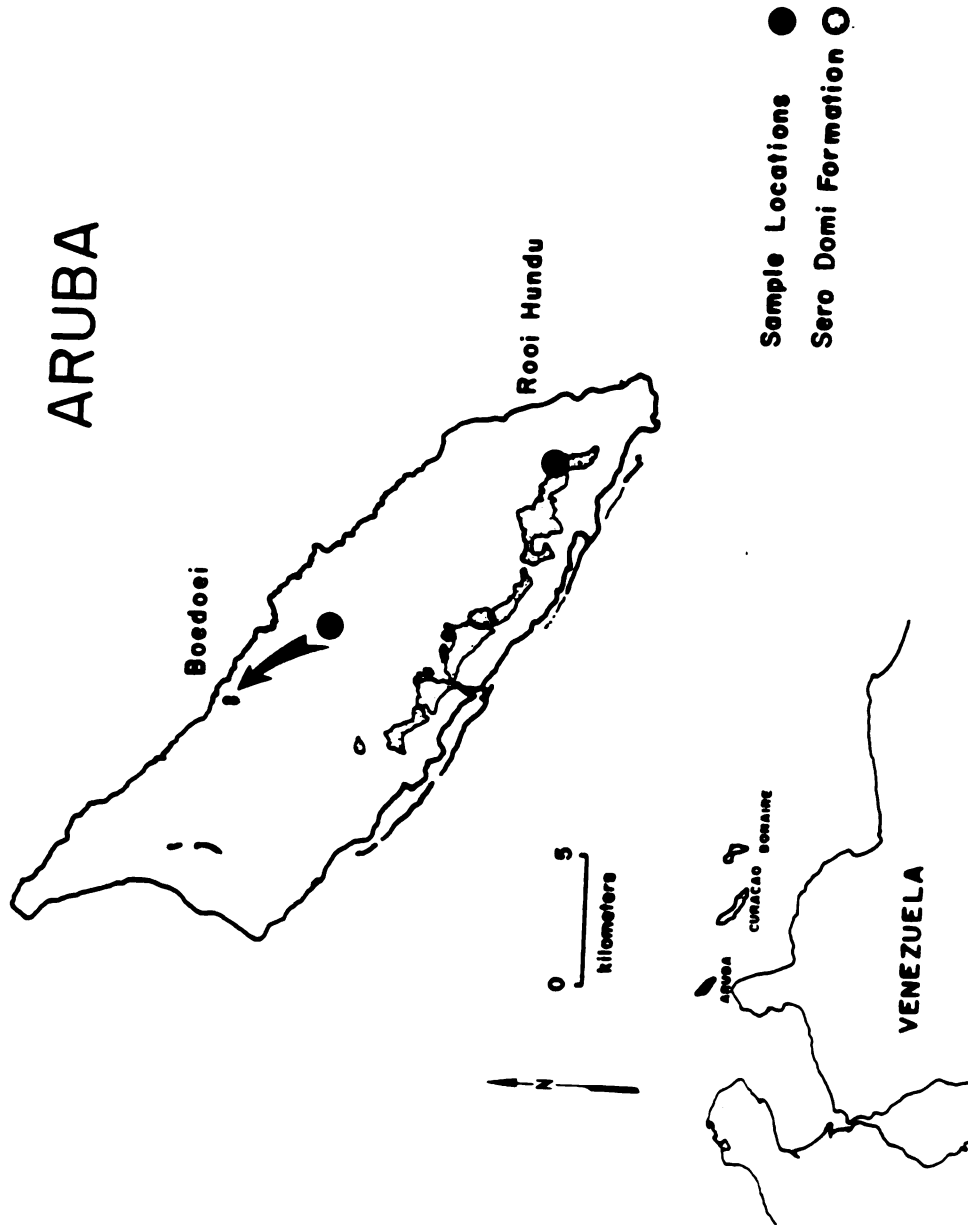


Figure 25. Location map for the Sero Domi Formation outcrops on Aruba, Netherlands Antilles.

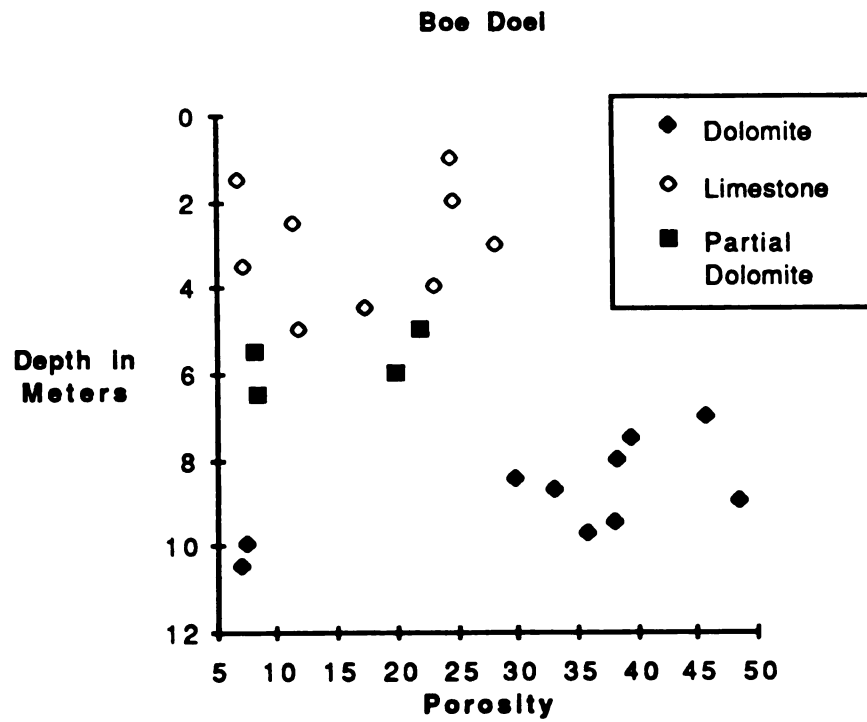


Figure 26. Percent porosity versus depth for the carbonates from Boe Doel (Aruba, N.A.).

TABLE 16. POROSITY AND PERMEABILITY OF THE BOE DOEI CARBONATES (ARUBA, NA)

SAMPLE	DEPTH IN METERS	LITHOLOGY	PERMEABILITY (MILLIDARCIES)	POROSITY	METHOD
BD2A	1.0	LIMESTONE	1.5	24.7	PLUG
BD2B	1.5	LIMESTONE		7.0	TS
BD3A	2.0	LIMESTONE	6434.0	24.8	PLUG
BD3B	2.5	LIMESTONE		11.6	TS
BD4A	3.0	LIMESTONE	7275.0	28.4	PLUG
BD4B	3.5	LIMESTONE		7.4	TS
BD7A	4.0	LIMESTONE	9530.0	23.3	PLUG
BD7B	4.5	LIMESTONE		17.6	TS
BD9A	5.0	LIMESTONE	1.4	11.9	PLUG
BD1A	5.2	DS, LIMESTONE	4202.0	22.0	PLUG
BD1B	5.5	DS, LIMESTONE		18.2	TS
BD8A	6.0	DS, LIMESTONE	1615.0	20.1	PLUG
BD8B	6.5	DS, LIMESTONE		8.4	TS
BD5A	7.0	DOLOMITE	29128.0	45.8	PLUG
BD5B	7.5	DOLOMITE		39.6	TS
BD6A	8.0	DOLOMITE	8654.0	38.5	PLUG
BD6B	8.5	DOLOMITE		30.0	TS
BD6C	8.8	DOLOMITE		33.2	TS
BD10A	9.0	DOLOMITE	OFF SCALE	48.5	PLUG
BD10B	9.5	DOLOMITE		38.2	TS
BD10C	9.8	DOLOMITE		35.9	TS
BD11A	10.0	DOLOMITE	0.02	7.6	PLUG
BD11B	10.5	DOLOMITE		7.2	TS

Limestone porosity average = 17.1 %

Standard deviation = 8.2%

Permeability average = 4648md

Standard deviation = 4390md

Partial dolomite porosity average = 17.2%

Standard deviation = 6.1%

Permeability average = 2909md

Dolomite porosity average = 32.5 %

Standard deviation = 14.3%

composition ranges from -8.42 to -5.51 ‰ and averages -7.05 ‰ PDB (Table 17).

The dolomites are planar, uniform dolomite rhombohedra with an average crystal size of 230 micrometers. Inclusions of allochems and calcite cement are rare, making the texture of the limestone that the dolomite replaced difficult to decipher. There are patterns of inclusions present however, that can be identified as replaced foraminifera. Inclusions of low magnesium-calcite cement in the dolomite are similar in morphology to the low magnesium-calcite cement in the overlying limestone (Figure 27). This indicates that a period of cementation preceded dolomitization in this area. Glauconite pellets are observed in the dolomites, but comprise less than one percent of the total volume. The dolomites are calcium-rich with a mean value of 57 mole percent CaCO_3 (XRD). The dolomite trace element data and the whole rock stable isotope composition are presented in table 18. The strontium concentration of the dolomites ranges from 277 to 140 ppm and averages 176 ppm. The iron concentration of the dolomites ranges from 2663 to 1265 ppm and averages 1961 ppm. The zinc concentration of the dolomites ranges from 67 to 15 ppm and averages 37 ppm. Whole rock oxygen isotopes of the dolomites range from 3.74 to 2.26 ‰ PDB and average 3.32 ‰ PDB. Whole rock carbon isotopes of the dolomites range from -3.75 to -3.09 ‰ PDB and average -3.24 ‰ PDB. The porosity of the dolomites ranges from 7.2 to 48.5 percent, with an average porosity of 32.5 percent (Fig. 26 and Table 16). The porosity in the dolomites is intercrystalline. The permeabilities of the dolomites vary widely from 0.02md to a permeability that went off scale (Table 16).

TABLE 17. OXYGEN AND CARBON ISOTOPE ANALYSES OF THE SERO DOMI LIMESTONES, (BOE DOEI).

Sample	Lithology	$\delta^{18}\text{O}_{\text{PDB}}$ (‰)	$\delta^{13}\text{C}_{\text{PDB}}$ (‰)
Boe Doei			
A	Limestone	-3.51	-7.42
B	"	-2.20	-5.51
C	"	-3.55	-7.18
D	"	-3.07	-6.10
E	"	-3.35	-7.60
F	"	-3.76	-8.42
G	"	-2.71	-6.87
H	"	<u>-3.03</u>	<u>-7.30</u>
		Mean =	-3.15
		S.D. =	0.51
			-7.05
			0.90

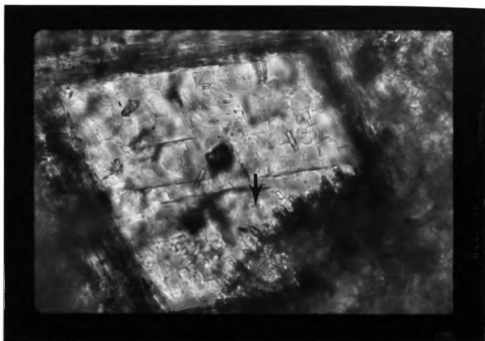


Figure 27. Blade shaped low magnesium calcite cement crystal included in a dolomite crystal from Boe Doei (Aruba, N.A.). Width of field = 0.6mm.

TABLE 18. STABLE ISOTOPE AND TRACE ELEMENT ANALYSES OF THE SERO DOMI DOLOMITES (BOE DOEI).

Sample	$\delta^{18}\text{O}_{\text{PDB}}$ (‰)	$\delta^{13}\text{C}_{\text{PDB}}$ (‰)	Sr (ppm)	Fe (ppm)	Zn (ppm)
Boe DoeI					
5	2.26	-3.75	277	2029	59
			183	1664	67
6	3.43	-3.13	168	1620	63
			171	1954	55
6	3.50	-3.18	165	1273	19
10	3.72	-3.14	176	2595	26
			169	2590	29
11	3.74	-3.16	140	2663	26
			157	1265	15
<u>11</u>	<u>3.25</u>	<u>-3.09</u>	<u>157</u>	<u>1273</u>	<u>15</u>
Mean =	3.32	-3.24	176	1961	39
S.D. =	0.55	0.25	37	554	21

The limestone-dolomite contact parallels bedding, and occurs over a vertical distance of approximately one meter. Across the contact, the number of dolomite rhombs decreases but the size of the dolomite rhombs remains the same (average of 256 micrometers). The dolomites in this zone also exhibit the same calcium rich zone as dolomites from the areas of 100 percent dolomite (Figure 28). There were therefore fewer dolomite nuclei in these limestones, but the rhombs grew at the same rate and at the same time as the rhombs in the completely dolomitized section. The fact that the dolomitization parallels bedding is also consistent with the idea that the degree of dolomitization is related to the original sediment texture or composition.

Discussion of Substrate Surface Area Affects

On the island of Aruba, most of the dolomites from the Boe Doei outcrop are very porous, but two have a very low porosity (Figure 26 and Table 16). The difference in the porosity of the dolomites at Boe Doei can also be explained due to a difference in the host rock texture. A number of factors that influence dolomite porosity could be constrained, specifically: 1) that the porosity variation was not a function of differences in solution chemistry or temperature, and 2) that parent mineralogy has no verifiable control on the resultant dolomite porosities.

First, the similarity in oxygen isotopes and the trace elements of the dolomites (Table 18) argues against a major difference in pore fluid chemistry and temperature.

Second, differences in the strontium content of the porous and

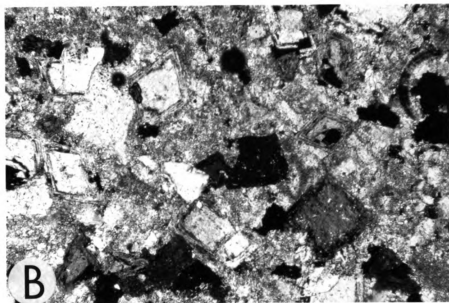
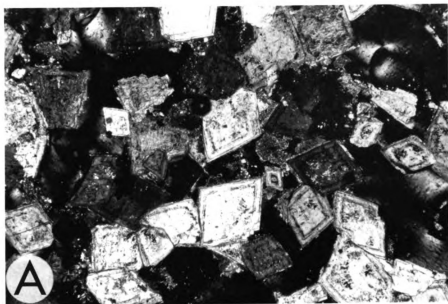


Figure 26. Dolomite crystals from Boe Doei under crossed-polars. Note the calcium-rich zone towards the outer edge of the crystals in the completely dolomitized section (A). The same high calcium zone is seen in the dolomites from the partially dolomitized horizons (B). Width of field = 1.5mm.

nonporous dolomites are not significant enough to suggest that there was a major difference in the amount of aragonite between the samples (eg. Rao et al, 1987).

Third, both the high and low porosity areas have dolomite crystals of similar size. The lower porosity of the dolomites in this portion of the section was therefore the result of a higher initial packing of dolomite nuclei. The subsequent growth of the dolomite crystals with the more dense nuclei resulted in a lower porosity dolomite.

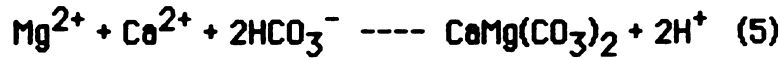
BICARBONATE FLUX

The flux of bicarbonate affects the porosity of a dolomite in that it controls the amount of material available for the precipitation of dolomite cement. Systems having high flux rates of bicarbonate, are able to precipitate greater quantities of cement.

To form a dolomite with a porosity less than or equal to the porosity of the precursor limestone, the amount of dolomite cement that must be precipitated is at least 13 percent of the solid volume of the limestone. The limiting ion for this precipitate is likely to be HCO_3^- because its concentration in solution is much less than the concentration of magnesium ions in most dolomitizing solutions.

The amount of cement that has been precipitated can be easily determined from the porosities of limestones with the same original texture as the dolomites. Once the amount of cement precipitated has been determined, the amount of time required to precipitate this cement can be calculated. To calculate the amount of time required to precipitate the

cement, the mass flux of the reactants must be modelled. The dolomite cementation equation used for modelling is:



The mass flux equation is:

$$\text{Mass Flux} = dqc \quad (6)$$

d = water density

q = Darcy velocity

c = molality of the reactant

The Darcy velocities used are from Simms (1984; table 19). If the mass flux of the reactants, the thickness of the dolomitized unit (assuming vertical flow), and the amount of cement to be precipitated are known, the minimum time for the precipitation of the cement can be determined from the following:

$$\text{Times (years)} = \frac{\left(\frac{2 \text{ moles HCO}_3^-}{\text{mole Ds}} \right) \times [(L_s \phi - D_s \phi) + 1.13(1 - L_s \phi)] \times (\text{thickness (m)})}{\left(\frac{\text{mass flux (moles HCO}_3^-)}{\text{m}^2\text{-year}} \right) \times \left(\frac{\text{molar volume of Ds} - \left(\frac{\text{m}^3}{\text{mole Ds}} \right)}{\right)} \quad (7)$$

Three different dolomitizing solutions were examined for use in the bicarbonate flux model. These solutions are; 1) mixed fresh/seawater, 2)

seawater, and 3) evaporatively concentrated seawater. It is difficult to find examples where both the chemical analyses of the solutions and their activity coefficients are listed. The activities for modelling a mixed water flux are obtained from Badiozamani (1973). The data are for a mixture of 5 percent seawater with 95 percent freshwater. The activities for modelling sea water were obtained from Millero and Schreiber (1982) with the absolute concentrations of the ions from Drever (1982). The activities of ions in brine solutions are difficult to determine and are therefore often not reported. The activities and concentrations for modelling brine reflux are from Krumgalz and Millero (1982). The concentration of the brine is approximately ten times the concentration of sea water.

The amount of bicarbonate available for cementation was determined by taking bicarbonate and Ca^{2+} out of solution down to calcite equilibrium. Recall that the "local source theory" invokes the local dissolution of the CaCO_3 substrate for dolomitization to proceed. By staying above calcite equilibrium, the amount of dolomite cement that can be precipitated from solution can be determined because dissolution of the substrate has not yet commenced.

The flux of bicarbonate for the various flow systems modelled is presented in table 19. The highest flux rates are in the mixed water flow process and the lowest flux rates are in the refluxing brines. The flux rates for seawater circulation are those associated with mixing zones. The high flux rates for mixed waters is due to the high Darcy velocity of this system. This particular mixed water however is undersaturated with respect to calcite and therefore cannot precipitate dolomite cement according to this method. Neither of the two locations examined in this

TABLE 19. DARCY VELOCITIES AND MASS FLUXES

Flow Process	Darcy Velocity* (meters/year)	Mass Flux (moles/meter ² year) HCO_3^-
Reflux	0.01 - 0.1	8.0×10^{-2} - 8.0×10^{-1}
Kohout	0.3 - 1.0	2.7×10^{-1} - 9.2×10^{-1}
Coastal Flows		
Mixing zone	5.0 - 20.0	6.5×10^0 - 2.6×10^1
Seawater	0.5 - 3.0	4.6×10^{-1} - 2.76×10^0
Circulation		

*Simms (1984)

study however, are suggested to have been dolomitized by mixed water.

The flux model will be applied to two study areas. First, the Pliocene carbonates on Aruba (Netherlands Antilles) are examined because they provide an opportunity to compare limestones and dolomites that had similar original textures. By comparing porosities of the limestones and dolomites one can estimate the amount of bicarbonate that has been imported to, or exported from, the system. Second, the Miocene carbonates of the Eniwetok Atoll are examined because constraints on the timing of dolomitization and the type of dolomitizing solution are available from previous work.

Pliocene Sero Domi Formation Aruba, Netherlands Antilles

The rocks at Rooi Hundu (Figure 25) were used for mass flux modelling because the original texture and porosity of the limestones can be deciphered. This allows one to determine the amount of bicarbonate that was fluxed through the system to produce the observed porosity in the dolomite. The limestones range in composition from wackestones to packstones. The major allochems are coralline algae which comprise up to 48 percent of the rock volume, and benthic foraminifera which comprise up to 30 percent of the rock volume. Minor constituents include echinoderms and rarely coral fragments. Bulk mineralogy as determined by x-ray diffraction is low magnesium calcite. There is a very finely crystalline acicular calcite cement in the limestones. Supko (1971) and Chafetz et al (1985) suggest that cement crystals of this morphology are indicative of

vadose cementation. The limestones near the top of the outcrop are the most tightly cemented. Based on the crystal morphology and the proximity to the top of the present outcrop, the calcite cement is probably modern vadose cement. The porosity of the limestones varies from 6.8 to 32.2 percent, with an average porosity of 21.7 percent. The porosity in the limestones is intercrystalline, intracrystalline and vuggy. The whole rock oxygen isotopes of the limestones range from -5.25 to -3.93 ‰ and average -4.64 ‰ PDB. The whole rock carbon isotope values range from -9.92 to -6.53 ‰ and average -8.00 ‰ PDB (Table 20).

The dolomites at Rool Hundu are planar nonuniform dolomites with rhombs averaging 13.8 micrometers in diameter. The coralline algae in the rocks were mimically replaced whereas the foraminifera were generally dissolved and left as molds (Figure 29 a, b and c). There are however some forams that have been replaced by dolomite. In contrast to the dolomites at Boe Doel, there is no evidence of predolomitization cementation in the rocks from this location. Minor compaction fractures are observed in the coralline algae at this site. This compaction occurred prior to the dissolution of the foraminifera. This is evidenced by coralline algae that have been deformed around what are currently foram molds (Figure 30). There is some post-dolomitization calcite cementation in the dolomites near the quartz diorite basement rock. This cement is a blocky phreatic low-magnesium calcite cement. The dolomite is calcium-rich with a mean value of 57 mole percent CaCO_3 (XRD). The dolomite trace element data and whole rock stable isotopic composition is presented in table 21. The strontium concentration of the dolomites ranges from 375 to 197 ppm and averages 259 ppm. The iron concentration of the dolomites ranges from

TABLE 20. OXYGEN AND CARBON ISOTOPE ANALYSES OF THE SERO DOMI LIMESTONES, (ROOI HUNDU).

Sample	Lithology	$\delta^{18}\text{O}_{\text{PDB}}$ (‰)	$\delta^{13}\text{C}_{\text{PDB}}$ (‰)
Roof Hundu			
A	Limestone	-5.25	-9.92
B	"	-5.09	-6.53
C	"	-4.49	-7.07
D	"	-3.93	-9.10
E	"	<u>-4.42</u>	<u>-7.40</u>
Mean =		-4.64	-8.00
S.D. =		0.54	1.44

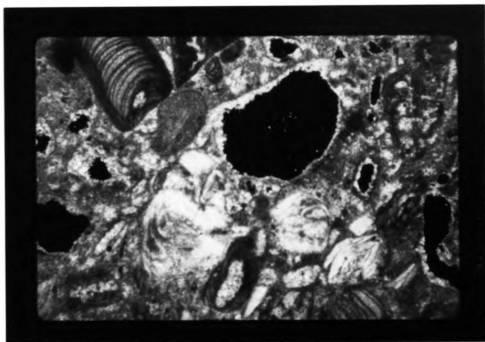


Figure 29a. Typical limestone from Rooi Hundu. Note the presence of coralline algae and benthic foraminifera. Width of field = 3.8mm.

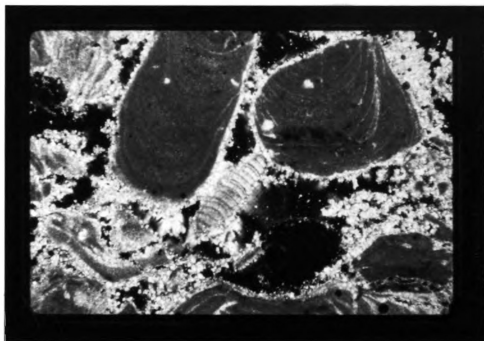


Figure 29b. Dolomites from Rooi Hundu showing the mimic replacement of the coralline algae. Width of field = 3.8mm.

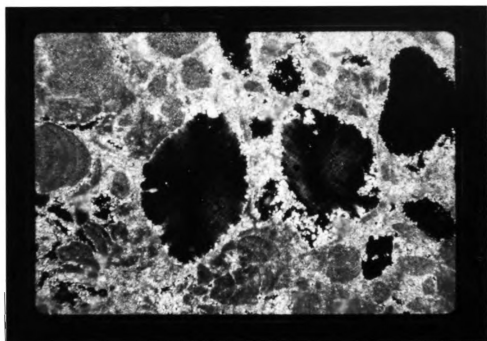


Figure 29c. Foram molds in the dolomites from Rooi Hundu. Width of field = 3.8mm.



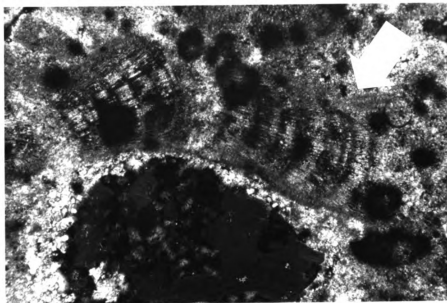


Figure 30. Coralline algae fractured around what is currently a foram mold from Rooi Hundu. Width of field 1.5mm.

TABLE 21. STABLE ISOTOPE AND TRACE ELEMENT ANALYSES OF THE SERO DOMI DOLOMITES, (ROOI HUNDU).

Sample	$\delta^{18}\text{O}_{\text{PDB}}$ (‰)	$\delta^{13}\text{C}_{\text{PDB}}$ (‰)	Sr (ppm)	Fe (ppm)	Zn (ppm)
Roai Hundu					
A	3.08	-2.12	375 293	820 918	21 21
B	3.17	-1.92	271 286	725 898	18 18
C	1.90	-3.51	232 250	776 351	10 20
D	2.20	-4.05	263 227	358 324	25 6
E	1.77	-2.23	197	308	25
F	<u>2.21</u>	<u>-4.12</u>	<u>199</u>	<u>310</u>	<u>21</u>
Mean =	2.39	-2.99	259	579	19
S.D. =	0.60	1.01	52	268	6

918 to 308 ppm and averages 579 ppm. The zinc concentrations of the dolomites range from 25 to 6 ppm and averages 19 ppm. Oxygen isotopes of the dolomites range from 3.17 to 1.77 ‰ and averages 2.39 ‰ PDB. Carbon isotopes of the dolomites range from -4.12 to -1.92 ‰ and average -2.99 ‰ PDB. The porosity of the dolomites ranges from 20.7 - 35.5 percent, with an average porosity of 28.6 percent (Figure 31 and Table 22). Vug and fossil moldic porosity are dominant in the dolomites. The permeabilities of the limestones range from 5.9 to 6217md.

The limestones conformably overlie the dolomites, but it is possible that these sediments were deposited after the underlying sediments had been dolomitized. This is postulated because the limestone-dolomite contact is sharp, parallels bedding, and partially dolomitized rocks are absent.

Both the limestones and dolomites are coralline algal packstones to wackestones. The effect of dolomitization on the porosity of these rocks can be estimated by subtracting the post-dolomitization calcite cements in the dolomites and the calcite cement in the limestones. With this correction, the porosity of the dolomites (ave. 28.1 percent) is less than the porosity of the limestones (ave. 39.9 percent) (Figure 31 and Table 22). The dolomitization of these rocks has therefore lowered porosity, despite the fact that fossil molds were created. This indicates that there must be some dolomite cementation. The permeabilities of the dolomites range from 594 to 19,997 md (Table 22).

Rooi Hundu

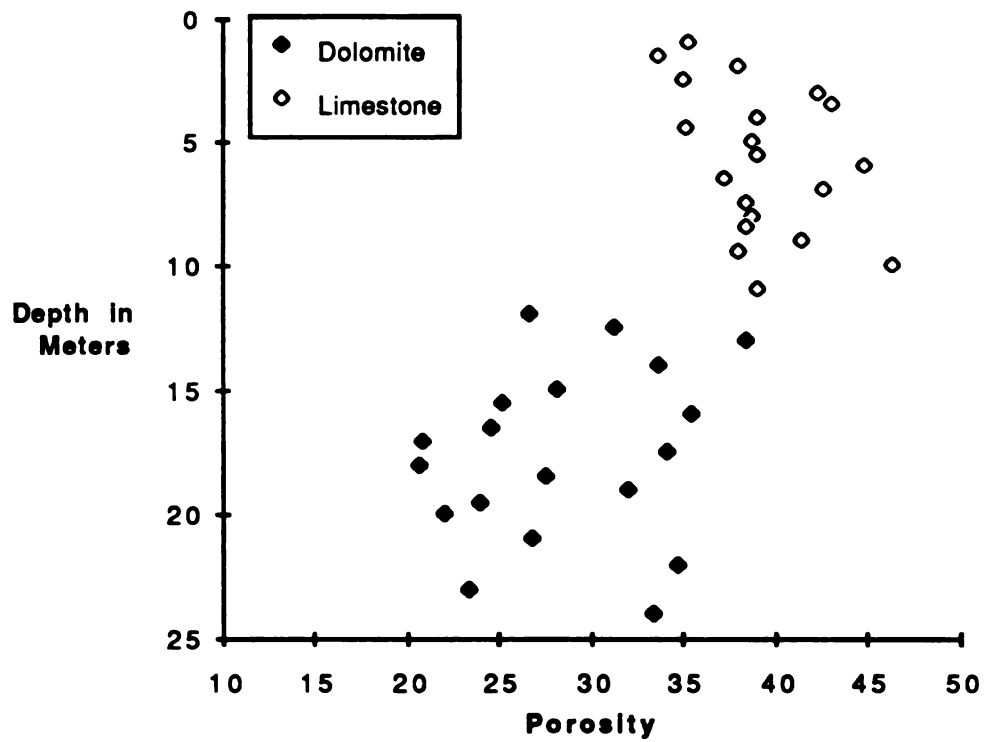


Figure 31. Percent porosity versus depth for the carbonates from Rooi Hundu. The limestone porosities have been corrected for calcite cementation.

TABLE 22. POROSITY AND PERMEABILITY OF THE ROOI HUNDU CARBONATES (ARUBA, NA)

SAMPLE	DEPTH IN METERS	LITHOLOGY	PERMEABILITY (MILLIDARCIES)	POROSITY	METHOD
A07A	1.0	LIMESTONE		35.4	PLUG,TS
A07B	1.5	LIMESTONE		33.8	PLUG,TS
A07C	2.0	LIMESTONE		38.1	PLUG,TS
5	2.5	LIMESTONE	4514.0	35.1	PLUG,TS
B4-4	3.0	LIMESTONE		42.4	TS
A08B	3.5	LIMESTONE		43.2	PLUG,TS
B4-7	4.0	LIMESTONE		39.2	TS
14	4.5	LIMESTONE	4786.0	35.2	PLUG,TS
A09A	5.0	LIMESTONE		38.9	PLUG,TS
A09B	5.5	LIMESTONE		39.1	PLUG,TS
A09C	6.0	LIMESTONE		45.0	PLUG,TS
16	6.5	LIMESTONE	4634.0	37.3	PLUG,TS
A10A	7.0	LIMESTONE		42.7	PLUG,TS
A10B	7.5	LIMESTONE		38.6	PLUG,TS
18	8.0	LIMESTONE	4278.0	38.9	PLUG,TS
B4-10	8.5	LIMESTONE		38.9	TS
B4-13A	9.0	LIMESTONE	5.9	41.5	PLUG,TS
B4-13B	9.5	LIMESTONE		38.1	TS
B4-14A	10.0	LIMESTONE		46.4	TS
20	10.5	LIMESTONE	6217.0	39.2	PLUG,TS
A01A	12.0	DOLOMITE		26.7	TS
A01B	12.5	DOLOMITE		31.4	TS
A01C	13.0	DOLOMITE	2496.0	38.5	PLUG
A01D	14.0	DOLOMITE		33.8	TS
A02A	15.0	DOLOMITE		28.2	TS
A02B	15.5	DOLOMITE		25.3	TS
A02C	16	DOLOMITE	594.0	35.5	PLUG
A03A	16.5	DOLOMITE		24.6	TS
A03B	17.0	DOLOMITE		20.9	TS

Table 22 (cont'd.)

A03C	17.5	DOLOMITE	19997.0	34.2	PLUG
A03D	18.0	DOLOMITE		20.7	TS
A04A	18.5	DOLOMITE		27.6	TS
A04B	19.0	DOLOMITE		32.1	TS
A04C	19.5	DOLOMITE		24.0	TS
A05A	20.0	DOLOMITE		22.1	TS
A05B	21.0	DOLOMITE		26.9	TS
A06A	22.0	DOLOMITE		34.8	TS
A06B	23.0	DOLOMITE		23.5	TS
A06C	24.0	DOLOMITE		33.5	TS

Limestone porosity average = 39.9%

Standard deviation = 3.9%

Permeability average = 4072md

Standard deviation = 2107md

Dolomite porosity average = 28.6 %

Standard deviation = 5.4%

Permeability average = 7696md

Standard deviation = 10,696md

T - test of the limestone porosity versus dolomite porosity

t = 3.75

n = 39

Origin of the Sero Domi Dolomites

Determining the origin of the Sero Domi dolomites will afford some constraints on the type of dolomitizing solution to use for the bicarbonate mass flux modelling. The origin of the dolomite in the Sero Domi Formation on the neighboring island of Bonaire (Netherlands Antilles) was suggested to have been due to either a refluxing brine (Deffeyes et al, 1965; Bandoian and Murray, 1977) or an evaporatively concentrated fresh water/seawater mix (Sibley, 1980). It is also possible, however, that the dolomitizing solution was cold seawater (e.g. Saller, 1984a and Aharonson et al, 1987). The evidence presented is consistent with dolomitization by either cold seawater or evaporatively concentrated brines.

The carbon isotopic values of the Sero Domi dolomites are lighter than dolomites precipitated from seawater (Veiser, 1983 and Saller, 1984a). The light carbon signature of the dolomites could be the result of; 1) carbon inherited from the limestones, 2) elevated temperature, and/or 3) the influence of organic carbon (soil gas or sulfate reduction) in the dolomitizing solution. The negative carbon in the dolomites from Rooi Hindu (if it was inherited from the limestones) was probably due to the influence of organic carbon from sulfate reduction. The amount of organic carbon that needs to be incorporated into the limestones can be determined from the following equation (Lawrence, 1973):

$$\delta^{13}\text{C of Bulk} = \mu_1\delta_a + (1-\mu_1)\delta_b \quad (8)$$

where

μ_1 = mole fraction of authigenic carbonate

δ_a = $\delta^{13}\text{C}$ of the carbon going into the authigenic carbonate

$(1-\mu_1)$ = mole fraction of original carbonate

δ_b = $\delta^{13}\text{C}$ of original carbonate

Curtis (1978), and Presley and Kaplan (1968) reported that organically derived carbon from the sulfate reduction zone ranges from -21 to -25 ‰ PDB. With this range of values, approximately 15 percent of the carbon present must be authigenic in nature to produce a limestone with a carbon isotopic composition of -3 ‰ PDB. The negative carbon in the dolomites could therefore, be explained by the carbon in the precursor limestone.

Alternatively, the negative carbon values are probably not the result of an elevated temperature, because this is not consistent with the heavy oxygen isotopes observed.

The negative carbon could be from the dolomitizing solution. The light carbon could be due to the influence of soil gas CO_2 from a fresh water source, or to light carbon evolved during sulfate reduction. The heavy oxygen isotopes in the dolomites are not consistent with an influence of fresh water. The light carbon and the heavy oxygen isotopes could be due to sulfate reduction occurring in cold marine waters. The amount of authigenic carbonate that would need to be precipitated (see above) is not unreasonable considering the amount of cement that was precipitated at Roor Hundu.

The oxygen isotopic values of the Sero Dami Formation dolomites are enriched in $\delta^{18}\text{O}$ as compared to dolomites precipitated from normal sea

water. This enrichment in oxygen isotopic values could be due to the influence of either dolomitization by evaporatively concentrated waters, or cold sea water. The temperature of the dolomitizing solution (with an initial composition of 0 ‰ SMOW) would be about 16° C (equation from Matthews and Katz, 1977) to produce a dolomite with an oxygen isotopic composition of +3.5 ‰ PDB.

At least two models can be proposed for the occurrence of positive oxygen isotopes and negative carbon isotopes in these dolomites. First, an isotopically heavy water passed through an isotopically light substrate. Oxygen will exchange 3 to 1 versus the carbon in the carbonate structure and would therefore equilibrate with the solution's isotopic signature more rapidly than carbon. In the second model, dolomitization is due to cold seawater in the sulfate reduction zone. The clustering of oxygen isotopes suggests a fluid with a relatively constant isotopic signature over a few hundred thousand years (the time necessary to precipitate the amount of cement observed at Rooi Hindu by sea water - see the discussion of flux modelling below). A constant isotopic signature for this prolonged time period without a large constant reservoir like the ocean is not likely. Sabkha hydrology demonstrates widely varying oxygen isotopic signatures from their landward extent to their seaward extent.

The trace element composition of dolomites has often been used as a tool to determine the origin of the dolomitizing solution. The usefulness of trace elements however is hampered by an inability to accurately determine distribution coefficients for species in dolomites at low temperatures. As a first approximation, strontium data were collected in order to model the origin of the dolomites by looking for consistent trends

in the data. A compilation of isotopic and strontium compositions in some relatively recent dolomites is presented in table 23.

The distribution coefficient of strontium in dolomite is still debated (Land, 1980). Katz and Matthews (1977) suggest a distribution coefficient of 0.025 from experimental evidence, whereas Baker and Burns (1985) determined a distribution coefficient of 0.06 from Recent sediments. Using these values as upper and lower limits, a dolomite precipitated from seawater should have a strontium concentration of between 120 and 280 ppm. The concentration of strontium in the Sero Dumi dolomites (176-259 ppm) falls within this range and suggests the possibility of seawater as a dolomitizing solution. These values are also similar to the concentrations of strontium in the dolomites from the Eniwetok and Niue Atolls (Table 23) which are both thought to have been dolomitized by seawater.

Refluxing brines should have higher concentrations of strontium due to the evaporative concentration of the strontium in the waters. Dolomites formed from this water should therefore have higher concentrations of strontium (assuming a constant distribution coefficient). Dolomites theorized to have formed in this way however, do not show any significant difference in strontium concentrations from dolomites theorized to have formed from seawater (Table 23). Therefore, strontium cannot be used as a discriminator between the two diagenetic environments.

The similarity of the iron and zinc concentrations in the dolomite also supports the premise that there was not a major difference in solution chemistry.

The evidence presented is consistent with dolomitization by either cold seawater or evaporatively concentrated brines. A dolomitizing solution of seawater composition is however, more consistent with the

TABLE 23. STABLE ISOTOPIC (PDB) AND TRACE ELEMENT COMPOSITIONS (PPM) OF SELECTED CENOZOIC DOLOMITES

Location	Sr	Fe	Zn	$\delta^{13}\text{C}$	$\delta^{18}\text{O}$	Proposed Origin
Jamaica-Falmouth (Lend, 1973b)	3000			-8.4	-1.0	Mixed
Jamaica-Hopegate (Lend, 1973a)	220			+1.2	+2.2	Mixed
Bonaire (Sibley, 1980&Lend, 1973a)	210			+2.4	+3.1	Mixed
Colette Atoll (Repellin, 1977)	170			+4.0	+4.0	Mixed
El Naqb (Lend et al, 1975)	96			-0.5	-1.1	Mixed
Eniwetok Atoll (Saller, 1984a)	170	36		+2.3	+2.5	Cold Marine
Niue Atoll (Aheron et al, 1987)	223	1587	151	+2.0	+2.8	Marine
Sugarloaf Key, FL (Behrens and Lend, 1972& Cerbello et al, 1987)	620			-0.7	+3.0	Marine
Belize (Mazzullo et al, 1987)	600			-1.6	+1.6	Marine
Jamaica (Mitchell et al, 1987)	600			+1.6	+2.0	Marine
Monterey Fm, CA (Burns and Baker, 1987)	236 558			-6.13 +8.62	+0.73 +0.50	Marine Marine
Beheme Peri-platform (Mullins et al, 1985)	850			+2.82	+5.18	Cold Marine (Authogenic)
Israel Cretaceous (Sass and Katz, 1982)	97			+0.49	-0.33	Marine- Hypersaline
Sabkha (Tlig & M'Robet, 1985)	115				+0.4	Sabkha
Holocene Baffin Bay, TX (Behrens and Lend, 1972)	916			-0.9	+4.8	Hypersaline
Persian Gulf (Behrens and Lend, 1972)	640			+4.3	+3.7	Evaporative Brine

clustering of oxygen isotopic data.

Discussion of the Bicarbonate Flux Model

The Sero Domi Formation on the island of Aruba was probably dolomitized by either cold sea water or a refluxing brine. In order to evaluate the mass flux models, a time constraint on the time allowable for dolomitization needs to be determined. The Sero Domi dolomites are Pliocene in age and the overlying Pleistocene limestones were not dolomitized. The dolomitization then occurred in $< 3\text{myr}$. Mass flux modelling is used to estimate the amount of time necessary to precipitate the amount of dolomite cement observed in the Sero Domi by both a refluxing brine and normal seawater. The average porosity of the limestones at Rooi Hundu is 39.9 percent (corrected for calcite cement) and the section is approximately 15 meters thick. If the limestones were replaced by dolomite with a 13 percent volume loss of the solids, then 19.6 percent dolomite cement must have been added to account for the present dolomite porosity of 28.1 percent. If sea water was the dolomitizing solution, and HCO_3^- the controlling anion for cementation, then the required amount of dolomite cement could have been precipitated in .1 - .34 million years, fluxing HCO_3^- by Kohout convection. This amount of dolomite cement could be precipitated in .03-.2 million years fluxing HCO_3^- by sea water circulation associated with a mixing zone. If a brine was the dolomitizing solution, the required amount of cement could have been precipitated in .11 - 1.14 million years fluxing HCO_3^- by a refluxing

brine. As compared to the time available for dolomitization, the short time periods obtained from the modelling, support the idea that the flux of bicarbonate through the system is not the limiting factor to be considered in the porosity evolution of these dolomites.

Eocene Carbonates From The Eniwetok Atoll

The Eocene strata from Eniwetok Atoll (Fig. 32) are lime mudstones to grainstones with a thin horizon (8 m) of dolomite. The dolomite is planar and uniform with rhombs ranging from 50 to 310 microns in diameter, and averaging of 137 microns. Partially dolomitized rocks (coralline algal, foram grainstones and packstones) contain fabric-selective replacement dolomite and dolomite cement. The fabric selective dolomite preferentially replaces the coralline algae and mud (Figure 33). Dolomite cement is superimposed on calcite cement (Figure 34) and compaction fractures (Saller, 1984a). The dolomite in the partially dolomitized rocks is the same size as the dolomite in the completely dolomitized rock. The stable isotopes of the dolomite are 2.5 ^{18}O and 2.3 ^{13}C (Saller, 1984b). The dolomites are Ca-rich with 55.3 mole percent CaCO_3 and average 170 ppm strontium (Saller, 1984b). The porosity of the limestones ranges from 33.2 to 9.8 percent and averages 23.1 percent (Figure 35 and Table 24). The permeabilities of the limestones range from 2042 to 1658md (Table 24). The porosity of the dolomitized rocks ranges from 14.2 to 4.2 percent and averages 7.4 percent. Only one permeability measurement was taken on the dolomites and it was 1658md. The porosity of the partially dolomitized rocks

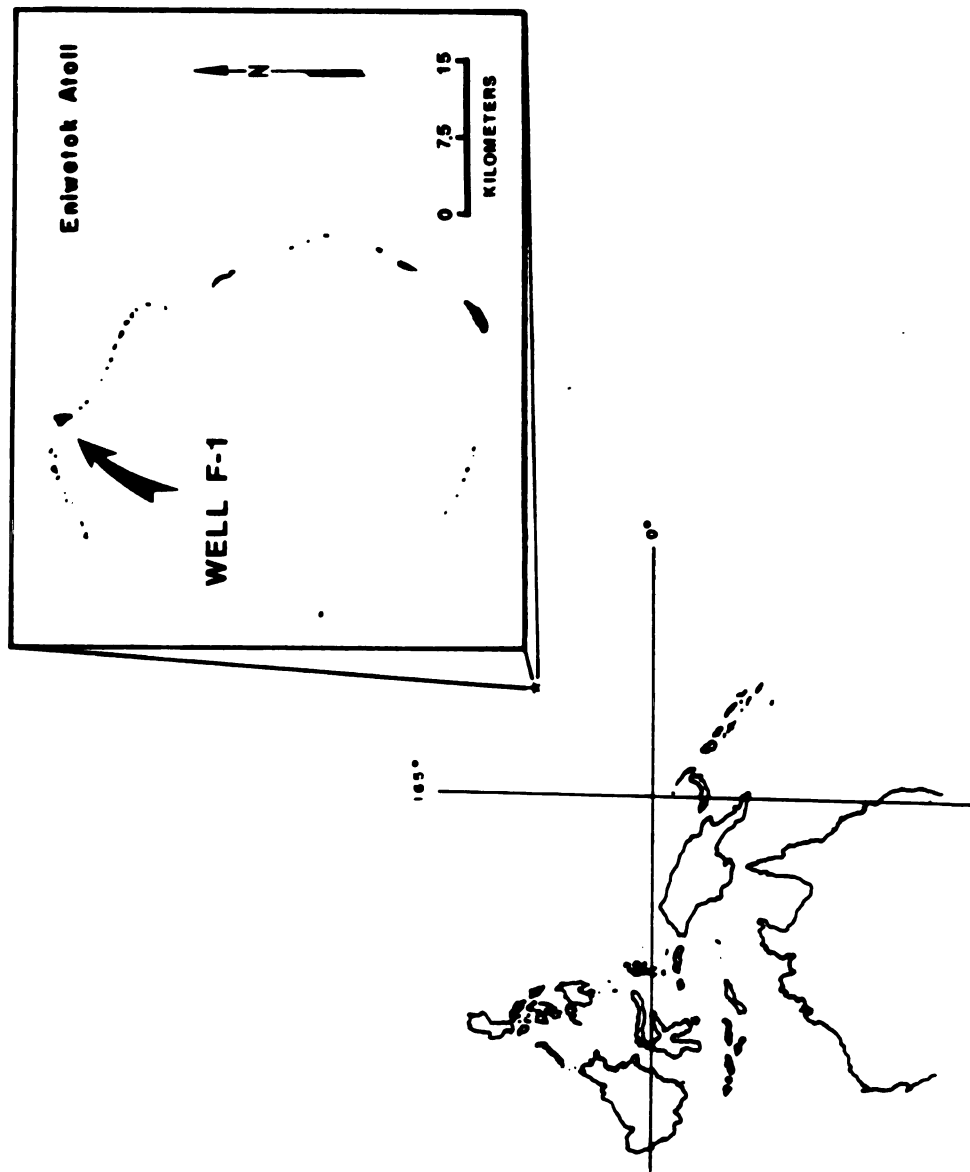


Figure 32. Location map for the core used from the Eniwetok Atoll.

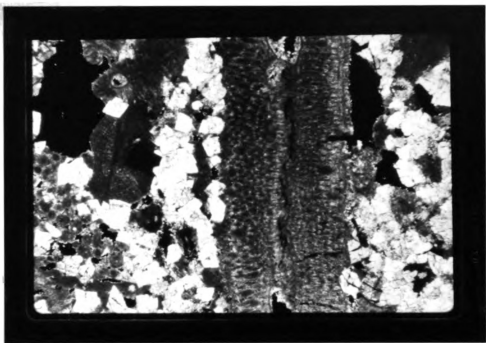


Figure 33. Selective replacement of the mud by dolomite and the resistance of the coarsely crystalline fossil fragments. Width of field = 3.8mm.

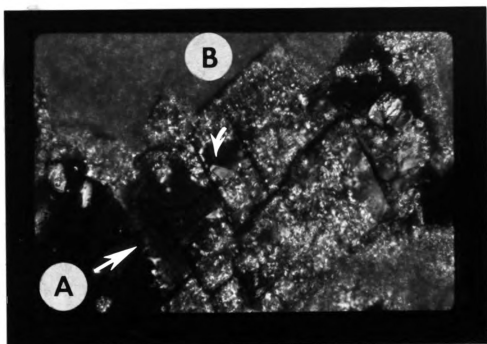


Figure 34. Dolomite cementation (A) after calcite cementation (B) on Eniwetok. Width of field = 0.2mm.

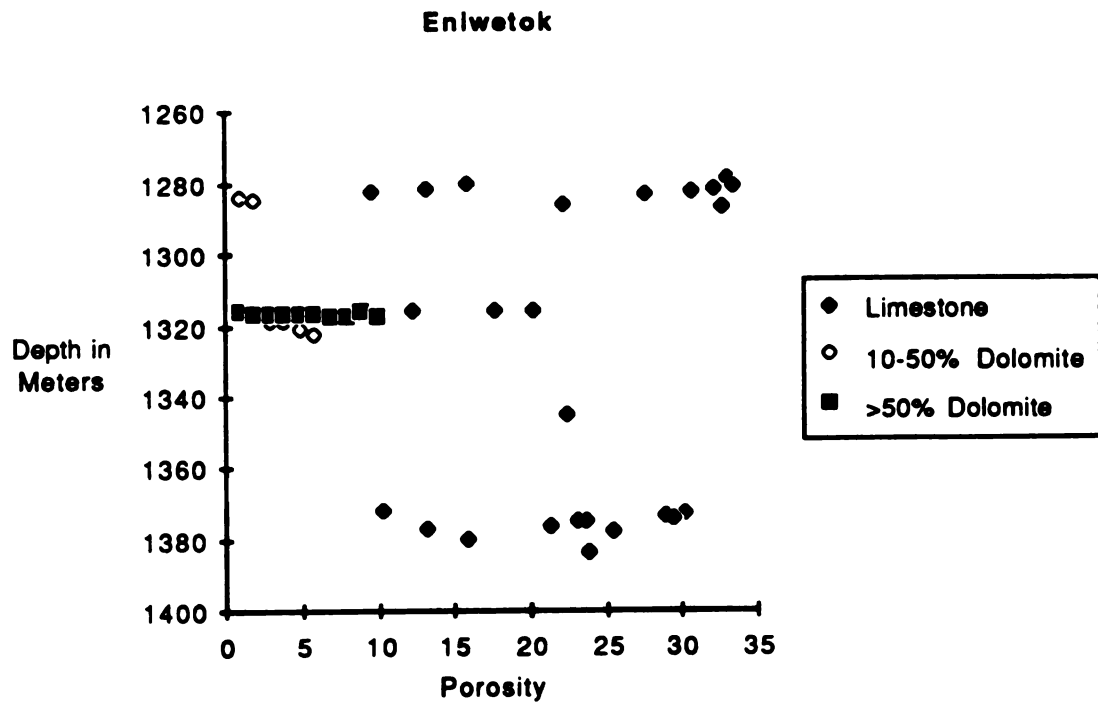


Figure 35. Percent porosity versus depth of the carbonates from the Eniwetok Atoll. Note the general decrease in porosity with the increase in percent dolomite.

TABLE 24. POROSITY AND PERMEABILITY OF THE ENIWETOK ATOLL CARBONATES

SAMPLE	DEPTH IN METERS	LITHOLOGY	PERMEABILITY (MILLIDARCIES)	POROSITY	METHOD
F1-11-4	1279.0	LIMESTONE	1921.0	33.2	PLUG
F1-11-5	1280.0	LIMESTONE		16.0	TS
F1-11-8	1281.0	LIMESTONE	1928.0	33.6	PLUG
F1-11-9	1281.4	LIMESTONE		13.4	TS
F1-11-12	1282.0	LIMESTONE	2042.0	32.2	PLUG
F1-11-16	1282.3	LIMESTONE	1675.0	30.8	PLUG
F1-11-18	1282.6	LIMESTONE		9.8	TS
F1-11-21	1283.2	LIMESTONE	1686.0	29.1	PLUG
F1-11-25	1283.5	LIMESTONE	1695.0	27.7	PLUG
F1-11-26	1283.8	10-50 DS		14.1	TS
F1-11-30	1285.0	10-50 DS		9.7	TS
F1-11-34	1286.3	LIMESTONE		22.4	TS
F1-11-36	1286.9	LIMESTONE	1501.0	32.8	PLUG
F1-12-1	1315.5	LIMESTONE		17.8	TS
F1-12-2	1315.6	LIMESTONE		20.3	TS
F1-12-3	1315.8	LIMESTONE		12.4	TS
F1-12-4	1316.1	>50 DS	1428.0	8.7	PLUG
F1-12-4T	1316.1	>50 DS		10.2	TS
F1-12-4B	1316.3	>50 DS		7.6	TS
F1-12-5T	1316.4	>50 DS		5.2	TS
F1-12-5B	1316.4	>50 DS		7.4	TS
F1-12-6	1316.6	>50 DS	1005.0	7.1	PLUG
F1-12-7T	1316.7	>50 DS		2.8	TS
F1-12-7B	1316.9	>50 DS		6.1	TS
F1-12-8	1317.3	>50 DS		4.2	TS
F1-12-9	1317.5	10-50 DS	1658.0	29.1	PLUG
F1-12-10	1317.7	>50 DS		14.2	TS
F1-12-12	1318.7	10-50 DS		10.4	TS
F1-12-14	1319.2	10-50 DS		7.7	TS
F1-12-16	1320.9	10-50 DS		11.6	TS

Table 24 (cont'd.)

F1-12-23	1322.8	10-50 DS		8.1	TS
F1-13-2	1345.7	LIMESTONE		22.5	TS
F1-14-2	1371.6	LIMESTONE		10.5	TS
F1-14-4	1372.5	LIMESTONE	1413.0	30.2	PLUG
F1-14-8	1373.7	LIMESTONE	1106.0	29.0	PLUG
F1-14-14	1374.0	LIMESTONE	1699.0	29.5	PLUG
F1-14-17	1374.7	LIMESTONE		23.2	TS
F1-14-20	1375.0	LIMESTONE	1634.0	23.7	PLUG
F1-14-25	1376.5	LIMESTONE	1713.0	21.5	PLUG
F1-14-28	1377.4	LIMESTONE		13.4	TS
F1-14-29	1377.7	LIMESTONE		25.6	TS
F1-15-3	1380.1	LIMESTONE		16.1	TS
F1-15-13	1383.0	LIMESTONE		24.0	TS

Limestone porosity average = 23.1%
Standard deviation = 7.5%

Permeability average = 1668md
Standard deviation = 250md

10-50% Dolomite porosity average = 13.0%
Standard deviation = 7.4%

Permeability = 1658md

>50% Dolomite porosity average = 7.4%
Standard deviation = 3.2%

Permeability average = 1216md
Standard deviation = 299md

appears to vary inversely with the amount of dolomite (Figure 35 and Table 24).

The fabric selective nature of the partial dolomites and the similarity of crystal size of all the dolomites is consistent with the hypothesis that the amount of dolomite in the rocks may have been controlled by the original rock texture. As in many ancient rocks, the dolomite may have selectively replaced mudstones. The fact that there are only rare fossil ghosts and molds in the completely dolomitized section is consistent with this hypothesis. If the original texture of the dolomites and limestones were different, then one can only speculate as to the original porosity of the sediments that were dolomitized. One can estimate the predolomitization porosity from the current porosities in the nondolomitized portion of the section. Enos and Sawatsky (1981), through their work on Holocene sediments, show that sediments containing higher proportions of mud were at least as porous as, or more porous than, sediments containing higher proportions of allochems. If this is the case, and only minor compaction and cementation is observed in the limestones, it is reasonable to assume that the low porosity dolomite that replaced the mud has resulted in a porosity loss of approximately 20 percent over the precursor limestone.

Discussion of the Bicarbonate Flux Model

To model the flux of HCO_3^- for these rocks requires assumptions about the porosity of the rocks that were dolomitized. The present porosity of the dolomites is 7.4 percent, whereas the the present porosity

of the limestones is approximately 24 percent. We will assume the predolomitization porosity of the limestones was approximately 24 percent. If the rocks were replaced with a 13 percent volume reduction, then approximately 26 percent dolomite cement must have been precipitated. Saller (1984a) presented strong evidence that the dolomitizing solution was sea water and that the dolomitization occurred within the past 24 myr. If sea water was the dolomitizing solution, and HCO_3^- the controlling anion for cementation, then the required amount of dolomite cement could have been precipitated in .1 to .24 million years fluxing sea water by Kohout convection. This amount of cement could have been precipitated in .02 to .14 million years fluxing HCO_3^- by sea water circulation associated with a mixing zone.

For most dolomites, the flux models are difficult to constrain. In the dolomites from Eniwetok, the dolomitizing solution and the maximum time allowable for dolomitization are relatively well constrained. In this case, we estimated a considerable porosity reduction within a time limit of .2 million years. As compared to the time available for dolomitization, the short time periods obtained from the modelling again support the idea that the flux of bicarbonate through the system is not the limiting factor to be considered in the porosity evolution of these dolomites.

DISCUSSION OF DOLOMITE POROSITY

The ability to determine which horizons within a dolomite are going to have a higher porosity is a very important in both reservoir exploration

and its subsequent development.

Early work on dolomitization and porosity concentrated on why dolomites are more porous than limestones (Van Tuyl, 1914; Murray, 1930; Landes, 1946; Murray, 1960 and Weyl, 1960). These models were based on the assumption that the dolomitizing solution contained little or no bicarbonate available for dolomite cementation. The flux modelling for the Eniwetok and Aruba dolomites suggests that the flux of bicarbonate is not always a limiting factor in the porosity evolution of a dolomite. The condition of porosity development with dolomitization is therefore not always the case. Often, coeval dolomites have a similar porosity to, or lower porosity than, their coeval limestones (Schmoker and Halley, 1982; Halley and Schmoker, 1983; Barrett, 1987 and this study).

The Trenton Formation dolomites have a higher porosity than their associated limestones. The dolomites however, are not 13 percent more porous than the limestones, which is what would be predicted by the "local source theory", but are only approximately two percent higher.

A fundamental problem with most studies of dolomite and porosity is that bulk dolomite and limestone porosities are compared. This causes problems in that porosity in limestones and in dolomites can vary on the scale of a thin section as well as between regional differences in facies. Dolomite porosities in the Trenton varied widely in the space of a few centimeters. Any attempt to truly assess the role that dolomitization plays in the evolution of porosity between limestones and dolomites needs to compare similar initial facies, that have been dolomitized by solutions with similar chemistries. For example, Schmoker et al (1985) compares dolomites (the bulk of which are from mid-lower Paleozoic) with limestones that are generally younger. With this type of analysis, one can

not assess the differences in diagenetic imprints over time. Also it is not possible to assess porosity variances due to differences in original facies or due to differing dolomitizing solutions.

Perhaps most dolomites initially have porosities similar to or even lower than their coeval limestones. Subsequent to the dolomitization episode, the unreplaced limestones will lose their porosity at a more rapid rate due to later cementation, or differences in pressure solution. Schmoker and Halley (1982) show that limestones from south Florida lose their porosity faster than their coeval dolomites due to the "porosity reducing effects of burial".

SUMMARY

Dolomite porosity is the result of the interplay of factors influencing reaction kinetics. These factors include: 1) the surface area of the substrate, 2) the saturation state of the solution, 3) temperature, 4) substrate mineralogy, and 5) the effect of inhibiting ions. The flux of bicarbonate also affects dolomite porosity in that it influences the amount of dolomite that can be precipitated.

The relationship between the bicarbonate flux, the surface area of the substrate, the solution chemistry, and the other factors influencing reaction kinetics and dolomite cementation are not clearly understood. The precise conditions under which any of the other kinetic effects listed may become the dominant textural (and therefore porosity) control are not known.

The effects that the substrate surface area, the saturation state of

the solution, and the flux of solute had on the resultant porosity of a dolomite were studied. The flux of bicarbonate determines the amount of dolomite cement that may be precipitated. The surface area of the substrate affects the porosity of a dolomite, in that it influences the nucleation rate of the dolomite. A high surface area substrate leads to a high nucleation rate and a low surface area leads to a low nucleation rate. A high nucleation rate leads to tightly packed dolomite crystals. A low nucleation rate leads to more loosely packed dolomite crystals. The saturation state of the solution also has an influence on the nucleation rate of dolomite. A high saturation state leads to a high nucleation rate, and a low saturation state leads to a low nucleation rate.

In the Trenton dolomites and the Sero Dumi dolomites, the surface area of the substrate has a control on the resultant porosity of the dolomite. The dolomitization of a finely crystalline (high surface area) limestone resulted in dense dolomite nucleation and a dolomite with porosities similar to or lower than the host. Dolomitization of a more coarsely crystalline (low surface area) limestone resulted in less dense dolomite nucleation and a dolomite with porosities higher than the host.

In the Trenton Formation dolomites, a change in fluid chemistry of the dolomitizing solution had no significant influence on the resultant porosity of the dolomites. This is not to say, however, that solution chemistry changes would never have an influence on the dolomite porosity. Perhaps the change in saturation state that the Trenton Formation was subjected to was simply not large enough to produce any significant difference in porosity.

The flux of the solute was not a limiting factor in the porosity evolution of the dolomites from the Eniwetok Atoll or the Sero Dumi

Formation. The amount of dolomite cement present in these rocks could have been precipitated in geologically reasonable time frames by reasonable concentrations of bicarbonate in solution.

CONCLUSIONS

The porosity of a dolomite is the result of the interplay of many factors that influence reaction kinetics. These factors control the texture and therefore the porosity of the resultant dolomite. The flux of bicarbonate through the system also affects dolomite porosity in that it influences the amount of dolomite cement that can be precipitated. In this study, the effect of two of factors influencing reaction kinetics; 1) the surface area of the substrate and 2) the saturation state of the solution were examined. The first conclusion is that the surface area of the substrate is a dominant control on dolomite texture and therefore porosity in these rocks. Finer-grained substrates that were dolomitized, resulted in dolomites with a low porosity. This occurred due to the high concentration of dolomite nuclei and the subsequent impingement of the numerous crystals with growth. Coarsely grained substrates resulted in textural reorganization and the development of more porous dolomites. This occurred due to the low concentration of dolomite nuclei, which led to more coarsely crystalline dolomite rhombohedra. The surface area of the substrate can be shown to affect other textural features in a dolomite. These features include: 1) rhombohedra size variations within a sample, 2) fossil moldic porosity and 3) textural preservation and/or textural obliteration.

Second, that the change in saturation state did not appear to have an influence on the porosity of the dolomite.

Third, that the flux of bicarbonate through the system is not always a limiting factor in the evolution of dolomite porosity.

The dolomitization process can either create, mimic or destroy porosity. The ultimate porosity of the dolomite is the result of the interplay between differences in the substrate surface area and the chemistry of the dolomitizing solution.

APPENDIX I

APPENDIX I

COMPARISON OF COMPENSATED NEUTRON LOG POROSITY WITH WHOLE CORE POROSITY

The following is a comparison of the whole core porosity with the compensated neutron log porosity. All of the logs in the area were run by Schlumberge, so that no correction is needed in comparing logs from different wells. In this comparison, since there are different correction factors involved in determining the porosity of limestones and dolomites from the logs, the simplest and least confusing way to compare the porosities is to compare the neutron porosities with a core that has all one lithology. In this case, the Total Petroleum Luck 1-12 well was chosen because the cored interval was completely dolomitized. In comparing the porosities listed below, one must keep in mind that the compensated neutron log porosities are an average porosity of the formation near the borehole, whereas the whole core porosity is an average over a smaller area. Therefore any localized deviations from the norm will be more apparent in the whole core porosity values.

TABLE A1-1. COMPARISON OF COMPENSATED NEUTRON AND WHOLE CORE POROSITY OF THE TRENTON DOLOMITES.

Depth (Feet)	Compensated Neutron Percent Porosity	Whole core Percent Porosity
4842	0.9	
4883		0.8
4844	0.5	1.1
4845		1.4
4846	0.9	1.0
4847		1.9
4848	1.7	2.2
4849		1.4
4850	1.7	2.0
4851		1.9
4852	2.0	2.4
4853		2.8
4854	2.5	2.7
4855		2.6
4856	3.0	2.9
4857		3.5
4858	2.5	5.3
4859		4.5
4860	2.0	6.4
4861		3.7
4862	4.4	4.3
4863		2.7

Table A1-1 (cont'd.)

4864	10.1	2.9
4865		1.8
4866	7.5	1.6
4867		8.9
4868	4.4	5.9
4869		8.9
4870	6.8	3.8
4871		3.1
4872	3.9	3.3
4873		5.2
4874	3.9	8.3
4875		6.4
4876	3.0	2.9
4877		3.2
4878	3.0	3.4
4879		3.7
4880	3.0	3.6
4881		3.5
4882	3.4	3.9
4883		2.7
4884	2.5	3.7
4885		4.0
4886	5.0	3.3
4887		4.8
4888	2.5	3.3

Table A1-1 (cont'd.)

4889		3.6
4890	3.1	3.2
4891		3.3
4892	2.2	2.4
4893		4.3
4894	1.4	3.6
4895		3.4
4896	1.4	3.6
4897		4.0
4898	2.0	2.5
4899		2.7
4900	2.0	2.9
4901		4.1
4902	2.0	3.5
4903		3.8
4904	5.0	2.3
4905		3.0
4906	3.0	3.7
4907		4.8
4908	2.2	3.0
4909		2.3
4910	2.0	3.2
4911		3.2
4912	2.0	3.8
4913		3.1

Table A1-1 (cont'd.)

4914	2.8	3.0
4915		2.7
4916	2.5	3.0
4917		3.4
4918	3.0	5.4
4919		7.1
4920	5.0	3.4
4921		3.0
4922	4.4	3.1
4923		4.6
4924	3.0	5.4
4925		5.1
4926	2.0	3.8
4927		3.6
4928	2.5	2.5
4929		3.0
4930	2.5	2.1
4931		2.1
4932	2.5	2.3
4933		2.6
4934	4.4	2.5
<u>4935</u>	<u>2.5</u>	<u>3.1</u>
Mean =	3.1	Mean = 3.5
S.D. =	1.8	S.D. = 1.5
n =	48	n = 93

A student T test indicates that the two methods of porosity analysis are not significantly different.

APPENDIX II

APPENDIX II

WHOLE CORE POROSITY AND PERMEABILITY ANALYSES OF THE TRENTON FORMATION CARBONATES

TABLE AII - 1. WHOLE CORE POROSITY AND PERMEABILITY ANALYSES OF THE TRENTON FORMATION.

Sample	Depth	Porosity	Permeability Max.	Permeability 90 Deg.	Lithology
<u>Total Luck 1-12</u>					
1	4843.0-44.0	0.8	0.2	<0.1	Ds,Sl/Anhy
2	4844.0-45.0	1.1	<0.1	<0.1	Ds,Sl/Anhy
3	4845.0-46.0	1.4	<0.1	<0.1	Ds,Sl/Anhy
4	4846.0-47.0	1.0	<0.1	<0.1	Ds,Sl/Anhy
5	4847.0-48.0	1.9	0.6	0.2	Ds,Sl/Anhy
6	4848.0-49.0	2.2	0.2	0.1	Ds,Sl/Anhy
7	4849.0-50.0	1.4	0.4	<0.1	Ds,Sl/Anhy
8	4850.0-51.0	2.0	<0.1	<0.1	Ds,Sl/Anhy
9	4851.0-52.0	1.9	<0.1	<0.1	Ds,Sl/Anhy
10	4852.0-53.0	2.4	<0.1	<0.1	Ds,Sl/Anhy
11	4853.0-54.0	2.8	<0.1	<0.1	Ds,Sl/Anhy
12	4854.0-55.0	2.7	0.1	<0.1	Ds,Sl/Anhy
13	4855.0-56.0	2.6	0.1	<0.1	Ds,Sl/Anhy
14	4856.0-57.0	2.9	0.1	<0.1	Ds,Sl/Anhy
15	4857.0-58.0	3.5	<0.1	<0.1	Ds
16	4858.0-59.0	5.3	1.0	0.4	Ds
17	4859.0-60.0	4.5	0.5	0.1	Ds
18	4860.0-61.0	6.4	1.0	1.0	Ds
19	4861.0-62.0	3.7	0.3	0.1	Ds
20	4862.0-63.0	4.3	0.7	0.5	Ds
21	4863.0-64.0	2.7	9.2	1.5	Ds
22	4864.0-65.0	2.9	11.0	0.1	Ds
23	4865.0-66.0	1.8	<0.1	<0.1	Ds
24	4866.0-67.0	1.6	*	<0.1	Ds
25	4867.0-68.0	8.9	27.0	9.1	Ds,Pyrite

Table All-I (cont'd.)

26	4868.0-69.0	5.9	10.0	5.7	Ds,Pyrite
27	4869.0-70.0	6.9	6.6	4.4	Ds,Pyrite
28	4870.0-71.0	3.8	0.4	0.2	Ds,Pyrite
29	4871.0-72.0	3.1	<0.1	<0.1	Ds
30	4872.0-73.0	3.3	<0.1	<0.1	Ds
31	4873.0-74.0	5.2	0.1	<0.1	Ds
32	4874.0-75.0	8.3	0.1	<0.1	Ds
33	4875.0-76.0	6.0	15.0	9.7	Ds
34	4876.0-77.0	2.9	<0.1	<0.1	Ds
35	4877.0-78.0	3.2	<0.1	<0.1	Ds
36	4878.0-79.0	3.4	0.5	0.4	Ds
37	4879.0-80.0	3.7	2.0	<0.1	Ds
38	4880.0-81.0	3.6	<0.1	<0.1	Ds
39	4881.0-82.0	3.5	0.5	<0.1	Ds
40	4882.0-83.0	3.9	<0.1	<0.1	Ds
41	4883.0-84.0	2.7	<0.1	<0.1	Ds
42	4884.0-85.0	3.7	<0.1	<0.1	Ds
43	4885.0-86.0	4.0	0.3	0.2	Ds
44	4886.0-87.0	3.3	0.3	0.1	Ds
45	4887.0-88.0	4.8	63.0	0.2	Ds,Y/F
46	4888.0-89.0	3.3	<0.1	<0.1	Ds
47	4889.0-90.0	3.6	*	<0.1	Ds
48	4890.0-91.0	3.2	*	<0.1	Ds
49	4891.0-92.0	3.3	<0.1	<0.1	Ds
50	4892.0-93.0	2.4	<0.1	<0.1	Ds
51	4893.0-94.0	4.3	0.1	<0.1	Ds
52	4894.0-95.0	3.6	<0.1	<0.1	Ds
53	4895.0-96.0	3.4	0.1	<0.1	Ds
54	4896.0-97.0	3.0	<0.1	<0.1	Ds
55	4897.0-98.0	4.1	0.6	0.4	Ds
56	4898.0-99.0	2.5	<0.1	<0.1	Ds
57	4899.0-00.0	2.7	<0.1	<0.1	Ds
58	4900.0-01.0	2.9	<0.1	<0.1	Ds
59	4901.0-02.0	4.1	0.3	0.1	Ds
60	4902.0-03.0	3.5	0.3	0.1	Ds
61	4903.0-04.0	3.8	0.5	0.4	Ds
62	4904.0-05.0	2.3	0.1	<0.1	Ds
63	4905.0-06.0	3.0	<0.1	<0.1	Ds

Table All-I (cont'd)

64	4906.0-07.0	3.7	0.1	<0.1	Ds
65	4907.0-08.0	4.8	2.8	1.1	Ds
66	4908.0-09.0	3.0	<0.1	<0.1	Ds
67	4909.0-10.0	2.3	0.1	<0.1	Ds
68	4910.0-11.0	3.2	1.9	<0.1	Ds,Y/F
69	4911.0-12.0	3.3	0.2	0.1	Ds
70	4912.0-13.0	3.0	0.1	<0.1	Ds
71	4913.0-14.0	3.1	<0.1	<0.1	Ds
72	4914.0-15.0	3.0	<0.1	<0.1	Ds
73	4915.0-16.0	2.7	<0.1	<0.1	Ds
74	4916.0-17.0	3.0	0.1	<0.1	Ds
75	4917.0-18.0	3.4	0.1	<0.1	Ds
76	4918.0-19.0	5.4	2.7	<0.1	Ds
77	4919.0-20.0	7.1	18.0	2.0	Ds,Sl/Lmy
78	4920.0-21.0	3.4	<0.1	<0.1	Ds
79	4921.0-22.0	3.0	0.5	0.2	Ds
80	4922.0-23.0	3.1	<0.1	<0.1	Ds,Sl/Lmy
81	4923.0-24.0	4.5	0.3	0.2	Ds
82	4924.0-25.0	5.4	0.5	0.3	Ds,Sl/Lmy
83	4925.0-26.0	5.1	0.3	0.1	Ds
84	4926.0-27.0	3.8	0.5	0.3	Ds
85	4927.0-28.0	3.6	<0.1	<0.1	Ds
86	4928.0-29.0	2.5	<0.1	<0.1	Ds
87	4929.0-30.0	3.0	<0.1	<0.1	Ds
88	4930.0-31.0	2.1	<0.1	<0.1	Ds
89	4931.0-32.0	2.3	<0.1	<0.1	Ds
90	4932.0-33.0	2.6	0.2	0.1	Ds
91	4933.0-34.0	2.5	0.4	0.1	Ds
92	4934.0-35.0	3.1	0.4	0.3	Ds

Total Emil Faist 2-12

1	5024.0-25.0	0.2	0.2	0.1	Ls,Sl/Ds,Sl/Shly
2	5026.0-27.0	0.2	<0.1	<0.1	Ls,Sl/Ds
3	5028.0-29.0	0.4	0.2	<0.1	Ls,Sl/Ds,Y/F
4	5030.0-31.0	0.4	<0.1	<0.1	Ls,Sl/Ds
5	5031.0-32.0	0.2	<0.1	<0.1	Ls,Sl/Ds

Table All-I (cont'd.)

6	5032.0-33.0	0.3	<0.1	<0.1	Ls,Sl/Ds
7	5033.0-34.0	0.4	15.0	<0.1	Ls,Sl/Ds,Y/F
8	5034.0-35.0	0.3	<0.1	<0.1	Ls,Sl/Ds,Y/F
9	5035.0-36.0	0.5	<0.1	<0.1	Ls,Sl/Ds,Y/F
10	5036.0-37.0	0.4	<0.1	<0.1	Ls,Sl/Ds,Y/F
11	5037.0-38.0	0.2	<0.1	<0.1	Ls,Sl/Ds
12	5038.0-39.0	0.3	<0.1	<0.1	Ls,Sl/Ds
13	5039.0-40.0	0.2	<0.1	<0.1	Ls,Sl/Ds
14	5040.0-41.0	0.3	<0.1	<0.1	Ls,Sl/Ds
15	5041.0-42.0	0.4	<0.1	<0.1	Ls,Sl/Ds
16	5042.0-43.0	0.2	<0.1	<0.1	Ls,Sl/Ds
17	5043.0-44.0	1.2	5.4	<0.1	Ls,Sl/Ds,Y/F
18	5044.0-45.0	0.3	<0.1	<0.1	Ls,Sl/Ds
19	5045.0-46.0	0.7	*	<0.1	Ls,Sl/Ds
20	5046.0-47.0	0.4	<0.1	<0.1	Ls,Sl/Ds
21	5047.0-48.0	0.2	*	<0.1	Ls
22	5048.0-49.0	0.4	<0.1	<0.1	Ls,Sl/Ds
23	5049.0-50.0	0.7	<0.1	<0.1	Ls,Sl/Ds
24	5050.0-51.0	0.7	<0.1	<0.1	Ls,Ds
25	5051.0-52.0	0.8	<0.1	<0.1	Ds,Lmy
26	5052.0-53.0	0.4	*	<0.1	Ls
27	5053.0-54.0	1.8	0.1	<0.1	Ds,Y/Sl/Ygy
28	5054.0-55.0	1.7	<0.1	<0.1	Ds,Sl/Ygy
29	5055.0-56.0	1.1	<0.1	<0.1	Ds,Sl/Ygy
30	5056.0-57.0	1.7	<0.1	<0.1	Ds
31	5057.0-58.0	2.6	*	<0.1	Ds
32	5058.0-59.0	2.7	*	<0.1	Ds
33	5059.0-60.0	3.7	*	<0.1	Ds
34	5060.0-61.0	1.9	0.1	<0.1	Ds
35	5061.0-62.0	2.1	<0.1	<0.1	Ds
36	5062.0-63.0	2.7	<0.1	<0.1	Ds,Sl/Lmy
37	5063.0-64.0	2.3	*	<0.1	Ds
38	5064.0-65.0	2.8	*	<0.1	Ds
39	5065.0-66.0	2.8	*	<0.1	Ds
40	5066.0-67.0	2.3	*	<0.1	Ds
41	5067.0-68.0	1.6	<0.1	<0.1	Ds
42	5068.0-69.0	2.7	<0.1	<0.1	Ds,Ygy,Sty,V/F
43	5069.0-70.0	2.0	*	<0.1	Ds

Table All-1 (cont'd.)

44	5070.0-71.0	2.7	*	<0.1	Ds
45	5071.0-72.0	1.4	0.2	<0.1	Ds,V/F
46	5072.0-73.0	3.8	<0.1	<0.1	Ds
47	5073.0-74.0	2.1	<0.1	<0.1	Ds
48	5074.0-75.0	2.8	*	<0.1	Ds
49	5075.0-76.0	2.3	268.0	<0.1	Ls,Ds,V/F
50	5076.0-77.0	3.3	<0.1	<0.1	Ls,Ds
51	5077.0-78.0	2.2	<0.1	<0.1	Ls,Ds
52	5078.0-79.0	2.5	<0.1	<0.1	Ls,Ds
53	5079.0-80.0	2.8	<0.1	<0.1	Ls,Ds
54	5080.0-81.0	2.1	<0.1	<0.1	Ls,Ds
55	5081.0-82.0	3.5	<0.1	<0.1	Ls,Ds
56	5082.0-83.0	4.6	<0.1	<0.1	Ds,Lmy
57	5083.0-84.0	4.7	*	<0.1	Ds,Lmy
58	5084.0-85.0	5.0	3.4	<0.1	Ds,Lmy,V/F
59	5085.0-86.0	4.2	*	<0.1	Ds
60	5085.0-86.0	1.1	0.2	<0.1	Ds,V/F
61	5087.0-88.0	2.8	*	<0.1	Ds,Lmy
62	5088.0-89.0	2.0	<0.1	<0.1	Ds,Sl/Lmy
63	5089.0-90.0	1.4	<0.1	<0.1	Ds,Lmy
64	5090.0-91.0	0.4	*	<0.1	Ls
65	5092.0-93.0	2.6	<0.1	<0.1	Ls,Ds
66	5093.0-94.0	2.1	<0.1	<0.1	Ds,Sl/Lmy
67	5094.0-95.0	1.2	<0.1	<0.1	Ds,Sl/Lmy
68	5095.0-96.0	3.1	<0.1	<0.1	Ds
69	5096.0-97.0	3.5	<0.1	<0.1	Ds
70	5097.0-98.0	6.1	0.4	0.4	Ds,Shr
71	5098.0-99.0	0.9	<0.1	<0.1	Ds
72	5099.0-00.0	2.2	*	0.2	Ds
73	5100.0-01.0	3.0	*	<0.1	Ds
74	5101.0-02.0	1.8	<0.1	<0.1	Ds
75	5102.0-03.0	1.2	<0.1	<0.1	Ds,Lmy
76	5103.0-04.0	2.1	21.0	<0.1	Ds,Lmy,Pyr,V/F
77	5104.0-05.0	2.6	702.0	<0.1	Ds,V/F
78	5105.0-06.0	2.0	*	16.0	Ds,V/F
79	5106.0-07.0	1.1	9.8	<0.1	Ds,V/F
80	5107.0-08.0	3.4	2.1	0.2	Ds,Sl/Vgy,V/F
81	5108.0-09.0	2.5	109.0	<0.1	Ds,Sl/Vgy,V/F

Table All-1 (cont'd.)

82	5109.0-10.0	2.6	*	0.2	Ds,V/F
83	5110.0-11.0	7.1	563.0	37.0	Ds,Sl/Vgy,V/F
84	5111.0-12.0	10.1	4.7	0.2	Ds,Lmy,Sl/Vgy,V/F
85	5112.0-13.0	8.3	*	0.2	Ds,Lmy
86	5113.0-14.0	6.3	202.0	0.1	Ds,Lmy,Sl/Vgy
87	5114.0-15.0	4.0	0.4	0.2	Ds,Sl/Vgy
88	5115.0-16.0	3.2	30.0	0.1	Ds,Sl/Vgy,V/F
89	5116.0-17.0	3.1	127.0	0.3	Ds,Sl/Vgy,V/F
90	5117.0-18.0	2.1	*	<0.1	Ds,Sl/Vgy
91	5118.0-19.0	1.3	254.0	0.3	Ds,Sl/Vgy,V/F
92	5119.0-20.0	2.3	0.1	<0.1	Ds,Sl/Vgy
93	5120.0-21.0	5.3	84.0	0.3	Ds,Lmy,Sl/Vgy,V/F
94	5121.0-22.0	3.4	<0.1	<0.1	Ds,Lmy,Sl/Vgy
95	5122.0-23.0	2.7	4.6	<0.1	Ds,Lmy,Sl/Vgy
96	5123.0-24.0	2.4	6.5	<0.1	Ds,Lmy,Sl/Vgy
97	5124.0-25.0	1.7	<0.1	<0.1	Ds,Lmy,Sl/Vgy
98	5125.0-26.0	2.4	0.6	<0.1	Ds,Lmy,Sl/Vgy,
99	5126.0-27.0	2.5	3.0	<0.1	Ds,Lmy,Sl/Vgy,V/F
100	5127.0-28.0	4.1	3.3	2.5	Ds,Lmy,Sl/Vgy,V/F
101	5128.0-29.0	1.7	<0.1	<0.1	Ds,Lmy,Sl/Vgy
102	5129.0-30.0	4.5	155.0	1.7	Ds,Lmy,Sl/Vgy,V/F
103	5130.0-31.0	2.3	*	<0.1	Ds,Sl/Vgy
104	5131.0-32.0	3.1	9.4	0.2	Ds,Lmy,Sl/Vgy,V/F
105	5132.0-33.0	5.3	320.0	44.0	Ds,sl/Vgy,V/F
106	5133.0-34.0	2.1	837.0	<0.1	Ds,Lmy,Sl/Vgy,V/F
107	5134.0-35.0	3.6	468.0	19.0	Ds,Lmy,Sl/Vgy,V/F
108	5135.0-36.0	3.6	*	2.0	Ds,Lmy,Sl/Vgy,V/F
109	5136.0-37.0	1.5	0.1	<0.1	Ls,Sl/Ds
110	5137.0-38.0	3.6	<0.1	<0.1	Ls,Ds
111	5138.0-39.0	0.9	*	<0.1	Ls,Ds
112	5139.0-40.0	0.5	*	<0.1	Ls,Ds
113	5140.0-41.0	0.3	*	<0.1	Ls
114	5141.0-42.0	0.6	*	<0.1	Ls
115	5142.0-43.0	0.9	<0.1	<0.1	Ls
116	5143.0-44.0	1.1	<0.1	<0.1	Ls
117	5144.0-45.0	1.1	<0.1	<0.1	Ls
118	5145.0-46.0	1.5	*	<0.1	Ls
119	5146.0-47.0	2.3	*	<0.1	Ls

Table All-I (cont'd.)

120	5147.0-48.0	1.3	*	<0.1	Ls
121	5148.0-49.0	0.2	*	<0.1	Ls
122	5149.0-50.0	0.8	<0.1	<0.1	Ls,Sl/Ds
123	5150.0-51.0	0.5	<0.1	<0.1	Ls,Sl/Ds
124	5151.0-52.0	0.8	0.2	<0.1	Ls,Sl/Ds
125	5152.0-53.0	0.8	<0.1	<0.1	Ls,Ds
126	5153.0-54.0	0.7	<0.1	<0.1	Ls,Ds
127	5154.0-55.0	2.1	4.1	1.5	Ds
128	5155.0-56.0	1.6	0.1	<0.1	Ds,Sl/Lmy
129	5156.0-57.0	2.1	0.2	<0.1	Ds
130	5157.0-58.0	6.3	14.0	2.5	Ds,V/F
131	5158.0-59.0	4.1	207.0	0.3	Ds,V/F
132	5159.0-60.0	4.3	0.1	<0.1	Ds
133	5160.0-61.0	7.3	1.3	0.2	Ds,Lmy
134	5161.0-62.0	5.5	<0.1	<0.1	Ds,Lmy
135	5162.0-63.0	4.4	0.1	<0.1	Ds,Lmy
136	5163.0-64.0	0.2	*	<0.1	Ds,Lmy
137	5164.0-65.0	2.0	<0.1	<0.1	Ds
138	5165.0-66.0	6.7	6.3	2.6	Ds
139	5166.0-67.0	4.5	0.1	<0.1	Ds
140	5167.0-68.0	2.1	0.3	<0.1	Ds
141	5168.0-69.0	2.5	0.2	<0.1	Ds
142	5169.0-70.0	4.7	3.5	2.1	Ds
143	5170.0-71.0	3.8	147.0	0.1	Ds,V/F
144	5171.0-72.0	3.4	43.0	1.8	Ds,Sl/Lmy,V/F
145	5172.0-73.0	3.4	<0.1	<0.1	Ds,Sl/Lmy,V/F
146	5173.0-74.0	4.8	*	<0.1	Ds,Sl/Lmy
147	5174.0-75.0	2.1	<0.1	<0.1	Ds
148	5175.0-76.0	3.0	<0.1	<0.1	Ds
149	5176.0-77.0	2.3	0.4	<0.1	Ds
150	5177.0-78.0	0.4	<0.1	<0.1	Ls,Ds
151	5178.0-79.0	0.9	<0.1	<0.1	Ls,Ds
152	5179.0-80.0	0.3	<0.1	<0.1	Ls,Ds
153	5180.0-81.0	0.3	<0.1	<0.1	Ls,Sl/Ds
154	5181.0-82.0	0.4	<0.1	<0.1	Ls,Sl/Ds
155	5182.0-83.0	0.3	<0.1	<0.1	Ls,Ds
156	5183.0-84.0	0.3	<0.1	<0.1	Ls,Ds
157	5184.0-85.0	0.5	<0.1	<0.1	Ls,Ds

Table All-I (cont'd.)

158	5185.0-86.0	0.3	<0.1	<0.1	Ls,Ds
159	5186.0-87.0	0.4	<0.1	<0.1	Ls
160	5191.0-92.0	0.7	<0.1	<0.1	Ls
161	5195.0-96.0	0.5	<0.1	<0.1	Ls
162	5199.0-00.0	0.2	<0.1	<0.1	Ls
163	5231.0-32.0	4.3	<0.1	<0.1	Ls
164	5234.0-35.0	3.5	0.3	<0.1	Ls
165	5239.0-40.0	2.2	0.1	<0.1	Ls
166	5243.0-44.0	0.7	<0.1	<0.1	Ls,Sl/Ds
167	5244.0-45.0	0.6	<0.1	<0.1	Ds,Lmy
168	5245.0-46.0	2.2	<0.1	<0.1	Ds,Lmy
169	5246.0-47.0	5.1	0.5	0.3	Ls,Ds
170	5247.0-48.0	9.2	201.0	172.0	Ds,Lmy,V/F
171	5248.0-49.0	3.3	<0.1	<0.1	Ls
172	5249.0-50.0	2.0	<0.1	<0.1	Ls
173	5250.0-51.0	1.7	<0.1	<0.1	Ls
174	5251.0-52.0	6.2	0.3	<0.1	Ls,Ds
175	5252.0-53.0	0.9	<0.1	<0.1	Ds,Lmy
176	5253.0-54.0	1.4	<0.1	<0.1	Ls
177	5254.0-55.0	1.7	<0.1	<0.1	Ls,Ds

Total Harmon-Luck 1-1

1	4965.0-66.0	0.9	*	<0.1	Ls
2	4966.0-67.0	1.1	*	<0.1	Ls
3	4967.0-68.0	1.1	*	<0.1	Ls
4	4968.0-69.0	1.1	*	<0.1	Ls
5	4969.0-70.0	1.0	*	<0.1	Ls
6	4970.0-71.0	1.1	*	<0.1	Ls
7	4971.0-72.0	1.3	*	<0.1	Ls
8	4972.0-73.0	2.0	*	<0.1	Ls
9	4973.0-74.0	3.2	*	<0.1	Ls
10	4974.0-75.0	1.4	*	<0.1	Ls
11	4975.0-76.0	1.3	*	<0.1	Ls
12	4976.0-77.0	1.5	*	<0.1	Ls
13	4977.0-78.0	1.3	*	<0.1	Ls
14	4978.0-79.0	1.3	*	<0.1	Ls
15	4979.0-80.0	0.9	*	<0.1	Ls

Table All-1 (cont'd.)

16	4980.0-81.0	1.2	*	<0.1	Ls
17	4981.0-82.0	1.9	*	<0.1	Ls
18	4982.0-83.0	3.1	*	<0.1	Ls
19	4983.0-84.0	0.9	*	<0.1	Ls,Sl/Ds
20	4984.0-85.0	2.2	*	<0.1	Ls
21	4985.0-86.0	2.4	*	<0.1	Ls
22	4986.0-87.0	3.2	*	<0.1	Ls
23	4987.0-88.0	1.3	*	<0.1	Ls
24	4988.0-89.0	2.1	*	<0.1	Ls
25	4989.0-90.0	2.2	*	<0.1	Ls
26	4990.0-91.0	0.8	*	<0.1	Ls
27	4991.0-92.0	0.7	*	<0.1	Ls
28	4992.0-93.0	0.7	*	<0.1	Ls
29	4993.0-94.0	0.7	*	<0.1	Ls
30	4994.0-95.0	0.7	*	<0.1	Ls

Total Hankerd 1-17

1	4841.0-42.0	0.6	<0.1	<0.1	Ls,Sl/Ds
2	4842.0-43.0	0.4	<0.1	<0.1	Ls,Ds
3	4843.0-44.0	0.4	<0.1	<0.1	Ls,Ds
4	4844.0-45.0	0.4	<0.1	<0.1	Ls,Ds
5	4880.0-81.0	0.4	<0.1	<0.1	Ls
6	4881.0-82.0	0.6	<0.1	<0.1	Ls
7	4882.0-83.0	0.5	<0.1	<0.1	Ls
8	4883.0-84.0	0.7	<0.1	<0.1	Ls,Sl/Ds
9	4884.0-85.0	0.7	<0.1	<0.1	Ls
10	4885.0-86.0	0.5	<0.1	<0.1	Ls
11	4886.0-87.0	0.4	<0.1	<0.1	Ls

Total Emil Faist 1-12

1	4896.0-97.0	3.0	<0.1	<0.1	Ds,V/Sl/Lmy
2	4897.0-98.0	3.2	<0.1	<0.1	Ds,V/Sl/Lmy
3	4898.0-99.0	1.7	<0.1	<0.1	Ds,V/Sl/Lmy

Table All-1 (cont'd)

Total Luck 2-12

1	4856.0-57.0	3.4	<0.1	<0.1	Ds
2	4857.0-58.0	3.0	<0.1	<0.1	Ds
3	5017.0-18.0	1.4	*	<0.1	Ds
4	5018.0-19.0	2.5	*	<0.1	Ds
5	5019.0-20.0	1.8	<0.1	<0.1	Ds
6	5020.0-21.0	0.9	<0.1	<0.1	Ls, Ds
7	5021.0-22.0	1.1	<0.1	<0.1	Ls, Ds
8	5022.0-23.0	1.2	<0.1	<0.1	Ds, Lmy
9	5023.0-24.0	7.2	5.9	0.8	Ds, Lmy, Sl/Vgy, V/F
10	5024.0-25.0	8.4	417.0	0.2	Ds, Lmy, Sl/Vgy, V/F
11	5025.0-26.0	2.7	*	<0.1	Ds
12	5026.0-27.0	4.1	*	<0.1	Ds, Lmy
13	5027.0-28.0	3.9	<0.1	<0.1	Ds
14	5028.0-29.0	5.4	*	<0.1	Ds, Lmy
15	5029.0-30.0	6.8	*	29.0	Ds
16	5030.0-31.0	4.7	4.1	0.1	Ds, V/F
17	5031.0-32.0	4.0	245.0	<0.1	Ds, V/F
18	5032.0-33.0	1.7	*	<0.1	Ds
19	5033.0-34.0	2.2	<0.1	<0.1	Ds, Lmy
20	5034.0-35.0	2.0	45.0	<0.1	Ds, V/F
21	5036.0-37.0	2.5	4.3	<0.1	Ds
22	5037.0-38.0	4.0	2.8	0.1	Ds
23	5038.0-39.0	2.7	0.1	<0.1	Ds
24	5039.0-40.0	1.8	<0.1	<0.1	Ds
25	5040.0-41.0	2.4	<0.1	<0.1	Ds
26	5041.0-42.0	3.2	0.1	<0.1	Ds
27	5042.0-43.0	1.2	<0.1	<0.1	Ds
28	5043.0-44.0	2.2	0.1	<0.1	Ds
29	5044.0-45.0	1.3	<0.1	<0.1	Ls, Ds
30	5045.0-46.0	1.3	<0.1	<0.1	Ls, Ds
31	5046.0-47.0	2.3	<0.1	<0.1	Ds
32	5047.0-48.0	3.2	0.5	0.2	Ds
33	5048.0-49.0	2.2	<0.1	<0.1	Ds
34	5049.0-50.0	1.8	<0.1	<0.1	Ds, Lmy
35	5050.0-51.0	1.3	<0.1	<0.1	Ls, Ds
36	5052.0-53.0	1.1	<0.1	<0.1	Ls, Ds

Table All-I (cont'd.)

37	5054.0-55.0	1.3	<0.1	<0.1	Ls,Ds
38	5056.0-57.0	0.8	<0.1	<0.1	Ls,Ds
39	5058.0-59.0	1.0	<0.1	<0.1	Ls,Ds
40	5060.0-61.0	1.0	<0.1	<0.1	Ls,SI/Ds
41	5062.0-63.0	0.9	<0.1	<0.1	Ls,SI/Ds
42	5064.0-65.0	1.0	<0.1	<0.1	Ls,SI/Ds
43	5066.0-67.0	0.6	<0.1	<0.1	Ls,SI/Ds
44	5068.0-69.0	0.6	<0.1	<0.1	Ls,Ds
45	5070.0-71.0	0.5	<0.1	<0.1	Ls,SI/Ds
46	5075.0-76.0	1.2	<0.1	<0.1	Ls
47	5077.0-78.0	0.7	<0.1	<0.1	Ls,Ds
48	5080.0-81.0	0.9	<0.1	<0.1	Ls,Ds
49	5082.0-83.0	1.2	<0.1	<0.1	Ls,SI/Ds
50	5083.0-84.0	0.8	<0.1	<0.1	Ls,Ds
51	5084.0-85.0	1.2	<0.1	<0.1	Ls,SI/Ds
52	5085.0-86.0	1.0	<0.1	<0.1	Ls/Ds
53	5086.0-87.0	0.7	<0.1	<0.1	Ls,Ds
54	5087.0-88.0	0.7	<0.1	<0.1	Ls,Ds
55	5088.0-89.0	0.9	<0.1	<0.1	Ls
56	5089.0-90.0	1.0	<0.1	<0.1	Ls,SI/Ds
57	5090.0-91.0	0.6	<0.1	<0.1	Ls,Ds
58	5091.0-92.0	0.9	<0.1	<0.1	Ls,Ds
59	5092.0-93.0	1.8	<0.1	<0.1	Ls,Ds
60	5093.0-94.0	3.8	1.8	1.7	Ls,Ds
61	5094.0-95.0	0.7	<0.1	<0.1	Ls,Ds
62	5095.0-96.0	1.0	23.0	<0.1	Ls,Ds,V/F
63	5096.0-97.0	0.9	<0.1	<0.1	Ls,Ds
64	5097.0-98.0	1.2	<0.1	<0.1	Ls,Ds
65	5098.0-99.0	1.4	<0.1	<0.1	Ls,Ds
66	5099.0-00.0	1.5	<0.1	<0.1	Ls,Ds
67	5100.0-01.0	1.6	<0.1	<0.1	Ls,Ds
68	5101.0-02.0	0.5	<0.1	<0.1	Ls,SI/Ds
69	5102.0-03.0	0.8	<0.1	<0.1	Ls,Ds
70	5103.0-04.0	1.7	<0.1	<0.1	Ls,Ds
71	5104.0-05.0	0.8	<0.1	<0.1	Ls,Ds
72	5105.0-06.0	1.5	0.1	0.1	Ds,Lmy
73	5106.0-07.0	1.8	0.1	<0.1	Ls,Ds
74	5107.0-08.0	1.6	0.1	0.1	Ls,Ds

Table All-I (cont'd.)

75	5108.0-09.0	1.6	0.1	<0.1	Ls,Ds
76	5109.0-10.0	2.7	0.7	0.6	Ls
77	5110.0-11.0	2.0	<0.1	<0.1	Ls,Ds
78	5111.0-12.0	2.1	0.1	<0.1	Ls,Ds
79	5113.0-14.0	1.5	<0.1	<0.1	Ls,Ds
80	5115.0-16.0	1.8	86.0	<0.1	Ls,Ds,Y/F
81	5117.0-18.0	1.0	<0.1	<0.1	Ls,Ds
82	5119.0-20.0	1.0	<0.1	<0.1	Ls,Sl/Ds
83	5121.0-22.0	1.1	<0.1	<0.1	Ls,Sl/Ds
84	5123.0-24.0	1.2	<0.1	<0.1	Ls,Ds
85	5125.0-26.0	0.7	<0.1	<0.1	Ls
86	5127.0-28.0	1.3	<0.1	<0.1	Ls,Ds
87	5129.0-30.0	1.5	<0.1	<0.1	Ls,Ds
88	5131.0-32.0	1.4	<0.1	<0.1	Ls,Ds

* Indicates plug permeability

Total Average
Dolomite Porosity 3.1
Standard Deviation 1.4
Number of Samples 170

Total Average
Limestone Porosity 1.3
Standard Deviation 0.9
Number of Samples 62

Total Average
Partial Dolomite Porosity 1.9
Standard Deviation 1.9
Number of Samples 169

Symbols Used:

Anhy - anhydrite

Sl - slight

Sty - stylolites

Ygy - vuggy

Ds - dolomite

Ls - limestone

Shly - shale

APPENDIX III

APPENDIX III

W-TEST TO DETERMINE THE NORMALITY OF THE TRACE ELEMENT DATA IN THE TRENTON DOLOMITES

The following is the statistical analysis to determine if the geochemical data has a normal or lognormal distribution. This was done in order to define which test would be used to determine if the data sets were statistically different.

The W-test is a method for testing whether a data set has been drawn from a normal distribution (Gilbert, 1987). If the test is conducted on the logarithms of the data, the hypothesis of a lognormal distribution can also be evaluated. This test is good for data sets of 50 samples or less. All of the samples tested were from the Total Luck 1-12 and 2-12 wells, because these wells have the greatest number of samples.

The W-test

The first step is to determine the null hypothesis;

Ho = the population has a normal distribution

1) $d = \sum (x_i - \bar{x})^2$

2) Arrange data from the smallest to the largest

3) Compute K

$$K = n/2 \quad \text{if } n \text{ is even}$$

$$K = n-1/2 \quad \text{if } n \text{ is odd}$$

4) Obtain coefficients a_1 -- a_k from a statistical table

5) Compute

$$W = 1/d [\sum a_i (x_{[n-1+j]} - x_{[i]})^2]$$

6) Reject H_0 at the α significance level if W is less than the quartile given in the table.

STRONTIUM

The strontium values are from the Total Luck 1-12 and Total Luck 2-12 cores ($n= 29$).

$$\begin{aligned} W = 1/18,343 \quad & [0.4291(203-96) + 0.2968(202-102) + 0.2499(188-122) + \\ & 0.2150(181-123) + 0.1864(162-125) + 0.1616(161-125)+ \\ & 0.1395(159-127) + 0.1192(157-129) + 0.1002(155-129)+ \\ & 0.0822(155-130) + 0.0650(150-134) + 0.0483(149-135)+ \\ & 0.0320(144-139) + 0.0159(141-139)]^2 \end{aligned}$$

$$W = 1/18,343 * \{131\}^2$$

$$W = 0.936$$

W at (95% CI) = 0.926

The calculated W is greater than W_{α} , we therefore accept the null hypothesis that this population has been drawn from a normal population.

MANGANESE

The manganese values are from the Total Luck 1-12 and 2-12 cores (n=25).

$$W = 1/1,391,308 \{0.4450[2079-1213] + 0.3069[2078-1268] + \\ 0.2543[2001-1287] + 0.2148[1850-1298] + \\ 0.1822[1819-1385] + 0.1539[1791-1425] + \\ 0.1283[1777-1489] + 0.1046[1768-1518] + \\ 0.0823[1736-1557] + 0.0610[1714-1589] + \\ 0.0403[1708-1622] + 0.0200[1685-1626]\}^2$$

$$W = 1/1,391,308 * (1160)^2$$

$$W = 0.967$$

W at (95% CI) is 0.918

The calculated W is greater than W_{α} , we therefore accept the null hypothesis that this population has been drawn from a normal population.

IRON

The iron values are from the Total Luck 1-12 and Total Luck 2-12 cores

(n= 25).

$$W = 1/7.14 \times 10^8 [.4493(36486-15676) + .3098(34918-16221) + .2554(29329-17778) + .2145(28200-18188) + .1807(27236-18329) + .1512(27143-18329) + .1245(25891-18879) + .0997(25057-18913) + .0764(24563-19090) + .0539(23056-19262) + .0321(22677-19634) + .0107(22112-21015)]^2$$

$$W = 1/7.14 \times 10^8 [25400]^2$$

$$W = .904$$

W at (98% CI) is 0.901

The calculated W is greater than W_{α} , we therefore accept the null hypothesis that this population has been drawn from a normal population.

Zinc

The zinc values are from the Total Luck 1-12 and 2-12 cores (n=25).

$$W = 1/123 [.4450(10-1) + .3069(9-2) + .2543(6-2) + .2148(6-2) + .1822(5-2) + .1539(5-2) + .1283(5-2) + .1046(5-2) + .0823(5-2) + .0610(5-2) + .0403(4-3) + .0200(4-3)]^2$$

$$W = 1/123 [9]^2$$

$$W = .660$$

W at (95% CI) is 0.918

The calculated W is lower than W_α , we therefore reject the null hypothesis that this population has been drawn from a normal population.

Taking the natural log of the values and performing the same test results in:

$$W = 1/7.82 \quad [.4450(2.3-0.0) + .3069(2.2-.69) + .2543(1.79-.69) + .2148(1.79-.69) + .1822(1.61-.69) + .1539(1.61-.69) + .1283(1.61-.69) + .1046(1.61-.69) + .0823(1.61-.69) + .0610(1.61-.69) + .0403(1.39-1.10) + .0200(1.39-1.10)]^2$$

$$W = 1/7.82 [2.71]^2$$

$$W = .939$$

W at (95% CI) is 0.918

The calculated W is greater than W_α , we therefore accept the null hypothesis that this population has been drawn from a lognormal population.

APPENDIX IV

APPENDIX IV

A COMPARISON OF COMPENSATED NEUTRON LOG POROSITIES OF THE NONCONGLOMERITIC ZONES AND WHOLE-CORE POROSITIES OF THE CONGLOMERITIC ZONES IN THE TRENTON FORMATION DOLOMITES

TABLE AIV-1. COMPENSATED NEUTRON LOG POROSITY COMPARISON OF THE
NONCONGLOMERITIC ZONES IN THE TRENTON FORMATION DOLOMITES.

Sample	Total Hicks-Martin 1-11 (West)	Total Luck 2-12 (East)
1	2.0	2.0
2	2.0	1.0
3	2.0	1.0
4	2.0	2.7
5	2.0	8.0
6	2.5	6.0
7	3.0	8.0
8	4.0	8.0
9	4.0	7.5
10	5.0	6.0
11	5.0	5.8
12	5.0	5.0
13	1.0	4.0
14	1.0	3.0
15	1.5	2.0
16	1.5	4.5
17	2.0	2.8
18	2.3	0.5
19	2.5	0.2
20	2.5	1.0
21	2.0	0.2
22	2.0	0.3
23	1.0	0.3
24	1.0	0.2

Table AIV1-1 (cont'd.)

25	1.0	0.0
26	1.0	0.5
27	1.0	2.0
28	1.0	2.5
29	1.0	1.0
30	0.5	
31	0.5	
32	1.0	
33	2.0	
34	2.0	
35	1.0	
36	1.0	
37	1.0	
38	1.0	
39	1.0	
40	0.5	
41	0.8	
42	0.8	
43	0.8	
44	0.8	
45	0.8	
46	0.8	

Mean	=	1.7	2.9
S.D.	=	1.2	2.7

Applying a standard T-test to the data indicates that there is no significant difference in porosity between the two populations.

TABLE AIV-2. WHOLE CORE POROSITY COMPARISON OF THE CONGLOMERITIC HORIZON IN THE TRENTON FORMATION DOLOMITES.

Sample	Total Emil Faist 2-12 (West)	Total Luck 1-12 (East)
1	1.7	3.5
2	1.1	5.3
3	1.7	4.5
4	2.6	6.4
5	2.7	3.7
6	3.7	4.3
7	1.9	2.7
8	2.1	2.9
9	2.3	1.8
10	2.8	1.6
11	2.3	8.9
12	1.6	5.9
13	2.7	6.9
14	2.0	3.8
15	2.7	3.1
16	1.4	3.0
17	3.8	6.2
18	2.1	8.3
19	2.8	6.4
20	4.2	2.9
21	1.1	3.2
22	3.1	3.4
23	3.5	3.7
24	6.1	3.6
25	0.9	3.5
26	2.2	3.9
27	3.0	2.7
28	1.8	3.7
29	2.6	4.0
30	2.0	3.3
31	1.1	4.8
32	3.4	3.3
33	2.5	3.6

Table AIV-2 (cont'd.)

34	2.6	3.2
35	7.1	3.3
36	4.0	2.4
37	3.2	3.6
38	3.1	3.4
39	2.1	3.0
40	1.3	4.0
41	2.3	2.5
42	2.3	2.7
43	5.3	2.9
44	2.1	4.1
45	2.1	3.5
46	6.3	3.8
47	4.1	2.3
48	4.3	3.0
49	2.0	3.7
50	6.7	4.8
51	4.5	3.4
52	2.1	2.3
53	2.5	3.2
54	4.7	3.0
55	3.8	3.0
56	2.1	3.1
57	3.0	3.0
58	2.3	2.7
59		3.4
60		3.4
61		5.4
62		3.4
63		3.0
64		4.5
65		5.1
66		3.8
67		3.6
68		2.5
69		3.0
70		2.1
71		2.3
72		2.6

Table AIV-2 (cont'd.)

73		2.5
74		3.1
<hr/>		
Mean =	2.9	3.7
S.D. =	1.4	1.4

Applying a standard T-test to the data indicates that there is no significant difference in porosity between the two populations.

REFERENCES

REFERENCES

- ADAMS, J.E. AND RHODES, M.L., 1960, Dolomitization by seepage refluxion: American Association of Petroleum Geologists Bulletin, v. 44, p. 1912-1920.
- AHARON, P., SOCKI, R.A. AND CHAN, L., 1987, Dolomitization of atolls by sea water convection flow: test of a hypothesis at Niue, South Pacific: Journal of Geology, v. 95, p. 187 - 203.
- ARMSTRONG, A.K., 1970, Mississippian dolomites from Lisburne Group, Killik River, Mount Bupto region, Brooks Range, Alaska: American Association of Petroleum Geologists Bulletin, v. 54, p. 251-264.
- BADIOZAMANI, K., 1973, The Dorag dolomitization model application to the Middle Ordovician of Wisconsin: Journal of Sedimentary Petrology, v. 43, p. 965-984.
- BAKER, P.A. AND BURNS, S.J., 1985, Occurrence and formation of dolomite in organic-rich continental margin sediments: American Association of Petroleum Geologists, v. 69, p. 1917-1930.
- BAKER, P.A. AND KASTNER, M., 1981, Constraints on the formation of sedimentary dolomite: Science v. 213, p. 214-216.
- BANDOIAN, C.A. AND MURRAY, R.C., 1977, Plio-Pleistocene carbonate rocks of Bonaire, Netherlands Antilles: Geological Society of America Bulletin, v. 85, p. 965-984.
- BARBER, C., 1974, Major and trace element associations in limestones and dolomites: Chemical Geology, v. 14, p. 273-280.
- BARRETT, M.L., 1986, Replacement geometry and fabrics of the Smackover (Jurassic) dolomite, southern Alabama: Transactions Gulf Coast Association of Geological Societies, v., 36, p. 9-18.

- BARTLETT, T.R., 1984, Synthetic dolomitization: Rate effects of variable mineralogy, surface area, external CO_3^{2-} - and crystal seeding: M.S. Thesis, Michigan State University.
- BATHURST, R.C., 1975, Carbonate Sediments and Their Diagenesis: Developments in Sedimentology, 12, New York, Elsevier, 658 p.
- BAUM, G.R., HARRIS, W.B. and DREZ, P.E., 1985, Origin of dolomite in the Eocene Castle Hayne limestone, North Carolina: Journal of Sedimentary Petrology, v. 55, p. 506-517.
- BEHRENS, W.E. AND LAND, L.S., 1972, Subtidal Holocene dolomite, Baffin Bay, Texas, Journal of Sedimentary Petrology, v.42, p. 155-161.
- BOISTELLE, R., 1982, Mineral crystallization from solution, in Rodriguez, R., and Sunagawa, I., eds., Crystal Growth in Sedimentary Environments: Estudios Geol. Proceedings of the First International Symposium on Crystal Growth, Processes in Sedimentary Environments, Madrid, v. 38, p. 135-152.
- BULLEN, S.B. AND SIBLEY, D.F., 1984, Dolomite selectivity and mimic replacement: Geology, v. 12, p. 655-658.
- BURNS, S.J. AND BAKER, P.A., 1987, A geochemical study of dolomite in the Monterey Formation, California: Journal of Sedimentary Petrology, v. 57, p. 128-139.
- CARBALLO, J.D., LAND, L.S. AND MISER, D.E., 1987, Holocene dolomitization of supratidal sediments by active tidal pumping, Sugarloaf Key, Florida: Journal of Sedimentary Petrology, v. 57, p. 153-165.
- CHAFETZ, H.S., WILKINSON, B.H. AND LOVE, K.M., 1985, Morphology and composition of non-marine carbonate cements in near surface settings: in Schneidermann, N. and Harris, P.M. eds., Carbonate Cements: Society of Economic Paleontologists and Mineralogists Special Publication 36, p. 337-347.
- CHILINGER, G.V., 1956, Use of Ca/Mg ratio in porosity studies: Bulletin of American Association of Petroleum Geologists, v. 40, p. 2489-2493.

- CHOQUETTE, P.W. AND STEINEN, R.P., 1980, Mississippian non-supratidal dolomite, Ste. Genevieve limestone, Illinois Basin: evidence for mixed water dolomitization: in Zenger, D.H., and Dunham, J.B., eds., Concepts and Models of Dolomitization: Society of Economic Paleontologists and Mineralogists Special Publication 28, p. 163-196.
- CHOQUETTE, P.W. AND STEINEN, R.P., 1985, Mississippian oolite and non-supratidal dolomite reservoirs in the Ste. Genevieve Formation, North Bridgeport Field, Illinois Basin: in Roehl, P.O. and Choquette, P.W. eds., Carbonate Petroleum Reservoirs, Springer-Verlag New York, Inc., p. 207-225.
- CHRISTIAN, J.W., 1975, The Theory of Transformations in Metals and Alloys: Part 1, Equilibrium and General Kinetic Theory, New York, Pergamon Press, second edition, 586 p.
- CHURNET, H.G. AND MISRA, K.C., 1981, Genetic implications of the trace element distribution pattern in the Upper Knox carbonate rocks, Copper Ridge District, East Tennessee: *Sedimentology*, v. 30, p. 173-194.
- CLEMENT, J.H., 1985, Depositional sequences and characteristics of Ordovician Red River reservoirs, Pennel Field, Williston Basin, Montana: in Roehl, P.O. and Choquette, P.W. eds., Carbonate Petroleum Reservoirs, Springer-Verlag New York, Inc., p. 72-84.
- CRAIG, H., 1957, Isotopic standards for carbon and oxygen and correction factors for mass-spectrometric analysis of carbon dioxide: *Geochimica et Cosmochimica Acta*, v. 12, p. 133-149.
- CURTIS, C.D., 1978, Possible links between sandstone diagenesis and depth-related geochemical reactions occurring in enclosing mudstones: *Journal of the Geological Society of London*, v. 135, p. 107-117.
- DEBUISONJE, P.H., 1974, Neogene and Quaternary geology of Aruba, Curacao and Bonaire: The Hague, Martinus Nijhoff, 291 p.
- DEFFEYES, K.S., LUCIA, F.J., AND WEYL, P.K., 1965, Dolomitization of Recent and Plio-Pleistocene sediments by marine evaporate waters on

- Bonaire, Netherlands Antilles: in Pray, L.C., and Murray, R.C., eds., Dolomitization and Limestone Diagenesis: Society of Economic Paleontologists and Mineralogists Special Publication 13, p. 71-88.
- DRAVIS, J.J. AND YUREWICZ, D.A., 1985, Enhanced carbonate petrography using fluorescence microscopy: *Journal of Sedimentary Petrology*, v. 55, p. 795-804.
- DREYER, J.I., 1982, *The Geochemistry of Natural Water*, Englewood Cliffs, New Jersey, Prentice-Hall, 388 p.
- DUNHAM, J.B. AND OLSEN, E.R., 1980, Shallow subsurface dolomitization of subtidally deposited carbonate sediments in the Hanson Creek Formation (Ordovician-Silurian) of central Nevada: in Zenger, D.H., and Dunham, J.B., eds., *Concepts and Models of Dolomitization*: Society of Economic Paleontologists and Mineralogists Special Publication 28, p. 139-161.
- ELLS, G.D., 1962, Structures associated with the Albion-Scipio Oil Field trend: Michigan Department of Conservation, Geological Survey Division, 86 p.
- ENOS, P. AND SAWATSKY, L.H., 1981, Pore networks in Holocene carbonate sediments: *Journal of Sedimentary Petrology*, v. 51, p. 961-985.
- FISHER, W.L. AND RODDA, P.U., 1969, Edwards Formation (Lower Cretaceous), Texas: Dolomitization in a carbonate platform system: *American Association of Petroleum Geologists*, v. 53, p. 55-72.
- FROELICH, P.N., KLINKHAMMER, G.P., BENDER, M.L., LUEDTKE, N.A., HEATH, G.R., CULLEN, D. AND DAUPHIN, P., 1979, Early oxidation of organic matter in pelagic sediments of the eastern equatorial Atlantic: Suboxic diagenesis: *Geochimica et Cosmochimica Acta*, v. 43, p. 1075-1090.
- GAINES, A.M., 1980, Dolomitization kinetics: Recent experimental studies: in Zenger, D.H., and Dunham, J.B., eds., *Concepts and Models of Dolomitization*: Society of Economic Paleontologists and Mineralogists Special Publication 28, p. 81-86.
- GAWTHORPE, R.L., 1987, Burial dolomitization and porosity development in a mixed carbonate-clastic sequence: an example from the Bowland

- Basin, northern England: Sedimentology, v. 34, p. 533-558.**
- GRAF, D.L. AND GOLDSMITH, J.R., 1956, Some hydrothermal syntheses of dolomite and protodolomite: Journal of Geology, v. 64, p. 173-186.**
- GREGG, J.M. AND SIBLEY, D.F., 1984, Epigenetic dolomitization and the origin of xenotopic dolomite texture: Journal of Sedimentary Petrology, v. 54, p. 908-931.**
- GREGG, J.M. AND SHELTON, K.L., in press, Minor and trace element distributions in the Bonneterre dolomite (Cambrian), southeast Missouri - Evidence for multiple basin fluid sources and pathways during lead-zinc mineralization:**
- GUEDDARI, M., MONNIN, C., PERRET, B.F., AND TARDY, Y., 1983, Geochemistry of brines of the Chott El Jerid in southern Tunisia - application of Pitzer's equations: Chemical Geology, v. 39, p. 165-178.**
- HALLEY, R.B. AND SCHMOKER, J.W., 1983, High-porosity Cenozoic rocks of South Florida: progressive loss of porosity with depth: American Association of Petroleum Geologists Bulletin, v. 67, p. 191-200.**
- HANSHAW, B.B., BACK, W. AND DEIKE, R.G., 1971, A geochemical hypothesis for dolomitization by ground water: Economic Geology, v. 66, p. 710-724.**
- JODRY, R.L., 1969, Growth and dolomitization of Silurian reefs, St. Clair County, Michigan: American Association of Petroleum Geologists Bulletin, v. 53, p. 957-981.**
- KATZ, A. AND MATTHEWS, A., 1977, The dolomitization of CaCO_3 : an experimental study at 252-295°C: Geochimica et Cosmochimica Acta, v. 41, p. 297-308.**
- KRUMGALZ, B.S. AND MILLERO, F.J., 1982, Physico-chemical study of the Dead Sea waters, I. Activity coefficients of major ions in Dead Sea water: Marine Chemistry, v. 11, p. 209-222.**
- LAND, L.S., 1973a, Contemporaneous dolomitization of Middle Pleistocene reefs by meteoric water, North Jamaica: Bulletin of Marine Science, v.**

23, p. 64-92.

- LAND, L.S., 1973b, Holocene meteoric dolomitization of Pleistocene limestones, North Jamaica: *Sedimentology*, v. 20, p. 411-424.
- LAND, L.S., SALEM, M.R.I. AND MORROW, D.W., 1975, Paleohydrology of ancient dolomites: Geochemical evidence: *American Association of Petroleum Geologists Bulletin*, v. 59, p. 1602-1625.
- LAND, L.S., 1980, The isotopic and trace element geochemistry of dolomite: The state of the art, in Zenger, D.H., and Dunham, J.B., eds., *Concepts and Models of Dolomitization*: Society of Economic Paleontologists and Mineralogists Special Publication 28, p. 87-110.
- LANDES, K.K., 1946, Porosity through dolomitization: *American Association of Petroleum Geologists Bulletin*, v. 30, p. 305-318.
- LAWRENCE, J.R., 1973, Interstitial water studies, LEG 15 - Stable oxygen and carbon isotope variations in water, carbonates, and silicates from the Venezuela Basin (SITE 149) and the Aves Rise (SITE 148): in HEEZEN, B.C. and MACGREGOR, I.D. eds., *Initial Reports of the Deep Sea Drilling Project, Volume 20*, Washington (U.S. Government Printing Office) p. 891- 899.
- LONGMAN, M.W., FERTAL, T.G., AND GLENNIE, J.S., 1983, Origin and Geometry of Red River Dolomite Reservoirs, Western Williston Basin: *American Association of Petroleum Geologists Bulletin*, v. 67, p. 744-771.
- LUCIA, F.J., 1962, Diagenesis of a crinoidal sediment: *Journal of Sedimentary Petrology*, v. 32, p. 848-865.
- MACHEL H.G., in press, Fluid flow direction during dolomitization as deduced from trace element trends: in BAKER, P.A. and SHUKLA, V.J. eds., *Dolomite Formation and Diagenesis - Recent Advances and Unsolved Problems*: Society of Economic Paleontology and Mineralogy Special Publication,
- MACHEL, H.G. AND MOUNTJOY, E.W., 1986, Chemistry and environments of dolomitization - a reappraisal: *Earth Science Reviews*, v. 23, p. 175-222.

- MAGARITZ, M., ISSAR, A. AND AZMON, E., 1983, On the genesis of discordant dolostone bodies in the Northeastern Negev, Israel: *Chemical Geology*, v. 39, p. 93-114.
- MATTES, B.W. AND MOUNTJOY, E.W., 1980, Burial dolomitization of the Upper Devonian Miette Buildup, Jasper National Park, Alberta: in Zenger, D.H., and Dunham, J.B., eds., *Concepts and Models of Dolomitization: Society of Economic Paleontologists and Mineralogists Special Publication 28*, p. 259-297.
- MAZZULLO, S.J., REID, A.M. AND GREGG, J.M., 1987, Dolomitization of Holocene Mg-calcite supratidal deposits, Ambergris Cay, Belize: *Geological Society of America Bulletin*, v. 98, p. 224-231.
- MESHER, P.K., 1980, Structural evolution of SE Michigan - Middle Ordovician to Middle Silurian; MS Thesis Michigan State University.
- MILLERO, F.J. and SCHREIBER, D.R., 1982, Use of the ion pairing model to estimate activity coefficients of the ionic components of natural waters: *American Journal of Science*, v. 282, p. 1508-1540.
- MITCHELL, J.T., LAND, L.S. AND MISER, D.E., 1987, Modern marine dolomite cement in a North Jamaican fringing reef, *Geology*, v. 15, p. 557-560.
- MULLINS, H.T., WISE Jr, S.W., LAND, L.S., SIEGEL, D.I., MASTERS, P.M., HINCHEY, E.J. AND PRICE, K.R., 1985, Authigenic dolomite in Bahamian peri-platform slope sediment: *Geology*, v. 13, p. 292-295.
- MURRAY, A.N., 1930, Limestone oil reservoirs of the northeastern United States and Ontario, Canada: *Economic Geology*, v. 25, p. 452-469.
- MURRAY, R.C., 1960, Origin of porosity in carbonate rocks: *Journal of Sedimentary Petrology*, v. 30, p. 58-84.
- MURRAY, R.C. AND LUCIA, F.J., 1967, Cause and control of dolomite distribution by rock selectivity: *Geological Society of America Bulletin*, v. 78, p. 21-35.
- PARKER, W.C., RAGLANG, P.C. AND TEXORIS, D.A., 1985, Controls on trace

elements in the Ordovician Black River Group, New York, U.S.A.:
Chemical Geology, v. 53, p. 83-94.

- PRESLEY, B.J. AND KAPLAN, I.R., 1968, Changes in dissolved sulfate, calcium and carbonate from interstitial water of near-shore sediments: *Geochimica et Cosmochimica Acta*, v. 32, p. 1037-1048.
- POWERS, R.W., 1962, Arabian Upper Jurassic carbonate reservoir rocks: in Ham, W.E., ed., *Classification of carbonate rocks - a symposium*: American Association of Petroleum Geologists Memoir 1, p. 122-192.
- RAO, N.V.N.D., AL-IMAM, O.A.O. AND BEHAIRY, A.K.A., 1987, Early mixed-water dolomitization in the Pleistocene reef limestones, West coast of Saudi Arabia: *Sedimentary Geology*, v. 53, p. 231-245.
- ROSEN, M.R., MISER, D.E. AND WARREN, J.K., 1988, Sedimentology, mineralogy and isotopic analysis of Pellet Lake, Coorong Region, South Australia, *Sedimentology*, v. 35, p. 105-122.
- RUZYLA, K AND FREIDMAN, G.M., 1985, Factors Controlling porosity in dolomite reservoirs of the Ordovician Red River Formation, Cabin Creek Field, Montana: in Roehl, P.O. and Choquette, P.W. eds., *Carbonate Petroleum Reservoirs*, Springer-Verlag New York, Inc., p. 40-58.
- SALLER, A.H., 1984a, Petrologic and geochemical constraints on the origin of subsurface dolomite, Enewetak Atoll: an example of dolomitization by normal seawater: *Geology*, v. 12, p. 217-220.
- SALLER, A.H., 1984b, Diagenesis of Cenozoic limestones on Enewetak Atoll: Ph.D. Dissertation, Louisiana State University, 363p.
- SASS, E. AND KATZ, A., 1982, The origin of platform dolomites: New evidence: *American Journal of Science*, v. 282, p. 1184-1213.
- SCHMOKER, J.W. AND HALLEY, R.B., 1982, Carbonate porosity verses depth: A predictable relation for south Florida: *American Association of Petroleum Geologists Bulletin*, v. 66, p. 2561-2570.
- SCHMOKER, J.W., KRYSTINIK, K.B., AND HALLEY, R.B., 1985, Selected characteristics of limestone and dolomite reservoirs in the United States: *American Association of Petroleum Geologists Bulletin*, v. 69,

p. 733-741.

- SEARS, S.O. AND LUCIA, F.J., 1980, Dolomitization of northern Michigan Niagaran reefs by brine refluxion and freshwater/seawater mixing: in Zenger, D.H., and Dunham, J.B., eds., Concepts and Models of Dolomitization: Society of Economic Paleontologists and Mineralogists Special Publication 28, p. 215-235.
- SHAW, B., 1975, Geology of the Albion-Scipio Trend, southern Michigan. MS Thesis, University of Michigan.
- SIBLEY, D.F., 1980, Climatic control of dolomitization, Sero Domi Formation (Pliocene), Bonaire, N.A., in Zenger, D.H. and Dunham, J.B., eds., Concepts and Models of Dolomitization: Society of Economic Paleontologists and Mineralogists Special Publication 28, p. 247-258.
- SIBLEY, D.F., 1982, The origin of common dolomite fabrics: clues from the Pliocene: *Journal of Sedimentary Petrology*, v. 52, p. 1087-1100.
- SIBLEY, D.F. AND GREGG, J.M., 1987, Classification of dolomite rock textures: *Journal of Sedimentary Petrology*, v. 57, p. 967-975.
- SIBLEY, D.F., DEDDOES, R.E. AND BARTLETT, T.R., 1987, Kinetics of dolomitization: *Geology*, v. 15, p. 1112-1114.
- SIMMS, M., 1984, Dolomitization by groundwater-flow systems in carbonate platforms: *Transactions - Gulf Coast Association of Geological Societies*, v. 34, p. 411-420.
- SUPKO, P.R., 1971, "Whisker" crystal cement in a Bahamian rock, in Carbonate Cements, Studies in Geology 19: Johns Hopkins Press, Baltimore, Maryland, p. 143-146.
- TAYLOR, T.R., 1982, Petrographic and geochemical characteristics of dolomite types and the origin of ferroan dolomite in the Trenton Formation, Michigan Basin: Ph.D. Dissertation, Michigan State University, 75p.
- TAYLOR, T.R. AND SIBLEY, D.F., 1986, Petrographic and geochemical characteristics of dolomite types and the origin of ferroan dolomite

in the Trenton Formation, Ordovician, Michigan Basin, U.S.A.:
Sedimentology, v. 33, p. 61-86.

TLIG, S. AND M'RABET, A., 1985, A comparative study of Rare Earth Element (REE) distributions within the Lower Cretaceous dolomites and limestones of Central Tunisia: Sedimentology, v. 32, p. 897-907.

VAN TUYL, F.M., 1914, The origin of dolomite: Iowa Geological Survey Annual Report, v. 25, 251-422.

VEIZER, J., 1983, Trace elements and isotopes in sedimentary carbonates: in REEDER, R.J. ed., Carbonates: Mineralogy and Chemistry: Reviews in Mineralogy, v. 11, p. 265 - 299.

VEIZER, J. AND HOEFS, J., 1976, The nature of $\delta^{18}\text{O}/\delta^{16}\text{O}$ and $\text{C}^{13}/\text{C}^{12}$ secular trends in sedimentary carbonate rocks: Geochimica et Cosmochimica Acta, v. 40, p. 1387-1395.

WALTER, L.M. AND MORSE, J.W., 1984, Reactive surface area of skeletal carbonates during dissolution: Effect of grain size: Journal of Sedimentary Petrology, v. 54, p. 1081 - 1090.

WARD, W.C. AND HALLEY, R.B., 1985, Dolomitization in a mixing zone of near-seawater composition, Late Pleistocene, northeastern Yucatan Peninsula: Journal of Sedimentary Petrology, v. 55, p. 407 - 420.

WARDLAW, N.C., 1979, Pore systems in carbonate rocks and their influence on hydrocarbon recovery efficiency: Geology of Carbonate Porosity, Education Course Note Series #11, p. E1-E24.

WEBER, J.N., 1964, Trace element composition of dolostones and dolomites and its bearing on the dolomite problem: Geochimica et Cosmochimica Acta, v. 28, p. 1817-1868.

WEYL, P.K., 1960, Porosity through dolomitization: conservation of mass requirements: Journal of Sedimentary Petrology, v. 30, p. 85-90.

WILSON, J.L. AND SENGUPTA, A., 1985, The Trenton Formation in the Michigan Basin and Environs: pertinent questions about its stratigraphy & diagenesis: in Cercone, K.C., and Budai, J.M., eds., Ordovician and Silurian rocks of the Michigan Basin and its margins:

Michigan Basin Society Special Paper Number 4, p. 1-13.

YANGUAS, J.E. AND DRAVIS, J.J., 1985, Blue fluorescent dye technique for recognition of micro porosity in sedimentary rocks: Journal of Sedimentary Petrology, v. 55, p. 600-601.